TESTING PHYSICS BEYOND THE STANDARD MODEL IN NEUTRINO SECTOR

THESIS SUBMITTED TO THE UNIVERSITY OF DELHI

FOR THE DEGREE OF

DOCTOR OF PHILOSOPHY

By

Poonam Mehta

November 2004

DECLARATION

This work has been carried out in Department of Physics & Astrophysics of the University of Delhi under the supervision of Dr. Ashok K. Goyal. The work reported in the thesis is original and has not been submitted earlier for any degree to any University.

(Poonam Mehta)

(Dr. Ashok K. Goyal)
Supervisor

(Professor M. P. Srivastava)
Head of Department

Department of Physics & Astrophysics
University of Delhi
Delhi - 110 007, India.

Dedicated to

My parents, sister & hubby

Acknowledgements

First and foremost, I would like to thank my advisor, Ashok K. Goyal for carrying out a liberal yet vigilant supervision of my Ph. D. project and giving me full academic freedom for pursuing my interests in physics. He has given me exceptional advice, help and support throughout the course of my graduate career. I have benefitted greatly from him. I would also like to thank the faculty members in my department, specially the members of my thesis advisory committee, Amitabha Mukherjee and V. K. Gupta.

I would like to express my gratitude to H. S. Mani, Biswarup Mukhopadhyaya, Debajyoti Choudhury, Debashis Ghoshal, Dileep Jatkar, D. Gaitonde, Satchitananda Naik, Ashoke Sen, T. R. Seshadri and Shiv Sethi for giving wonderful courses on specialized topics in the graduate school course work at HRI. It is my pleasure to thank the full physics faculty at HRI, for whatever physics I have learnt over the past few years.

A warm thanks goes to Biswarup Mukhopadhyaya and Raj Gandhi for suggesting the first problem and motivating me to work in field of physics beyond the standard model of particle physics in neutrino sector. I owe special thanks to Raj Gandhi for providing me motivation and encouragement throughout my career. He has been extremely patient towards me and has been very generous in spending time for discussions, which were both enlightening and inspiring. I am very grateful to Sukanta Dutta and Anindya Datta for training me in the initial period of my Ph. D. on the computational details and who always had answers to all my questions. I sincerely wish to express my gratitude to my collaborator, S. Uma Sankar, for highly stimulating and fruitful discussions. It is a pleasure to thank Srubabati Goswami

for the numerous insightful and enjoyable discussions we had during the last two years of my Ph. D.

I am indebted to my friends: Aarti, Sarita, Rashmi, Debrupa, Mimi, Pomita, Chandrima, Rajesh, Swapan, Partha, Sanjeev, Surjo, Namit, Shalini, Jaswant, Pranav, Sanoli, Purusottam, Anupam, Siddhartha for many hours of fun and good discussions. They have all helped me at several instances in whatever way they could. Their presence really made a difference. I would like to thank Naveen Gaur for his help and for providing me his style files for writing the thesis.

I would like to extend my special thanks to my parents-in-law and sister-in-law for their loving support during the last few years of my Ph. D.

No words can ever describe the level of support and encouragement that I got from my family. I would like to convey my deep regards to my parents for their selfless love, affection and care. Special thanks are due to my younger sister, Sunnu for her cheerful support and for taking care of things at home while I was engrossed in my research.

Last but not the least, thanks are due to my husband, Sourin for the tremendous encouragement and care he had given to me. Despite tremendous academic pressure of his own, he has always patiently helped me out with various things during the last five years. Ultimately, it is his constant support and immense confidence in me that made it possible.

My research has been funded by Council for Scientific and Industrial Research, India. I would like to acknowledge the infrastructural help from the Department of Science and Technology (India) Project Number SP/S2/K-20/99.

List of Publications

1. Signals of R-parity violating supersymmetry in neutrino scattering at muon storage rings (with A. Datta, R. Gandhi and B. Mukhopadhyaya), **Phys. Rev. D 64**, 015011 (2001) [hep-ph/0011375].

2. Leptoquark signals via neutrino interactions at neutrino factories (with S. Dutta and A. Goyal) **Phys. Lett. B 535**, 219 (2002) [hep-ph/0107214].

3. Heavy quark production via leptoquarks at a neutrino factory (with A. Goyal and S. Dutta), **Phys. Rev. D 67**, 053006 (2003) [hep-ph/0209019].

4. Atmospheric neutrinos as a probe of CPT Violation (with A. Datta, R. Gandhi and S. Uma Sankar), **Phys. Lett. B 597**, 356 (2004) [hep-ph/0312027].

Contents

List of Figures

List of Tables

Chapter 1

Introduction

This chapter serves as the introduction to the thesis, and also reviews the basic requirements necessary to study a class of exotic processes mediated by non-standard interactions in neutrino sector at a neutrino factory (NF) set-up. At the level of our present day understanding, the standard model (SM) of particle physics (with massless neutrinos) is capable of successfully describing a large amount of experimental data. In the neutrino sector, it is no longer adequate since a series of recent solar, atmospheric, accelerator and reactor experimental results point to the fact that neutrinos do oscillate and that they are massive ! In fact, neutrinos provide an unmatched window to probe physics beyond the SM. In this dissertation, we will try to address some of the issues related to non-oscillation new physics signatures in the neutrino sector at proposed NF.

1.1 Neutrinos and the Standard Model

Over the last three decades experimental and theoretical efforts to understand the fundamental constituents of matter have condensed into a theory called the SM. This theory, initially devised by Glashow, Weinberg and Salam, includes the unified theory of electroweak interactions and the theory of strong interactions, quantum chromodynamics. Many excellent texts describing

the SM in detail are available and so only a brief discussion of the structure of the theory will be made here. To begin with let us briefly review the particle content of the SM. In the next subsection we will discuss the neutrino interactions in the SM.

1.1.1 Review of the Standard Model

In this section we define the SM of elementary particles by introducing its particle content and parameters of this model. We aim at giving a short introduction, to go deeper into the subjects touched here, we refer the reader to the seminal papers on the SM [1] and to standard books and reviews [2]. The SM of particle physics gives a comprehensive description of fundamental particles of matter and their interactions. It is built from 3 types of particles : the Gauge Bosons which mediate the interactions, Fermions (*i.e.* the leptons and the quarks) and the Higgs sector. The SM is a quantum field theory of electromagnetic, weak and strong interactions based on a gauge theory with an $\mathrm{SU(3)_c} \bigotimes \mathrm{SU(2)_L} \bigotimes \mathrm{U(1)_Y}$ gauge group. The symmetry group of strong interactions is $\mathrm{SU(3)_c}$ where c is the color quantum number carried by the gauge bosons which mediate the strong interactions. The $\mathrm{SU(2)_L} \bigotimes \mathrm{U(1)_Y}$ is the symmetry group of electroweak interactions where L is the left chirality and Y is the weak hypercharge, which is defined below.

Fermionic content of the SM : The basic constituents of matter are the spin-half fermions which comprise of *the leptons* and *the quarks*. There are 3 generations of leptons and quarks in the SM.

$$l_{iL} \ : \ \begin{pmatrix} \nu_i \\ e_i \end{pmatrix}_L \quad e_{iR} \ ; \ \ q_{iR} \ : \ \begin{pmatrix} u_{i\alpha} \\ d_{i\alpha} \end{pmatrix}_L \quad u_{i\alpha R} \quad d_{i\alpha R} \ ; \quad i = 1,2,3 \quad \& \quad \alpha = 1,2,3$$

Here i is the generation index and α is the colour index. In SM, the quarks and leptons transform according to left-handed (LH) doublet and right-handed (RH) singlet representations of $\mathrm{SU(2)_L}$ to account for the V-A nature of the charged current weak interactions. The quarks (both LH and RH) transform as triplets of $\mathrm{SU(3)_c}$ of colour, in order to account for the strong interactions of quarks, while the leptons are singlets under $\mathrm{SU(3)_c}$. The assignment of weak

Generation	Particles	Symbol	Mass	Q	T_3	Y	Lepton no.		
	Leptons		in MeV/c^2				L_e	L_μ	L_τ
I	Electron neutrino	ν_e	$< 3 \times 10^{-6}$	0	$+\frac{1}{2}$	$-\frac{1}{2}$	+1	0	0
	Electron	e^-	0.511	-1	$-\frac{1}{2}$	$-\frac{1}{2}$	+1	0	0
I	Electron	e_R^-	0.511	-1	0	-1	+1	0	0
II	Muon neutrino	ν_μ	< 0.19	0	$+\frac{1}{2}$	$-\frac{1}{2}$	0	+1	0
	Muon	μ^-	105.66	-1	$-\frac{1}{2}$	$-\frac{1}{2}$	0	+1	0
II	Muon	μ_R^-	105.66	-1	0	-1	0	+1	0
III	Tau neutrino	ν_τ	< 18	0	$+\frac{1}{2}$	$-\frac{1}{2}$	0	0	+1
	Tau	τ^-	1777	-1	$-\frac{1}{2}$	$-\frac{1}{2}$	0	0	+1
III	Tau	τ_R^-	1777	-1	0	-1	0	0	+1

Table 1.1: Properties of 6 known leptons in the SM. The corresponding anti-leptons have equal mass but opposite charge and additive quantum numbers.

hypercharge corresponding to the $U(1)_Y$ group to the various $SU(2)_L$ and $SU(3)_c$ multiplets is according to the charge formula : $Q = T_3 + Y$, where T_3, Y and Q denote the third component of weak isospin corresponding to $SU(2)_L$, weak hypercharge and the electric charge generators respectively. Note that electric charge is independent of colour, since no generator of $SU(3)_c$ appears in the charge formula. In Table 1.1 and Table 1.2 respectively, we have listed the three generations of leptons and quarks and their properties like mass (in units of MeV/c^2), electric charge (Q in units of $|e|$), the third component of the weak isospin ($T_3 = \pm 1/2$ for a weak isospin doublet and 0 for a singlet), the average charge of the weak isospin multiplet called the hypercharge assignments for fermions and the individual lepton family and baryon numbers.

Bosonic content of the SM : The scalar sector of the theory has one elementary particle called the *Higgs boson*. In the SM the Higgs boson transforms according to doublet representation of $SU(2)_L$ while under $SU(3)_c$ it is a singlet. The complex scalar doublet is given

Generation	Particles	Symbol	Mass	Q	T_3	Y	Baryon no.
	Quarks		in MeV/c^2				B
I	Up	u	$1.5-4.5$	$+\frac{2}{3}$	$+\frac{1}{2}$	$+\frac{1}{6}$	1/3
	Down	d	$5-8.5$	$-\frac{1}{3}$	$-\frac{1}{2}$	$+\frac{1}{6}$	1/3
I	Up	u_R	$1.5-4.5$	$+\frac{2}{3}$	0	$+\frac{2}{3}$	1/3
	Down	d_R	$5-8.5$	$-\frac{1}{3}$	0	$-\frac{1}{3}$	1/3
II	Charm	c	$1000-1400$	$+\frac{2}{3}$	$+\frac{1}{2}$	$+\frac{1}{6}$	1/3
	Strange	s	$80-155$	$-\frac{1}{3}$	$-\frac{1}{2}$	$+\frac{1}{6}$	1/3
II	Charm	c_R	$1000-1400$	$+\frac{2}{3}$	0	$+\frac{2}{3}$	1/3
	Strange	s_R	$80-155$	$-\frac{1}{3}$	0	$-\frac{1}{3}$	1/3
III	Top	t	$174.3 \pm 5.1 \times 10^3$	$+\frac{2}{3}$	$+\frac{1}{2}$	$+\frac{1}{6}$	1/3
	Bottom	b	$4000-4500$	$-\frac{1}{3}$	$-\frac{1}{2}$	$+\frac{1}{6}$	1/3
III	Top	t_R	$174.3 \pm 5.1 \times 10^3$	$+\frac{2}{3}$	0	$+\frac{2}{3}$	1/3
	Bottom	b_R	$4000-4500$	$-\frac{1}{3}$	0	$-\frac{1}{3}$	1/3

Table 1.2: Properties of six known quarks in the SM. The corresponding anti-quarks have equal mass but opposite charge and additive quantum numbers.

by

$$\Phi \;=\; \begin{pmatrix} \phi^+ \\ \phi^0 \end{pmatrix} \;,$$

The two complex scalars carry an electric charge $Q = +1, 0$ and a weak hypercharge $Y = Q - T_3 = 1/2$. Note that the Higgs boson is the only boson in the theory which is not a gauge boson.

In the gauge sector, we have *eight gluons* which are the gauge bosons of $\mathrm{SU(3)_c}$ and are the mediators of strong interactions. For the broken $\mathrm{SU(2)_L} \bigotimes \mathrm{U(1)_Y}$, we have *three weak gauge bosons* : the $W^{\pm}$ and the Z and one photon (γ) which mediates the electromagnetic interactions. The gluons are chargeless and massless objects and carry colour quantum number.

The $W^{\pm}$ are charged and massive particles while Z is electrically neutral but massive and the photon is both chargeless and massless. The 8 gluons (g) and the 3 weak bosons ($W^{\pm}, Z$) are self-interacting but the photon (γ) is not. The properties of the gauge bosons and their interactions *etc* are listed in Table 1.3.

In the gauge invariant theory, none of the fields correspond to massive particles. Fermion mass terms are forbidden by global gauge invariance. Gauge boson mass terms are forbidden by local gauge invariance. The way to give masses without sacrificing the renormalizability of the theory is to allow for spontaneous symmetry breaking. The Higgs bosons induce this spontaneous symmetry breaking of the gauge group $\mathrm{SU(3)_c} \bigotimes \mathrm{SU(2)_L} \bigotimes \mathrm{U(1)_Y}$ to $\mathrm{SU(3)_c} \bigotimes \mathrm{U(1)_Y}$.

Particles	Symbol	Mass	Q	Symmetry	Interaction(strength)
Gauge bosons		in MeV/c^2			
8 Gluons	g	0	0	SU(3)	Strong(1)
Photons	c	0	0	U(1)	Electromagnetic(10^{-2})
Intermediate vector	$W^{\pm}$	80.423	±1	SU(2)	Weak(10^{-5})
bosons	Z^0	91.1876	0	SU(2)	Weak(10^{-5})

Table 1.3: Properties of gauge bosons and their interactions and underlying symmetries in SM.

A Remark : The neutrino sector in the SM has only LH neutrinos and RH anti-neutrinos which form doublets with corresponding charged leptons. With one Higgs field Φ in the theory, only the Yukawa couplings $\bar{l}_{iR} l_{iL} \Phi + h.c.$ are present in the SM and we have a global symmetry corresponding to lepton number conservation. Thus, neutrinos are massless in the SM. There are many possible extensions of the SM to give $m_\nu \neq 0$; they can be broadly categorized as

1. *Extension of the Higgs sector only :* Other scalars besides the Higgs doublet, Φ can join the lepton bilinear to form $\mathrm{SU(2)_L} \bigotimes \mathrm{U(1)_Y}$ gauge-invariant Yukawa couplings. These can be triplet : H, singly charged singlet : h^+ and doubly charged singlet : R^{++}. For example, when the triplet, H develops a vacuum expectation value (v_H), a Majorana

mass term for the neutrino, $(v_H f)\bar{\nu}^c_{iL}\nu_{iL}$, results.

2. *Extension of the lepton sector only :* The simplest scheme is obviously the addition of three neutral singlets, the RH neutrinos, ν_{eR} $\nu_{\mu R}$ and $\nu_{\tau R}$ in the theory. These are singlets under $\mathrm{SU(3)_c}$ and $\mathrm{SU(2)_L}$ and carry no hypercharge. In this extension we get additional terms in the Lagrangian of the type : $D\bar{\nu}_{iL}\nu_{iR} + B\bar{\nu}^c_{iR}\nu_{iR} + h.c.$, where $D = (1/\sqrt{2})v_\Phi f$. A Majorana bare-mass term B is present because ν_R is totally neutral with respect to $\mathrm{SU(2)_L} \bigotimes \mathrm{U(1)_Y}$ group and we do not impose lepton number conservation on the theory. Thus in this extension we are naturally led to consider neutrino mass terms of the Dirac and Majorana types.

3. *Extension of both Higgs and lepton sectors :* This is the most general case where one adds new scalars like Higgs triplet mentioned above as well as RH singlet neutrinos to the theory. Here also, we can get neutrino mass terms of both Dirac and Majorana types.

1.1.2 Neutrino Interactions in the Standard Model

Neutrinos interact and scatter off matter as described by the electroweak theory of SM. Neutrinos make excellent probes of hadronic matter. They are structureless, comparatively easy to generate in accelerators and their electroweak properties are well understood. One of the common methods of studying hadrons at quark level is by investigating the collisions of neutrinos with protons or neutrons in a fixed target. The effects of small interaction cross section for neutrinos has been overcome by modern experiments through the use of high-intensity beams coupled with massive detectors which give luminosities in the range of $10^{36}\mathrm{cm}^{-2}\mathrm{s}^{-1}$. Data samples in excess of one million events are now available, which allow measurements of strong and electroweak parameters comparable in precision to other fixed target and collider determinations. In the SM, neutrinos interact only weakly with matter, either via the exchange of a W boson or of a Z boson. Neutrino-nucleon interactions dominate over neutrino-electron interaction, due to the small electron mass and the composite structure of the nucleon. The

ratio $\sigma_{\nu-e}/\sigma_{\nu-p(n)}$ is of the order of m_e/m_p. The only exception is the $\nu_e - e$ interaction around E = 6.3×10^6 GeV, where the resonant W boson production enhances the cross section by two orders of magnitude.

- **Charged Current interactions** are given by

$$\mathcal{L}_{CC} = \frac{g_2}{2\sqrt{2}}(J^+_\mu W^{+\mu} + J^-_\mu W^{-\mu}) \tag{1.1}$$

where the strength g_2 is the $\mathrm{SU(2)_L}$ coupling constant and J^+_μ is the $V-A$ weak charged current (CC) and can be written as

$$J^+_\mu \;=\; \sum_i \bar{\psi}_f \gamma_\mu (1-\gamma_5)\psi_i \tag{1.2}$$

Here $'i'$ stands for charged leptons $(e, \mu, \tau, d', s', b')$ and $'f'$ is the corresponding weak isospin partner $(\nu_e, \nu_\mu, \nu_\tau, u, c, t)$ respectively. In short-hand notation, we may simply write

$$J^+_\mu = (\bar{u}\ d')_{V-A} + (\bar{c}\ s')_{V-A} + (\bar{t}\ b')_{V-A} + (\bar{\nu}_e\ e)_{V-A} + (\bar{\nu}_\mu\ \mu)_{V-A} + (\bar{\nu}_\tau\ \tau)_{V-A} \tag{1.3}$$

For the low-energy four-fermion interaction, we generate the following effective Lagrangian

$$\mathcal{L}^{CC}_{eff} \;=\; \frac{-g_2^2}{2M_W^2} J^+_\mu J^{-\mu} \tag{1.4}$$

We can make the identification that g_2 is related to the Fermi coupling constant G_F,

$$\frac{G_F}{\sqrt{2}} = \frac{g_2^2}{8M_W^2}$$

where M_W is the mass of the W boson.

- **Neutral Current interactions** are given by

$$\mathcal{L}_{NC} = eJ^{em}_\mu A^\mu + \frac{g_2}{2\ \cos\Theta_W} J^0_\mu Z^\mu \tag{1.5}$$

where e is the QED coupling constant, g_2 is the $\mathrm{SU(2)_L}$ coupling constant and Θ_W is the Weinberg angle. The electromagnetic and weak neutral current (NC) are given by

$$J_\mu^{em} = \sum_f Q_f \bar{f}\gamma_\mu f \tag{1.6}$$

$$\begin{aligned} J_\mu^0 &= \sum_f \left[g_L^f \bar{f}\gamma_\mu(1-\gamma_5)f + g_R^f \bar{f}\gamma_\mu(1+\gamma_5)f \right] \\ &= \sum_f \bar{f}\gamma_\mu(v_f - a_f\gamma_5)f \end{aligned} \tag{1.7}$$

where $'f'$ represents $(\nu_e, \nu_\mu, \nu_\tau, u, c, t)$ and their corresponding $\mathrm{SU(2)_L}$ partners. The sum is over 12 fermions (6 leptons and 6 quarks). We can express v_f and a_f in terms of g_L^f and g_R^f as

$$v_f = g_L^f + g_R^f = T_3^f - 2\ Q_f\ \sin^2\Theta_W \quad ; \quad a_f = g_L^f - g_R^f = T_3^f \tag{1.8}$$

where Q_f and T_3^f denotes the electric charge and the third component of the weak isospin of the LH fermion f_L respectively and Θ_W is the Weinberg angle. The electroweak charges of leptons and quarks in the SM are listed in Table 1.1 and Table 1.2 respectively. We can generate low-energy four-fermion interactions corresponding to the product of NC,

$$\mathcal{L}_{eff}^{NC} = \frac{-g_2^2}{2M_W^2} J_\mu^0 J^{0\mu} \tag{1.9}$$

where $M_Z \cos\Theta_W = M_W$ has been used, M_Z being the mass of Z-boson.

We see that the weak CC is exclusively LH as opposed to the weak NC which contains a RH component. This is why the RH quarks and charged leptons are in weak isospin singlets. The gauge bosons $W^\pm$ connect leptons within a family *e.g.* $(\bar{\psi}_{\nu_e}\psi_e W^+ + \text{h.c.})$. We can assign an additive "lepton family number" to each of the leptons : electron number, L_e is equal to 1 for e^- and ν_e, -1 for e^+ and $\bar{\nu}_e$, etc. As can be seen from the form of the weak CC and NC, the weak interactions conserve this lepton family number, which means ν_e induced interaction always has a e^- or ν_e in the final state for example. An important consequence of this is that in the SM neutrinos *cannot change flavour by any means.*

Neutrino-electron interactions

For completeness, we shall first review both the **elastic and inelastic scattering** of the neutrino off electron in standard electroweak theory. For the neutrino-electron scattering, the following reactions are accessible to experimental measurements [3]:

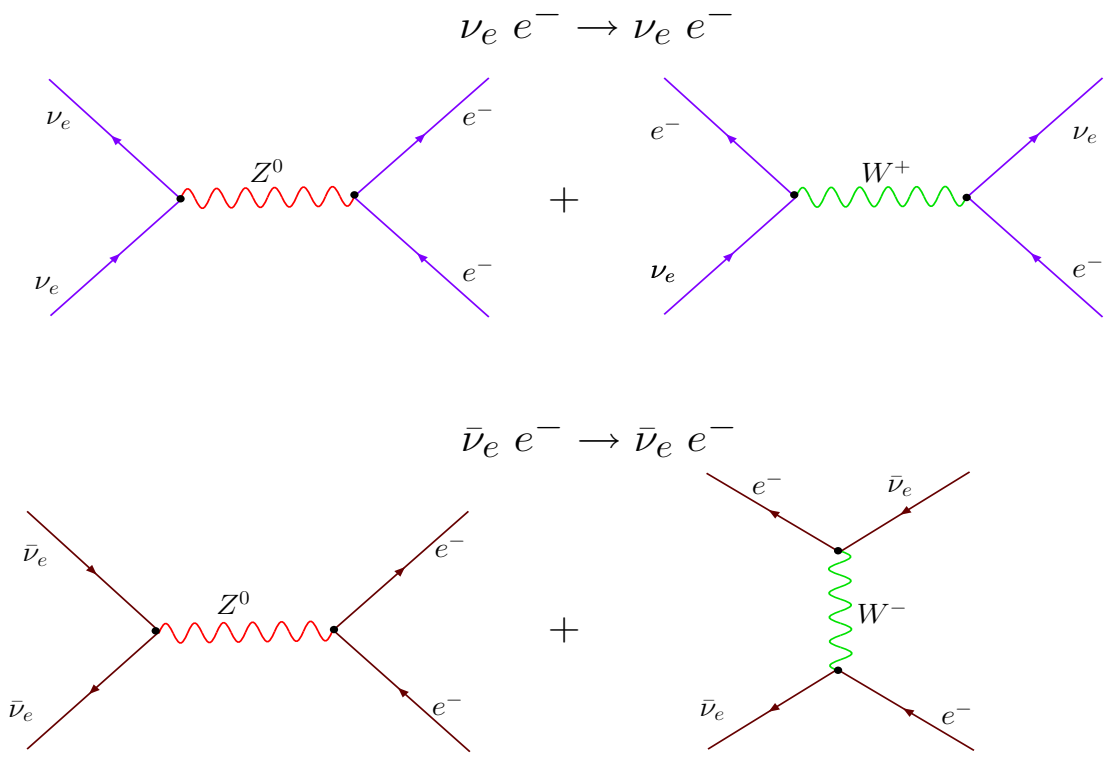

Figure 1.1: *The tree level Feynman diagrams for elastic $\nu_e - e^-$ and $\bar{\nu}_e - e^-$ scattering.*

$$
\begin{aligned}
\nu_\mu e^- &\rightarrow \nu_\mu e^-(NC) \\
\bar{\nu}_\mu e^- &\rightarrow \bar{\nu}_\mu e^-(NC) \\
\nu_e e^- &\rightarrow \nu_e e^-(CC+NC) \\
\bar{\nu}_e e^- &\rightarrow \bar{\nu}_e e^-(CC+NC)
\end{aligned}
$$

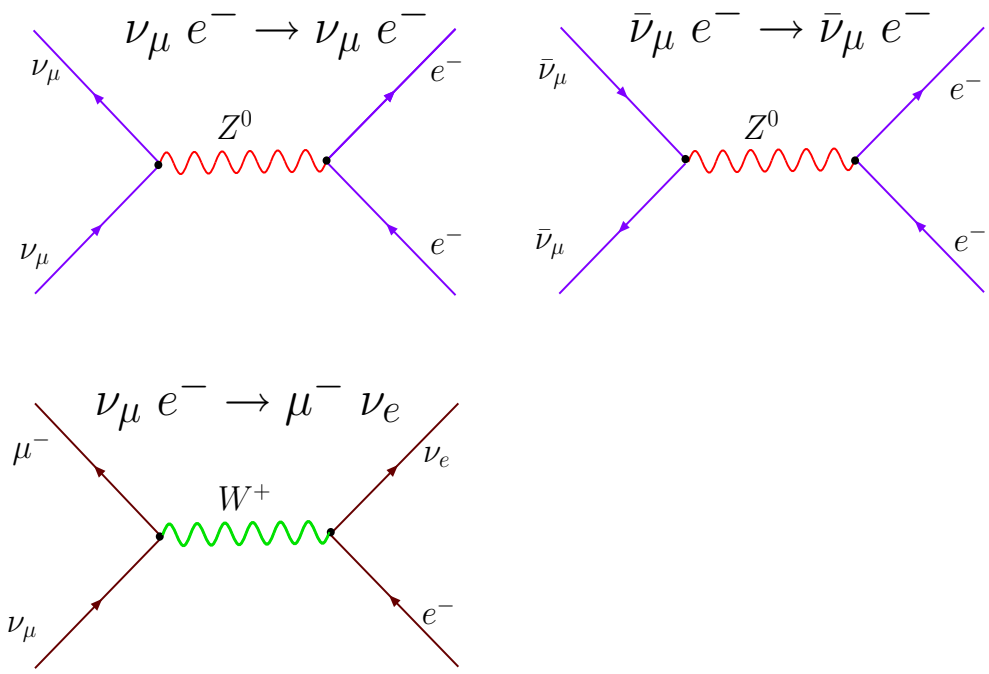

Figure 1.2: *The tree level Feynman diagrams for elastic and inelastic* $\nu_\mu - e^-$ *and* $\bar{\nu}_\mu - e^-$ *scattering.*

$$\nu_\mu e^- \quad \rightarrow \quad \mu^- \nu_e (CC) \tag{1.10}$$

Here, NC and CC refer to the neutral current (Z^0 exchange) and charged current ($W^\pm$ exchange) respectively. The tree level feynman diagrams for neutrino-electron scatterings are depicted in Figure 1.1 and Figure 1.2. We have the following differential cross sections for first four elastic reactions,

$$\frac{d\sigma^{\nu,\bar{\nu}}}{dy} \quad = \quad \frac{G_F^2(s-m_e^2)}{4\pi(1-q^2/M_W^2)^2} \times \left[A + B(1-y)^2 - C\frac{2m_e^2 y}{s-m_e^2}\right] \tag{1.11}$$

where, $G_F = 1.16639 \times 10^{-5}\text{GeV}^{-2}$ is the Fermi coupling constant and the coefficients, A, B and C for different initial and final states are listed in Table 1.4.

The total cross sections for the above interactions are obtained by integrating the differential cross section over y, which upon neglecting the m_e^2 term and the q^2 dependence of the propagator,

$$\begin{aligned}\sigma_{tot} &= \frac{G_F^2 s}{4\pi}\left(A+\frac{B}{3}\right) \\ &\approx 4.3\times 10^{-49}\mathrm{m}^2\left(\frac{E_\nu}{1\ \mathrm{MeV}}\right)\ \left(A+\frac{B}{3}\right)\end{aligned} \tag{1.12}$$

where, $s \simeq 2m_e E_\nu$ and E_ν is the lab energy of ν or $\bar{\nu}$. Hence unless E_ν is very large, experimental observation of these reactions is a formidable problem.

The presence of the final state muon in the inelastic process $\nu_\mu e^- \rightarrow \nu_e \mu^-$ (Figure 1.2) means that the reaction has a threshold of $E_\nu \sim m_\mu^2/(2m_e) \sim 11$ GeV. This process is related to $\mu^- \rightarrow e^- \nu_\mu \bar{\nu}_e$ by replacement of an outgoing $\bar{\nu}_e$ by an incoming ν_e, and is thus known as *inverse muon decay*. The differential cross section for this process is

$$\frac{d\sigma}{dy} = \frac{G_F^2(s-m_\mu^2)}{\pi(1-q^2/M_W^2)^2} \tag{1.13}$$

This gives at high energies,

$$\sigma_{tot} = \frac{G_F^2 s}{\pi} \approx 1.7\times 10^{-48} m^2\left(\frac{E_\nu}{1\ \mathrm{MeV}}\right) \tag{1.14}$$

For low energies, replace s by $(s-m_\mu^2)^2/s$. For the process $\bar{\nu}_\mu e^- \rightarrow \bar{\nu}_e \mu^-$, we get

$$\sigma_{tot} = \frac{G_F^2 s}{3\pi} \approx 5.7\times 10^{-49} m^2\left(\frac{E_\nu}{1\ \mathrm{MeV}}\right) \tag{1.15}$$

The total cross section of the electrons is slightly higher for ν_e's than for ν_μ's or ν_τ's because

Reaction	A	B	C
$\nu_\mu e^- \to \nu_\mu e^-$	$(g_V + g_A)^2$	$(g_V - g_A)^2$	${g_V}^2 - {g_A}^2)$
$\bar{\nu}_\mu e^- \to \bar{\nu}_\mu e^-$	$(g_V - g_A)^2$	$(g_V + g_A)^2$	${g_V}^2 - {g_A}^2)$
$\nu_e e^- \to \nu_e e^-$	$(g'_V + g'_A)^2$	$(g'_V - g'_A)^2$	${g'_V}^2 - {g'_A}^2)$
$\bar{\nu}_e e^- \to \bar{\nu}_e e^-$	$(g'_V - g'_A)^2$	$(g'_V + g'_A)^2$	${g'_V}^2 - {g'_A}^2)$

Table 1.4: The value of coefficients A, B and C for different reactions in $\nu(\bar{\nu}) - e$ scattering. Here $g_V = 2\sin^2\Theta_W - \frac{1}{2}$, $g_A = -\frac{1}{2}$, $g'_V = g_V + 1$ and $g'_A = g_A + 1$.

they have additional W-exchange channels available. The inverse muon decay is only possible for very high ν_μ energies ($E \geq 11$ GeV). However the neutrino-electron cross section is much lower than the neutrino-nucleon cross section (roughly by the mass ratio m_e/m_p). All data are consistent with a value of **Weinberg angle close to** $\sin^2\Theta_W \approx 0.23$. The tau neutrinos scatter in the same way as muon neutrinos.

Neutrino-nucleon interactions

Unlike the case of $\nu - e$ scattering, ingeneral three different classes of interactions of neutrinos with hadronic target can be distinguished : Elastic scattering, Quasi-elastic (QE) scattering off nucleons and inelastic interactions with nucleons. The tree level Feynman diagrams for each class of these processes are depicted in Figure 1.3, Figure 1.4 and Figure 1.5 respectively. We discuss these in turn below.

Quasi-elastic neutrino scattering : At low neutrino energies, charged current neutrino-hadron interactions are predominantly elastic and QE in which the neutrino scatters off an entire nucleon rather than the constituent partons. Nucleons are essentially point-like objects at very low energy (i.e. the elastic regime) but for $E > 30 - 50$ MeV, the structure of the nucleons must be taken into account (the QE regime). QE process has been studied at low energies (100 MeV - 10 GeV) mostly in bubble chamber experiments, light targets [4].

Consider the QE process for ν and $\bar{\nu}$:

$$\begin{aligned} \nu(k_1) + n(p_1) &\rightarrow l^-(k_2) + p(p_2) \\ \bar{\nu}(k_1) + p(p_1) &\rightarrow l^+(k_2) + n(p_2) \end{aligned} \tag{1.16}$$

The most general hadronic current for the above nucleon transition (for ν) can be written

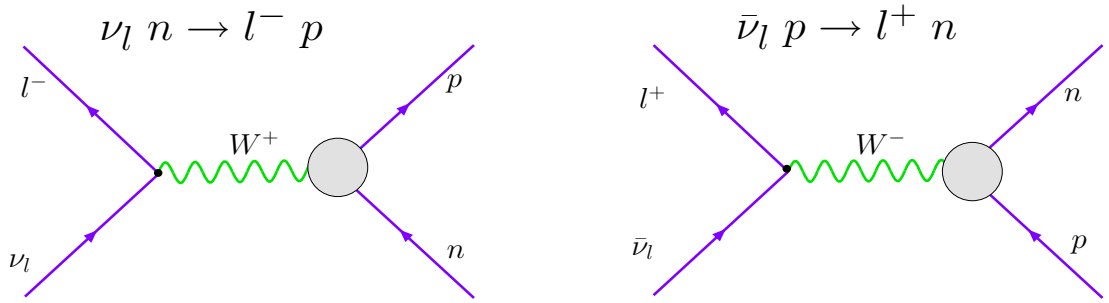

Figure 1.3: *The tree level Feynman diagrams for quasi-elastic ν_l and $\bar{\nu}_l$ scattering.*

as [5]

$$\begin{aligned} < p(p_2)|J^+_\lambda|n(p_1) > &= \bar{u}(p_2)\Big[\gamma_\lambda F_V^1(q^2) + \frac{i\sigma_{\lambda\nu}q^\nu \xi F_V^2(q^2)}{2M} + \frac{q_\lambda F_V^3(q^2)}{M} \\ &+ \gamma_\lambda\gamma_5 F_A(q^2) + \frac{q_\lambda\gamma_5 F_P(q^2)}{M} + \frac{\gamma_5(p_1+p_2)_\lambda F_A^3(q^2)}{M}\Big]u(p_1) \end{aligned} \tag{1.17}$$

where F_S, F_P, F_V, F_A, F_T describe the scalar, pseudoscalar, vector, axial-vector, and tensor form factors of the nucleon, respectively. $q = k_1 - k_2 = p_1 - p_2$, $\xi = (\mu_p - 1) - \mu_n$, and $M = (m_p + m_n)/2$. Here $\mu_p - 1 = 1.793$ and $\mu_n = -1.913$ are the proton and neutron anomalous magnetic moments.

Using the above current, the cross section (in the limit where $E_\nu >> m_l$) is [5]

$$\frac{d\sigma^{\nu,\bar{\nu}}}{dq^2} = \frac{M^2 G_F^2 \cos^2\theta_c}{8\pi E_\nu^2} \times \left[A(q^2) \mp B(q^2)\frac{(s-u)}{M^2} + C(q^2)\frac{(s-u)^2}{M^4}\right] \tag{1.18}$$

In this expression, G_F is the Fermi coupling constant and θ_c is the Cabibbo angle, $\cos\theta_c = 0.9740$. The functions $A(q^2), B(q^2)$ and $C(q^2)$ are convenient combinations of form factors (in the limit where m_l is negligible):

$$\mathrm{A(q^2)} = \frac{\mathrm{m^2 - q^2}}{\mathrm{4M^2}}\Big[\Big(4 - \frac{\mathrm{q^2}}{\mathrm{M^2}}\Big)|\mathrm{F_A}|^2 - \Big(4 + \frac{\mathrm{q^2}}{\mathrm{M^2}}\Big)|\mathrm{F_V^1}|^2 - \frac{\mathrm{q^2}}{\mathrm{M^2}}|\xi\mathrm{F_V^2}|^2\Big(1 + \frac{\mathrm{q^2}}{\mathrm{4M^2}}\Big) - \frac{\mathrm{4q^2 ReF_V^{1\star}}\xi\mathrm{F_V^2}}{\mathrm{M^2}}\Big]$$

$$\begin{aligned}
\mathrm{B(q^2)} &= -\frac{\mathrm{q^2}}{\mathrm{M^2}}\mathrm{ReF_A^\star}(\mathrm{F_V^1} + \xi\mathrm{F_V^2}) \\
\mathrm{C(q^2)} &= \frac{1}{4}\Big(|\mathrm{F_A}|^2 + |\mathrm{F_V^1}|^2\frac{\mathrm{q^2}}{\mathrm{M^2}}|\frac{\xi\mathrm{F_V^2}}{2}|^2\Big)
\end{aligned}$$

According to the conserved vector current (CVC) hypothesis, the vector part of the weak current and isovector part of the electromagnetic current form an isotriplet of conserved currents [6]. This allows us to relate the vector form factors ($F_V^1(q^2)$ and $\xi F_V^2(q^2)$) to the electromagnetic form factors of proton and neutron. which are better measured. Also the contribution of second class currents (that violate the symmetry of strong interactions called the G-parity where $G = CR_y$, C being charge conjugation and R_y being a rotation by an angle π around the isospin axis I_y) can be assumed to vanish (F_V^3 and $F_A^3 \to 0$), and one remains with two unknown functions the axial form factor F_A and the pseudoscalar form factor F_P. In terms of Sachs (electromagnetic) form factors, the vector form factors are given by

$$\begin{aligned}
\mathrm{F_V^1(q^2)} &= \Big(1 - \frac{\mathrm{q^2}}{\mathrm{4M^2}}\Big)^{-1}\Big[\mathrm{G_E^V(q^2)} - \frac{\mathrm{q^2}}{\mathrm{4M^2}}\mathrm{G_M^V(q^2)}\Big] \\
\xi\mathrm{F_V^2(q^2)} &= \Big(1 - \frac{\mathrm{q^2}}{\mathrm{4M^2}}\Big)^{-1}\Big[\mathrm{G_M^V(q^2)} - \mathrm{G_E^V(q^2)}\Big]
\end{aligned} \tag{1.19}$$

$F_V^1(q^2)$ and $F_V^2(q^2)$ are called Dirac and Pauli electromagnetic isovector form factors respectively. The electromagnetic form factors are determined from the electron scattering experi-

ments :

$$\mathrm{G_E^V(q^2) = G_E^p(q^2) - G_E^n(q^2)}, \qquad \mathrm{G_M^V(q^2) = G_M^p(q^2) - G_M^n(q^2)} \tag{1.20}$$

The vector form factors are often described by the dipole approximation (which matches with experiments well within $\pm 10\%$):

$$\begin{aligned} \mathrm{G_D(q^2)} &= \left(1 - \frac{\mathrm{q^2}}{\mathrm{M_V^2}}\right)^{-1}, \\ \mathrm{G_E^p = G_D(q^2)}, \quad \mathrm{G_E^n = 0}, \quad \mathrm{G_M^p = \mu_p G_D(q^2)}, \quad \mathrm{G_M^n = \mu_n G_D(q^2)}. \end{aligned} \tag{1.21}$$

So, the vector form factors are

$$\begin{aligned} \mathrm{F_V^1(q^2)} &= \left(1 - \frac{\mathrm{q^2}}{\mathrm{4M^2}}\right)^{-1} \mathrm{G_D(q^2)} \left[1 - \frac{\mathrm{q^2}}{\mathrm{4M^2}}(\mu_\mathrm{p} - \mu_\mathrm{n})\right], \\ \xi \mathrm{F_V^2(q^2)} &= \left(1 - \frac{\mathrm{q^2}}{\mathrm{4M^2}}\right)^{-1} \mathrm{G_D(q^2)} \left[\mu_\mathrm{p} - \mu_\mathrm{n} - 1\right] \end{aligned} \tag{1.22}$$

The above combinations of form factors is referred to as 'Dipole form factors'. Here $M_V^2 = 0.71$ GeV^2. It is an approximation that has been improved recently by Budd, Bodek and Arrington (BBA) who refer to the new form factors as 'BBA-2003 Form Factors' [7].
The axial form factor F_A (using dipolar parametrization) is given by

$$\mathrm{F_A(q^2)} = \mathrm{g_A} \left(1 - \frac{\mathrm{q^2}}{\mathrm{M_A^2}}\right)^{-1},$$

The value of F_A at $Q^2 = 0$ can be related to the axial coupling measured in $\beta-$decay experiments ($F_A(0) = g_A = -1.2670 \pm 0.0035$), but the q^2 dependence of F_A has to be determined

g_A = -1.267
G_F = 1.1803×10^{-5} GeV^{-2}
$\cos\theta_c$ = 0.9740
μ_p = 2.793 μ_N
μ_n = -1.913 μ_N
ξ = 3.706 μ_N
M_V^2 = 0.71 GeV^2

Table 1.5: The most recent values of the parameters used in QE scattering [7].

experimentally. In the dipolar parametrization, F_A depends on a single parameter, M_A which denotes the mass specifying the q^2 dependence of the axial form factor. Therefore, in first approximation the problem of the determination of the QE cross section can be identified with the measurement for M_A. The q^2 dependence of the differential scattering cross section has been measured in low energy experiments [4] and agrees well with the above expression. The updated value of M_A from BBA-2003 form factors is $M_A = 1.00 \pm 0.020$ GeV [7] which is in good agreement with the theoretically corrected value from pion electroproduction of $M_A = 1.014 \pm 0.016$ GeV. Studies of Δ production in, e.g. $\nu_\mu p \rightarrow \mu^- \Delta^{++}$ can also be used to study M_A, yielding a roughly similar value.

The contribution of the pseudoscalar form factor F_P to the QE cross section is proportional to $(m_l/M)^2$, therefore this term is important only for ν_τ. In muon neutrino interactions the effect of F_P is very small except at very low energy, below 0.2 GeV. Therefore some assumptions must be made about the pseudoscalar form factor F_P. One can use the Partially Conserved Axial Current (PCAC) hypothesis, $\partial\mu j_A^\mu = m_\pi^3 f_\pi \phi_\pi(x)$ (where, f_π is the pion decay constant and ϕ_π is the pion field) to postulate a form for F_P. A plausible parametrization that satisfies PCAC at low q^2 is [5]

$$\mathrm{F_P(q^2) = \frac{2M^2 F_A(q^2)}{(m_\pi^2 - q^2)}} \tag{1.23}$$

The inclusion of F_P leads to an approximately 5% reduction in both the ν_τ and $\bar{\nu}_\tau$ QE cross sections. The most recent parameter values appearing in QE form factors are listed in Table 1.5.

Elastic regime :

For really low energies, where the above expression (equation 1.18) is not valid, for example, $E_{\bar{\nu}_e} \approx 50\ MeV$ for $\bar{\nu}_e N \to e^+ N$ and $E_{\nu_\mu} \approx 110\ MeV$ for $\nu_\mu N \to \mu^- N$ we have the following formula for the elastic cross section :

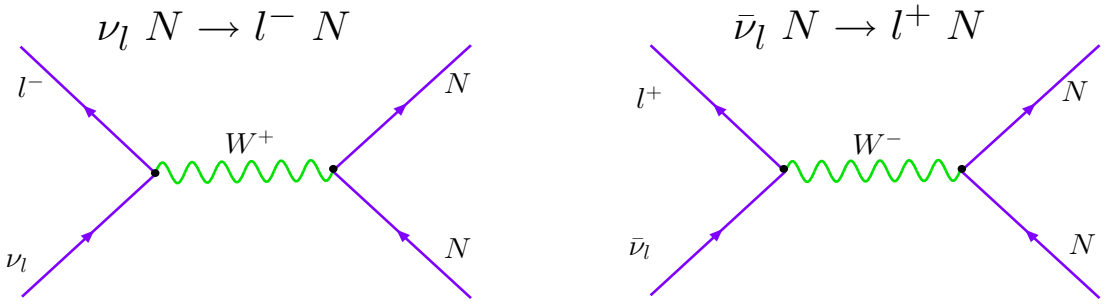

Figure 1.4: *The tree level Feynman diagrams for elastic ν_l and $\bar{\nu}_l$ scattering.*

$$\begin{aligned} \sigma^{\nu\bar{\nu}} &= \frac{G_F^2 (\hbar c)^2 E_\nu^2}{\pi} \left[{g_V}^2 + 3{g_A}^2 \right] \\ &\approx 9.77 \times 10^{-48}\ \mathrm{m}^2 \left(\frac{E_\nu}{1\ \mathrm{MeV}} \right)^2 \end{aligned} \tag{1.24}$$

where the mass difference between the proton and neutron is neglected and $g_V = 1$, $g_A = -1.267$ (previous neutrino experiments used $g_A = -1.23$) has been used, which are the current

best values.

A Comment on Resonance pion production :

Above the neutrino energy of 0.15 GeV, the threshold opens for pion production. Pion production becomes important at E > 0.34 GeV, when $\Delta_{33}(1232)$ is produced. Above 1 GeV multipion production dominates the neutrino-nucleon reactions.

Deep Inelastic Regime :

The tree level diagram for CC neutrino-nucleon scattering is shown in Figure 1.5. The interaction is mediated by a W-boson (W^+ for ν and W^- for $\bar{\nu}$) carrying a four momentum q.

At high enough energies ($E > 10$ GeV), the neutrino scatters off the partons present inside the nucleon. The deep inelastic neutrino-nucleon scattering has been studied with high precision in the energy range of $20 - 200$ GeV by numerous experiments (CCFRR, CHARM, CDHS) [8]. The CC neutrino-nucleon interaction $\nu N \rightarrow l^- X$ in the SM plays a central role in neutrino detection, since, except for the electron neutrino, only the hadronic component X produces visible signals to neutrino detectors. For the investigation of $\nu - N$ interactions in new physics models, this channel also constitutes the main background to the observation of neutrino-induced signals resulting from $\nu - N$ interactions in extensions of the SM.

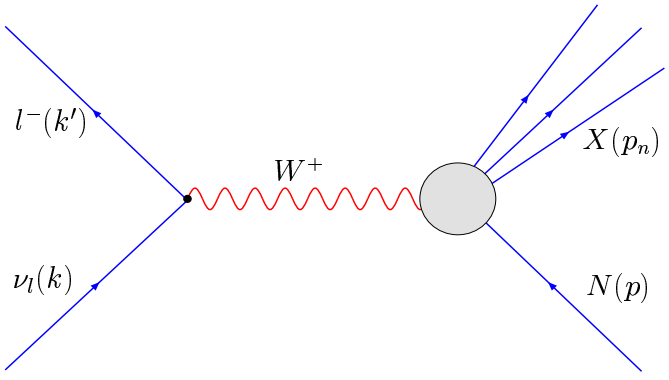

Figure 1.5: *The leading order diagram for deep inelastic $\nu - N$ scatttering. Here W^+ is the mediator for ν CC interactions and X is any possible final state.*

We consider the DIS process for ν and $\bar{\nu}$:

$$\begin{aligned} \nu_l(k) + N(p) &\rightarrow l^-(k') + X(p_n) \\ \bar{\nu}_l(k) + N(p) &\rightarrow l^+(k') + X(p_n) \end{aligned} \tag{1.25}$$

We perform the calculation within the renormalization group improved parton model, and focus on the inclusive process $\nu_l N \longrightarrow l^- +$ anything, where N is an isoscalar nucleon $N \equiv (n+p)/2$ of mass M and l stands for the lepton flavour. If we retain the effects of lepton-mass (where $l \equiv \tau, \mu$), the double differential cross section can be written in terms of the Bjorken scaling[1] variables $x = Q^2/2M\nu$ and $y = \nu/E_\nu$ as

$$\begin{aligned} \frac{d^2\sigma^{\nu,\bar{\nu}}}{dx\,dy} &= \frac{G_F^2\, M\, E_\nu}{\pi} \left[\left\{ xy + \frac{m_l^2}{2\,M\,E_\nu} \right\} F_1 + \left\{ (1-y) - \left(\frac{M}{2\,E_\nu} xy + \frac{m_l^2}{4\,E_\nu^2} \right) \right\} F_2 \right. \\ &\left. \pm \left\{ xy \left(1 - \frac{1}{2} y \right) - \frac{m_l^2}{4\,M\,E_\nu} y \right\} F_3 + \frac{m_l^2}{M^2} \left\{ \left(\frac{M}{2\,E_\nu} xy + \frac{m_l^2}{4\,E_\nu^2} \right) F_4 - \frac{M}{2\,E_\nu} F_5 \right\} \right] \end{aligned} \tag{1.26}$$

Here $-Q^2$ is the invariant momentum transfer between the incident neutrino and outgoing tau, $\nu = E_\nu - E_l$ is the energy loss in the lab (target) frame, M and M_W are the nucleon and intermediate boson masses respectively, and $G_F = 1.16632 \times 10^{-5}$ GeV^{-2} is the Fermi constant. The limits on x and y are

$$\frac{m_l^2}{2\,M\,(E_\nu - M)} \leq x \leq 1\,, \qquad\qquad A - B \leq y \leq A + B$$

where

[1]Bjorken scaling is the statement that in the large Q^2 limit with x fixed, the F_is are functions of x only. Thus, $F_i(x, q^2/M^2) = F_i(x)$ as $|q^2| \rightarrow \infty, x \rightarrow$ fixed. The dimensionless structure functions become independent of any mass scale. The functions F_is are called scaling functions. Experimentally, Bjorken scaling seems to be obtained for a rather modest value of $Q^2 \geq 2(GeV)^2$ in ep scattering.

$$
\begin{aligned}
A &= \frac{1}{2}\left(1-\frac{m_l^2}{2\,M\,E_\nu x}-\frac{m_l^2}{2\,E_\nu^2}\right)/\left(1+x\frac{M}{2E_\nu}\right),\\
B &= \frac{1}{2}\left|\left[\left(1-\frac{m_l^2}{2\,M\,E_\nu x}\right)^2-\frac{m_l^2}{2\,E_\nu^2}\right]\right|^{\frac{1}{2}}/\left(1+x\frac{M}{2E_\nu}\right).
\end{aligned}
\tag{1.27}
$$

Structure functions in the quark-parton model : In the quark parton model, the contributions to the structure functions F_i's can be expressed in terms of **quark distribution functions** $q(x,Q^2)$ of the proton, where $q = u,\ \bar{u},\ d,\ \bar{d}$ etc. The quantity $q(x,Q^2)dx$ is the number of quarks (or anti-quarks) of designated flavor that carry a momentum fraction between x and $x+dx$ of the proton's momentum in a frame in which the proton momentum is large.

Experimentally, massive neutrino detectors are constructed of materials of medium atmoic number, for *e.g.* , CHARM use marble (A=40) and CDHS use iron (A=56). Calcium is **isoscalar** (equal number of protons and neutrons) and iron is approximately so. Hence, structure functions are often measured per nucleon, reducing the number to half *i.e.* ,

$$
(F_i)_{nucleon} = \frac{(F_i)_{proton}+(F_i)_{neutron}}{2}
$$

For the process mediated by W^+, we have

$$
\begin{aligned}
F_2 &= x\left(u+d+\bar{u}+\bar{d}+2\,s+2\,\bar{b}\right),\\
F_1 &= \frac{F_2}{2\,x},\\
F_3 &= \left(u+d-\bar{u}-\bar{d}+2\,s-2\,\bar{b}\right),\\
F_4 &= \left(-\frac{M\,\nu}{Q^2}\right)^2 F_2+\left(-\frac{M\,\nu}{Q^2}\right)F_1,\\
F_5 &= \frac{F_2}{x}
\end{aligned}
$$

A straightforward application of the Callan-Gross equations ($2xF_1 = F_2$) shows that F_4 vanishes in this case. In the above, *u,d,c,s* and *b* denote the distributions for the various quark flavours in a proton. For W^-, the structure functions are obtained by flavour interchanges $d \leftrightarrow u$ and $s \leftrightarrow c$. For our calculations we use CTEQ4LQ parton distributions [9].

1.2 Directions beyond the Standard Model

Unification of all fundamental interactions observed in nature has been the dream of particle physic(ist)s. SM of particle physics has been a big step in this direction which successfully unified weak and electromagnetic interactions. But as has been well discussed in literature, the SM despite all successes also leave many questions unanswered. The SM also has known and well emphasized problems like naturalness, hierarchy etc. associated with it. So there are very strong reasons to believe that SM is a effective theory valid upto a certain energy scale ($\sim$ 1 TeV), and beyond this scale some new physics should take over.

As is already mentioned in the introduction, the SM is clearly inadequate to explain the phenomena of neutrino oscillations and masses. One is therefore interested in possible extensions of SM, which can accomodate the masses of neutrinos in a natural way. Here we will describe the possible candidates for theories beyond the SM including non-zero masses of neutrinos, viz, Supersymmetry (SUSY) and Leptoquarks (LQ). A possible extension of the SM can be found in the theory of SUSY, which proposes a massive supersymmetric "partner" for every particle in the conventional SM.

1.2.1 Supersymmetry

It is believed that the SM is an effective low energy theory branching out from a more fundamental theory at a very high scale (say GUT scale, $\sim 10^{16}$ GeV). So, one would expect that the gauge couplings meet at that high scale. In fact, experimental data shows converging be-

haviour of all the three couplings at $\sim 10^{16}$ GeV when extrapolating upto that very high scale. If we try to see the evolution of couplings in SM, then this unification comes very naturally.

SUSY implies symmetry between bosons & fermions, which is successful in protecting the scalar mass through the cancellation of quadratic divergences in scalar mass coming from bosonic and fermionic loops.

Minimal Supersymmetric Standard Model :

In the Minimal Supersymmetric Standard Model (MSSM), the gauge group is same as the SM gauge group, i.e, $\mathrm{SU(3)_c} \bigotimes \mathrm{SU(2)_L} \bigotimes \mathrm{U(1)_Y}$. The particle spectrum necessary to construct the MSSM consists of all the three generations of quarks and leptons and their superpartners, the $\mathrm{SU(3)_c}$ gauge bosons, gluons and their fermionic partners as well as the $\mathrm{SU(2)_L}$ and $\mathrm{U(1)_Y}$ gauge bosons and their superpartners. In addition, one needs two complex Higgs doublets and their corresponding superpartners. Each quark (lepton) has two scalar partners corresponding to two quark (lepton) chiralities.

The basic building blocks of $\mathrm{N} = 1$ Supersymmetric theories are supermultiplets containing following helicity states

$$\text{chiral} \ : \ \begin{pmatrix} \frac{1}{2} \\ 0 \end{pmatrix} \ , \ \text{gauge} \ : \ \begin{pmatrix} 1 \\ \frac{1}{2} \end{pmatrix} \ , \ \text{graviton} \ : \ \begin{pmatrix} 2 \\ \frac{3}{2} \end{pmatrix} \ ,$$

which are used to describe matter and higgses, gauge fields and gravity respectively. The MSSM is constructed out of SM particles alone. The MSSM has the same gauge interactions as the SM. In addition there are couplings derived from the superpotential :

$$W = \lambda_d \ Q \ D^C \ H + \lambda_\ell \ L \ E^C \ H + \lambda_u \ Q \ U^C \ \bar{H} + \mu \bar{H} H$$

Here, $Q[L]$ denote isodoublets of supermultiplets containing $(u,d)_L[(\nu,\ell)_L]$, $D^C[U^C, E^C]$ are singlets containing the left-handed conjugates $d_L^C[u_L^C, e_L^C]$ of the right-handed $d_R[u_R, e_R]$, and the superpotential couplings $\lambda_d[\lambda_{u,\ell}]$ correspond to the Yukawa couplings of the SM that give masses to the $d[u, \ell^-]$, respectively:

$$m_d = \lambda_d < H > \ , \ \ m_u = \lambda_u < \bar{H} > \ , \ \ m_\ell = \lambda_\ell < H > \ .$$

Each of these should be understood as a 3×3 matrix in generation space, which is to be diagonalized as in the SM. We require two Higgs doublets $H, \bar{H}$ with opposite hypercharges in order to give masses to all the matter fermions. In the SM , one doublet ϕ and its complex conjugate $\phi^\dagger$ would have sufficed. This does not work in the MSSM, because the superpotential W must be an analytic function of the fields. Moreover, Higgs supermultiplets include Higgsino fermions that generate triangle anomalies which must cancel among themselves, requiring at least two Higgs doublets. These couple via the μ term in superpotential. The particle content of SM and MSSM is given in Table 1.6.

Particle	Spin	Spartner	Spin
quark q	$\frac{1}{2}$	squark $\tilde{q}$	0
lepton ℓ	$\frac{1}{2}$	slepton $\tilde{\ell}$	0
photon γ	1	photino $\tilde{\gamma}$	$\frac{1}{2}$
W	1	wino $\tilde{W}$	$\frac{1}{2}$
Z	1	zino $\tilde{Z}$	$\frac{1}{2}$
Higgs H	0	higgsino $\tilde{H}$	$\frac{1}{2}$

Table 1.6: Particles in the SM and their supersymmetric partners.

MSSM is the simplest supersymmetric extension of SM in that it contains the fewest number of fields and superpotential interactions.

The presence of scalars carrying lepton (L) or baryon (B) number in a SUSY scenario makes it possible to have *one* of the above quantum numbers broken while the other is conserved. One can thus avoid undesirable consequences like fast proton decay, and can still be consistent with all other symmetries when R-parity [10] is violated. In such a scenario with broken lepton number, the corresponding part of the superpotential is given (suppressing colour and $SU(2)$ indices) by [11],

$$W_{\not L} = \epsilon_i \hat{L}_i \hat{H}_2 + \lambda_{ijk} \hat{L}_i \hat{L}_j \hat{E}^c_k + \lambda'_{ijk} \hat{L}_i \hat{Q}_j \hat{D}^c_k \tag{1.28}$$

where i, j and k are generation indices, $\hat{L}$ and $\hat{Q}$ represent the SU(2) doublet lepton and quark superfields, and $\hat{E}$, $\hat{U}$ and $\hat{D}$ denote the right-handed charged lepton, up-type quark and down-type quark superfields respectively. In terms of the component fields (with the sfermion fields characterised by the tilde sign), the trilinear terms above lead to interactions of the form

$$\begin{aligned} \mathcal{L} \;=\; & \lambda'_{ijk} \,[\, \tilde{d}^j_L \, \bar{d}^k_R \nu^i_L + (\tilde{d}^k_R)^* (\bar{\nu}^i_L)^c d^j_L + \tilde{\nu}^i_L \bar{d}^k_R d^j_L \\ & \qquad - \tilde{e}^i_L \bar{d}^k_R u^j_L - \tilde{u}^j_L \, \bar{d}^k_R e^i_L - (\tilde{d}^k_R)^* (\bar{e}^i_L)^c u^j_L \,] + h.c. \\ & + \lambda_{ijk} \,[\, \tilde{e}^j_L \, \bar{e}^k_R \nu^i_L + (\tilde{e}^k_R)^* (\bar{\nu}^i_L)^c e^j_L + \tilde{\nu}^i_L \bar{e}^k_R e^j_L - (i \leftrightarrow j) \,] + h.c \end{aligned} \tag{1.29}$$

It should be noted that these interaction terms violate both lepton flavour and lepton number. By suitable combinations of two such terms, it is possible to achieve contributions to processes which conserve lepton number but involve transition between different generations.

1.2.2 Leptoquarks

There are no interactions involving a quark, a lepton and a boson in the SM. There is a scalar Higgs doublet with electroweak quantum numbers, and vector bosons that are either coloured or charged, but no boson carrying colour and charge. This is a reflection of the fact that classically the leptons and quarks appear to be independant unrelated ingredients in the SM. However, in each generation of the quantum theory, they have equal and opposite contributions to the hypercharge anomaly, which must vanish for the quantum theory to make sense. It would therefore seem natural to have interactions between the quarks and leptons in any extension of the SM, and, in consequence, bosons coupling to a lepton and a quark.

The association between quarks and leptons exemplified by the cancellation of triangle anomalies preserving the renormalizability of the SM provide convincing hints at potential,

fundamental connections. Theories incorporating LQ furnish a mechanism whereby quarks and leptons can couple directly through a Yukawa-type interaction.

LQ are hypothetical particles which combine quantum numbers of the fundamental fermions of the SM and emerge as bosonic (scalar and vector) states in various extensions of the SM with extended gauge symmetries [12]. Lepton and quarks may be arranged in common multiplets, like in grand unified theories, and superstring motivated E_6 models, or they may have common sub-structure as in composite models. They are not part of MSSM, but can be accomodated in certain extended SUSY models. In most of these scenarios the mass spectrum of these states in not predicted. In a series of models, however, one expects states in the range of several hundred GeV to a few TeV.

LQ, as the name suggests, couple to a current comprising of a lepton and a quark. A LQ is a scalar (spin=0) or a vector (spin=1) particle carrying colour, fractional electric charge, and both lepton and baryon numbers. It may or may not have well-defined baryon and lepton number, depending on the choices of coupling. Those with B violating interactions would in general mediate proton decay, so their masses are expected to be very large ($\sim 10^{15}$ GeV). In many models, both baryon and lepton numbers are conserved, allowing low mass LQ to exist without mediating the proton decay. LQ with universal couplings to all flavours would give rise to flavour changing neutral currents (FCNC) and are severely constrained by low energy experiments. In most analyses it is assumed that there is no intergenerational mixing and that, for *e.g.* the first generation LQ couple only to e or ν_e and to u or d quarks in order to suppress FCNC. In this document, we shall only consider LQ with B and L conserving renormalizable couplings consistent with the symmetries of the SM. A fermion number $F = 3B + L$ is defined, which takes the value $|F| = 2$ for LQ coupling to $e^- q$ and $|F| = 0$ for $e^- \bar{q}$. For positrons, the fermion number F changes by two (since $L = -1$ for e^+).

Since LQ carry colour, they will not affect pure leptonic processes; thus $\nu e \rightarrow \nu e$ will not be affected. LQ will not mix with the weak intermediate bosons, which are colourless, so the masses of W and Z bosons will not be changed.

The interactions of LQ with known particles can be described by an effective Lagrangian valid at sufficiently low energies. The effective Lagrangian with the most general dimensionless, $\mathrm{SU(3)_c} \otimes \mathrm{SU(2)_L} \otimes \mathrm{U(1)_Y}$ invariant couplings of *scalar* and *vector* LQ satisfying baryon (B) and lepton number (L) conservation (suppressing colour, weak isospin and generation (flavour) indices) is given (we use the notation used in [13]) by:

LQ		Q	$\mathrm{T_3}$	Spin	$\lambda_L(lq)$	$\lambda_R(lq)$	$\lambda_L(\nu q)$
S_1	S_1	1/3	0	0	g_{1L}	g_{1R}	$-g_{1L}$
$\tilde{S}_1$	$\tilde{S}_1$	4/3	0	0	0	$\tilde{g}_{1R}$	0
$\vec{S}_3$	S_3^+	4/3	1	0	$-\sqrt{2}\,g_{3L}$	0	0
	S_3^0	1/3	0	0	g_{3L}	0	$-g_{3L}$
	S_3^-	−2/3	−1	0	0	0	$\sqrt{2}\,g_{3L}$
$V_{2\mu}$	$V_{2\mu}^b$	4/3	1/2	1	g_{2L}	g_{2R}	0
	$V_{2\mu}^a$	1/3	−1/2	1	0	g_{2R}	g_{2L}
$\tilde{V}_{2\mu}$	$\tilde{V}_{2\mu}^b$	1/3	1/2	1	$\tilde{g}_{2L}$	0	0
	$\tilde{V}_{2\mu}^a$	−2/3	−1/2	1	0	0	$\tilde{g}_{2L}$

Table 1.7: Coupling strengths of possible interactions allowed by LQ lagrangian for scalar & vector LQ corresponding to |F|=2.

$$
\begin{aligned}
\mathcal{L} &= \mathcal{L}_{|F|=2} + \mathcal{L}_{|F|=0} \qquad \text{where} \\
\mathcal{L}_{|F|=2} &= \left[g_{1L}\,\bar{q}_L^c\,i\,\tau_2\,l_L + g_{1R}\,\bar{u}_R^c\,e_R\right]\,S_1 + \tilde{g}_{1R}\,\bar{d}_R^c\,e_R\,\tilde{S}_1 + g_{3L}\,\bar{q}_L^c\,i\,\tau_2\,\vec{\tau}\,l_L\,\vec{S}_3 \\
&+ \left[g_{2L}\,\bar{d}_R^c\,\gamma^\mu\,l_L + g_{2R}\,\bar{q}_L^c\,\gamma^\mu\,e_R\right]\,V_{2\mu} + \tilde{g}_{2L}\,\bar{u}_R^c\,\gamma^\mu\,l_L\,\tilde{V}_{2\mu} + h.c.,
\end{aligned}
$$

$$
\mathcal{L}_{|F|=0} = \left[h_{2L}\,\bar{u}_R\,l_L + h_{2R}\,\bar{q}_L\,i\,\tau_2\,e_R\right]\,R_2 + \tilde{h}_{2L}\,\bar{d}_R\,l_L\,\tilde{R}_2 + \tilde{h}_{1R}\,\bar{u}_R\,\gamma^\mu\,e_R\,\tilde{U}_{1\mu}
$$

LQ		Q	T_3	Spin	$\lambda_L(lq)$	$\lambda_R(lq)$	$\lambda_L(\nu q)$
R_2	R_2^b	5/3	1/2	0	h_{2L}	h_{2R}	0
	R_2^a	2/3	$-1/2$	0	0	$-h_{2R}$	h_{2L}
$\tilde{R}_2$	$\tilde{R}_2^b$	2/3	1/2	0	$\tilde{h}_{2L}$	0	0
	$\tilde{R}_2^a$	$-1/3$	$-1/2$	0	0	0	$\tilde{h}_{2L}$
$U_{1\mu}$	$U_{1\mu}$	2/3	0	1	h_{1L}	h_{1R}	h_{1L}
$\tilde{U}_{1\mu}$	$\tilde{U}_{1\mu}$	5/3	0	1	0	$\tilde{h}_{1R}$	0
$U_{3\mu}$	$U_{3\mu}^+$	5/3	1	1	$\sqrt{2}\,h_{3L}$	0	0
	$U_{3\mu}^0$	2/3	0	1	$-h_{3L}$	0	h_{3L}
	$U_{3\mu}^-$	$-1/3$	-1	1	0	0	$\sqrt{2}\,h_{3L}$

Table 1.8: Coupling strengths of possible interactions allowed by LQ lagrangian for scalar & vector LQ corresponding to |F|=0.

$$+ \quad \left[h_{1L}\,\bar{q}_L\,\gamma^\mu\,l_L + \,h_{1R}\,\bar{d}_R\,\gamma^\mu\,e_R\right]\,U_{1\mu} + h_{3L}\,\bar{q}_L\,\vec{\tau}\,\gamma^\mu\,l_L\,U_{3\mu} + h.c. \tag{1.30}$$

where l_L, q_L are the LH lepton and quark doublets under $SU(2)_L$, *i.e.* $l_L = (\nu_L, e_L)$ and $q_L = (u_L, d_L)$ and e_R, d_R, u_R are the RH charged leptons, down- and up-quark singlets respectively. The scalar (*i.e.* S_1, $\tilde{S}_1$, S_3) and vector (*i.e.* V_2, $\tilde{V}_2$) LQ carry fermion number F=3B+L=-2, while the scalar (*i.e.* R_2, $\tilde{R}_2$) and vector (*i.e.* U_1, $\tilde{U}_1$, U_3) LQ have F=0. Decomposing the two terms corresponding to a fermion number on the right hand side of above equation, into scalar and vector parts, we have the following

$$\mathcal{L}_{|F|=i} \;=\; \mathcal{L}^{\rm Scalar}_{|F|=i} + \mathcal{L}^{\rm Vector}_{|F|=i} \qquad (\mathrm{i} = 2\,,\,0) \text{ with}$$

$$\mathcal{L}^{\rm Scalar}_{|F|=2} \;=\; g_{1L}\,\bar{u}^c_L\,e_L\,S_1 - \,g_{1L}\,\bar{d}^c_L\,\nu_L\,S_1 + \,g_{1R}\,\bar{u}^c_R\,e_R\,S_1 + \,\tilde{g}_{1R}\,\bar{d}^c_R\,e_R\,\tilde{S}_1$$

$$
\begin{aligned}
& - \sqrt{2}\, g_{3L}\, \bar{d}^c_L\, e_L\, S^+_3 + \sqrt{2}\, g_{3L}\, \bar{u}^c_L\, \nu_L\, S^-_3 - g_{3L}\, \bar{u}^c_L\, e_L\, S^0_3 \\
& - g_{3L}\, \bar{d}^c_L\, \nu_L\, S^0_3 + h.c., \\
\mathcal{L}^{\rm Vector}_{|F|=2} &= g_{2L}\, \bar{d}^c_R\, \gamma^\mu\, \nu_L\, V^a_{2\mu} + g_{2L}\, \bar{d}^c_R\, \gamma^\mu\, e_L\, V^b_{2\mu} + g_{2R}\, \bar{u}^c_L\, \gamma^\mu\, e_R\, V^a_{2\mu} \\
& + g_{2R}\, \bar{d}^c_L\, \gamma^\mu\, e_R\, V^b_{2\mu} + \tilde{g}_{2L}\, \bar{u}^c_R\, \gamma^\mu\, \nu_L\, \tilde{V}^a_{2\mu} + \tilde{g}_{2L}\, \bar{u}^c_R\, \gamma^\mu\, e_L\, \tilde{V}^b_{2\mu} + h.c., \\
\\
\mathcal{L}^{\rm Scalar}_{|F|=0} &= h_{2L}\, \bar{u}_R\, \nu_L\, R^a_2 + h_{2L}\, \bar{u}_R\, e_L\, R^b_2 - h_{2R}\, \bar{d}_L\, e_R\, R^a_2 + h_{2R}\, \bar{u}_L\, e_R\, R^b_2 \\
& + \tilde{h}_{2L}\, \bar{d}_R\, \nu_L\, \tilde{R}^a_2 + \tilde{h}_{2L}\, \bar{d}_R\, e_L\, \tilde{R}^b_2 + h.c., \\
\mathcal{L}^{\rm Vector}_{|F|=0} &= h_{1L}\, \bar{u}_L\, \gamma^\mu\, \nu_L\, U_{1\mu} + h_{1L}\, \bar{d}_L\, \gamma^\mu\, e_L\, U_{1\mu} + h_{1R}\, \bar{d}_R\, \gamma^\mu\, e_R\, U_{1\mu} \\
& + \tilde{h}_{1R}\, \bar{u}_R\, \gamma^\mu\, e_R\, \tilde{U}_{1\mu} + \sqrt{2}\, h_{3L}\, \bar{u}_L\, \gamma^\mu\, e_L\, U^+_{3\mu} + \sqrt{2}\, h_{3L}\, \bar{d}_L\, \gamma^\mu\, \nu_L\, U^-_{3\mu} \\
& + h_{3L}\, \bar{u}_L\, \gamma^\mu\, \nu_L\, U^0_{3\mu} - h_{3L}\, \bar{d}_L\, \gamma^\mu\, e_L\, U^0_{3\mu} + h.c.,
\end{aligned}
\tag{1.31}
$$

where $u_{L,R}$, $d_{L,R}$ are the generic LH (or RH) up- and down-type quarks of any generation and $e_{L,R}$, $\nu_{L,R}$ represent the LH (or RH) charged leptons and neutrinos of any generation respectively. The generation indices for both quarks and leptons are *not* explicitly mentioned here. Some LQ carry another index as a superscript, which represents the weak isospin, T_3. The isospin doublet LQ carry the indices *a, b*, where a = -1/2 and b = +1/2, while the triplet LQ carry indices *-, 0, +*, where "-" implies T_3=-1, "+" implies $T_3 = +1$ and "0" implies $T_3 = 0$. In our notation, $u^c_L \equiv (u_L)^c$ stands for anti-up quarks. We tabulate below the various interactions that are possible via LFV LQ. Table 1.7 gives the effective couplings for the LQ carrying fermion number |F|=2 while, Table 1.8 gives the couplings for LQ carrying fermion number |F|=0.

In another notation (called the **Aachen notation**, used in [14]), the LQ lagrangian is written in terms of seven renormalizable B and L conserving quark-lepton-boson couplings consistent with the $\mathrm{SU(3)_c} \bigotimes \mathrm{SU(2)_L} \bigotimes \mathrm{U(1)_Y}$ symmetries of the SM for both scalar and vector LQ, and each coupling carries generation indices for the two fermions (suppressed in the

Our Notation	Aachen Notation
S_1	S_0
$\tilde{S}_1$	$\tilde{S}_0$
$\vec{S}_3$	$\vec{S}_1$
$V_{2\mu}$	$V^{\mu}_{1/2}$
$\tilde{V}_{2\mu}$	$\tilde{V}^{\mu}_{1/2}$
R_2	$S^{\mu}_{1/2}$
$\tilde{R}_2$	$\tilde{S}^{\mu}_{1/2}$
$\tilde{U}_{1\mu}$	$\tilde{V}^{\mu}_{0}$
$U_{1\mu}$	V^{μ}_{0}
$U^{i}_{3\mu}$	$\tilde{V}^{i\mu}_{1}$

Table 1.9: LQ in our notation and the Aachen notation.

equation below). The scalar and vector interaction Lagrangians are therefore,

$$\begin{aligned}
\mathcal{L}_S &= \Big\{ \left(\lambda_{LS_0} \bar{q}^c_L i\tau_2 l_L + \lambda_{RS_0} \bar{u}^c_R e_R\right) S^{\dagger}_0 + \left(\lambda_{R\tilde{S}_0} \bar{d}^c_R e_R\right) \tilde{S}^{\dagger}_0 \\
&+ \left(\lambda_{LS_{1/2}} \bar{u}_R l_L + \lambda_{RS_{1/2}} \bar{q}_L i\tau_2 e_R\right) S^{\dagger}_{1/2} + \left(\lambda_{L\tilde{S}_{1/2}} \bar{d}_R l_L\right) \tilde{S}^{\dagger}_{1/2} \\
&+ \left(\lambda_{LS_1} \bar{q}^c_L i\tau_2 \tau^i l_L\right) S^i_1 \Big\} + h.c., \\
\\
\mathcal{L}_V &= \Big\{ \left(\lambda_{LV_0} \bar{q}_L \gamma_\mu l_L + \lambda_{RV_0} \bar{d}_R \gamma_\mu e_R\right) V^{\dagger\mu}_0 + \left(\lambda_{R\tilde{V}_0} \bar{u}_R \gamma_\mu e_R\right) \tilde{V}^{\mu\dagger}_0 \\
&+ \left(\lambda_{LV_{1/2}} \bar{d}^c_R \gamma_\mu l_L + \lambda_{RV_{1/2}} \bar{q}^c_L \gamma_\mu e_R\right) V^{\mu\dagger}_{1/2} + \left(\lambda_{L\tilde{V}_{1/2}} \bar{u}^c_R \gamma_\mu l_L\right) \tilde{V}^{\mu\dagger}_{1/2} \\
&+ \left(\lambda_{LV_1} \bar{q}_L \gamma_\mu \tau^i l_L\right) V^{\mu i\dagger}_1 \Big\} + h.c.,
\end{aligned} \tag{1.32}$$

where $\mathcal{L}_S$ and $\mathcal{L}_V$ contain the interactions with the scalar ($S_0,\ \tilde{S}_0,\ S_{1/2},\ \tilde{S}_{1/2}\ S^i_1$) and vectorial ($V^{\mu}_0,\ \tilde{V}^{\mu}_0,\ V^{\mu}_{1/2},\ \tilde{V}^{\mu}_{1/2},\ V^{i\mu}_1$) LQ fields, respectively. The subscript $(0, 1/2, 1)$ in each scalar

Our Notation	Aachen Notation
g_{1L}	λ_{LS_0}
g_{1R}	λ_{RS_0}
$\tilde{g}_{1R}$	$\lambda_{R\tilde{S}_0}$
g_{3L}	λ_{LS_1}
g_{2L}	$\lambda_{LV_{1/2}}$
g_{2R}	$\lambda_{RV_{1/2}}$
$\tilde{g}_{2L}$	$\lambda_{L\tilde{V}_{1/2}}$
h_{2L}	$\lambda_{LS_{1/2}}$
h_{2R}	$\lambda_{RS_{1/2}}$
$\tilde{h}_{2L}$	$\lambda_{L\tilde{S}_{1/2}}$
$\tilde{h}_{1R}$	$\lambda_{R\tilde{V}_0}$
h_{1L}	λ_{LV_0}
h_{1R}	λ_{RV_0}
h_{3L}	λ_{LV_1}

Table 1.10: LQ couplings in our notation and the Aachen notation.

and vectorial LQ indicates the *singlet*, *doublet*, and *triplet* $SU(2)_L$ representation, respectively, whereas the τ^is are the Pauli matrices. The quark fields $q^c_{L,R}$ are the corresponding conjugate of the $q_{L,R}$ fields respectively, where $q^c_{L,R} \equiv (P_{L,R}q)^c$. The L/R index reflects the lepton chirality. Here also the generation (flavor) and color indices in the fields appearing in equation 1.32 are omitted. The generation indices are usually mentioned as superscripts and the lepton family index comes first: λ^{ij} couples a LQ to an ith generation lepton and a jth generation quark. The relation between the two notations can be obtained by equating the interaction terms in the equation 1.31 and equation 1.32. The correspondence between various LQ and coupling constants is given in Table 1.9 and Table 1.10 respectively. In our entire analysis, we shall use

the former notation.

The main direct experimental searches for LQ investigate their production in the s-channel [13, 15], these searches are carried out at the e–p collider HERA at DESY [13, 16]. On the other hand, the indirect searches of LQ consist mainly in analyzing the anomalous effects induced by the LQ interactions in the DIS as well as in the low energy processes [14, 17]. Recently there has been a renewed interest in the subject [18] due to the high Q^2 anomalous events observed in the H1 [19] and ZEUS [20] experiments at HERA, although subsequent analyses of new data have shown a less significant discrepancy with the SM predictions [21].

1.3 Using the Neutrino Sector to learn about beyond the Standard Model

The study of neutrino properties is one of the most important probes of possible physics beyond the SM. Searching for the effects of neutrino mass and flavor mixing, the determination of the Dirac or Majorana character of neutrinos, searching for the neutrino magnetic moment, and accurate measurement of neutrino-nuclear cross sections all have a potentially significant impact on particle physics, astrophysics, and cosmology.

1.3.1 Present Status and Future Neutrino Experiments

First let us briefly review the present situation of the neutrino experiments. Results from atmospheric neutrino experiments [22–25], corraborated by the accelerator beam based K2K experiment [26] have provided firm evidence for $\nu_\mu \to \nu_\tau$ oscillations with maximal (or almost maximal) mixing. To this body of evidence have been added the solar neutrino results [27–33], which when combined with the results of the reactor based KamLAND experiment [34] have established the LMA-MSW solution [35] as the most favoured explanation for the solar neutrino deficit. As a result there has been a shift in the nature of goals in the neutrino sector.

The shift has been from a search for understanding the particle physics and/or the astrophysics driving the solar and atmospheric neutrino deficits to one where we seek to make increasingly precise measurements of neutrino mass and mixing matrix parameters.

Experiments planned to yield results over the next one or two decades thus reflect this change of emphasis. Almost all of the planned projects are long baseline (LBL)[2] endeavours using either

- a conventional proton beam colliding with a target to produce pions which then decay to give muon neutrinos, or
- superbeams, which are essentially technologically upgraded versions of present conventional beams,
- reactor sources with both near and far detectors for reduced systematic errors, and finally
- neutrino factory beams.

1.3.2 Future Neutrino Experiments Focus on Long Baselines and Neutrino Factories

Conventional neutrino beams are produced from a beam of charged pions decaying in a long ($\approx$ several hundred meters) decay channel. If positive (negative) pions are selected, the result is an almost pure $\nu_\mu(\bar{\nu}_\mu)$ beam from $\pi^+ \to \mu^+\nu_\mu(\pi^- \to \mu^-\bar{\nu}_\mu)$ decays, with a small $\mathcal{O}(1\%)$ component of ν_e from the three body decays of kaons.

The idea of superbeams was introducted by B. Richter. Superbeam experiments utilise the same basic principle used in conventional beam experiments mentioned above, but incorporate substantial technological improvements. This includes higher power beams and the idea of an

[2]By "long baseline" we actually mean the L/E range of about 50-500 km/GeV. For accelerator experiments, this translates to baselines conventionally termed "long", but for the lower reactor neutrino energies, the baselines are actually 1-2 km.

"off-axis" location for the detector. One of the planned projects is the 295 km Japanese J-PARC project [36], with Super-K (22.5 kT) as the detector and $< E_\nu > \simeq 0.76$ GeV. Similarly, NuMI [37] is planned for location in the US, with a 712 km (or possibly somewhat higher) baseline terminating in a 50 kT calorimeter and $< E_\nu > \simeq 2.2$ GeV. Both experiments primarily aim at heightened sensitivity to $\sin^2 \theta_{13}$ via the electron appearance channel. It is anticipated that the upper bound on this parameter will be improved by a factor of four over a five year running period.

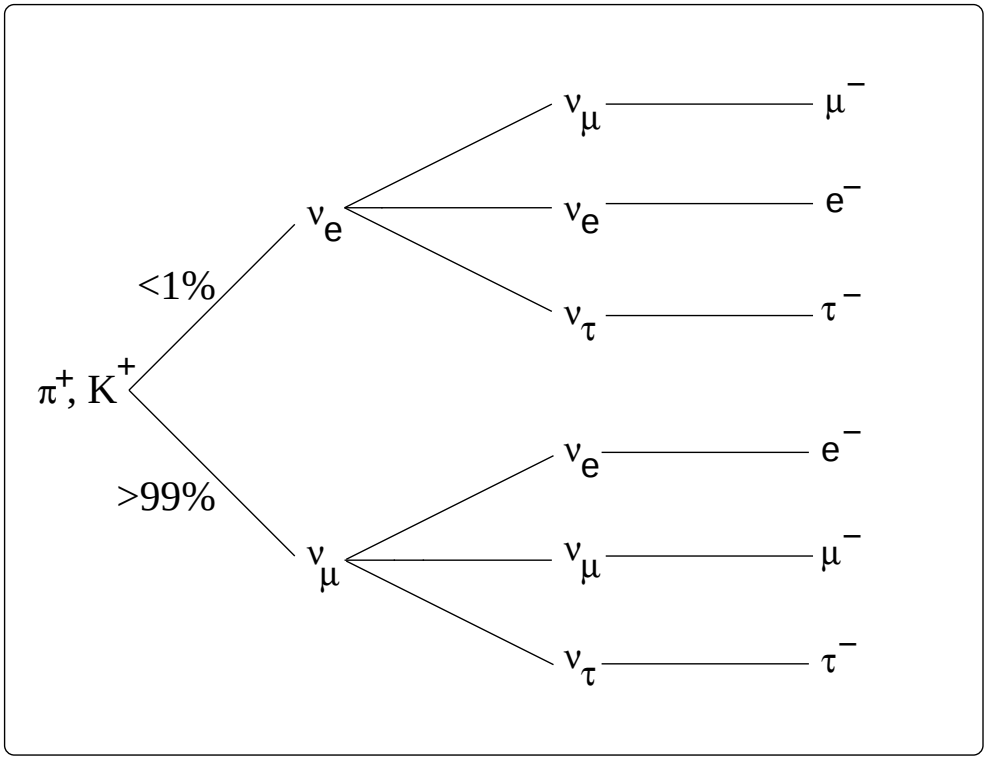

Figure 1.6: *Neutrino production, oscillation and detection via CC interactions for a superbeam set-up.*

Superbeam experiments, despite the fact that the neutrino beams produced are with high intensity are inadequate for $\nu_e \to \nu_X$ measurements (see Figure 1.6) since they are based on the same idea as conventional beams where the ν_e component is not large enough to be useful.

Conventional neutrino beams and superbeams are almost pure ν_μ beams, which therefore permit the study of $\nu_\mu \to \nu_e$ oscillations. The experiments must look for ν_e CC interactions in a distant detector. Backgrounds that fake ν_e CC interactions, together with a small ν_e component in the initial beam, account for $\mathcal{O}(1\%)$ of the total interaction rate. This makes it difficult for experiments using conventional beams to probe very small oscillation amplitudes, below the 0.01 - 0.001 range. This limitation motivates new types of neutrino facilities that provide ν_e beams, permitting the search for $\nu_e \to \nu_\mu$ oscillations, and if the beam energy is above the ν_τ CC interaction threshold, the search for $\nu_e \to \nu_\tau$ oscillations.

Hence, if we want both ν_e and $\bar{\nu}_e$ beams we will need a different sort of neutrino source. An obvious way to try to get ν_e and $\bar{\nu}_e$ beams is to exploit the decays :

$$\mu^- \to e^- \nu_\mu \bar{\nu}_e \qquad \text{or} \qquad \mu^+ \to e^+ \bar{\nu}_\mu \nu_e \tag{1.33}$$

This is the concept of a NF. To create a neutrino beam with sufficient intensity will require a very intense muon source. The decay of the muons and the relevant oscillation channels are shown in Figure 1.7.

The concept of a neutrino source based on a pion storage ring was originally considered by Koshkarev [38] in 1974. However the intensity of the muons created within the ring from pion decays was too low[3] to provide a useful neutrino source. The muon collider concept provided a way to produce a very intense muon source. To create a sufficiently intense muon source, a NF requires an intense multi-GeV proton source capable of producing a primary proton beam with a beam power of 1 MW or more on target. This is just the proton source required in medium term for neutrino superbeams. Hence, there is a natural evolution from superbeam experiments to NF experiments.

New accelerator technologies offer the possibility of building, within the next two decades, an accelerator complex that can produce and capture more than 10^{20} muons per year. In a NF, it has been proposed that muons from this intense source can be accelerated to energies

[3]The intensity of neutrino beam resulting from captured muon beam is a factor of 1000 less than that obtained with modern NF scheme.

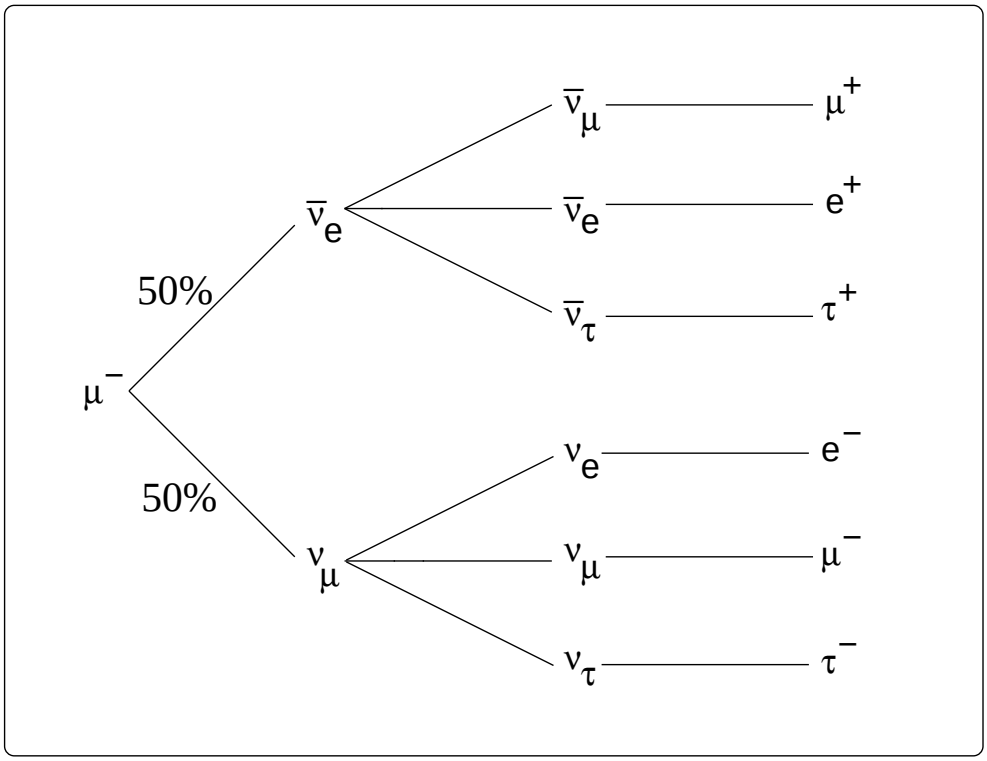

Figure 1.7: *Neutrino production, oscillation and detection via CC interactions for a NF for one polarity.*

of several GeV and then injected into a storage ring having long straight sections[4], where the muons decay to give rise to intense neutrino beams. The concept of a NF [39–41] therefore is to create a millimole/year muon source, rapidly accelerate the muons to the desired storage ring energy, and inject them into a storage ring wih long straight section that points in desired direction.

The design of NF is being pursued in the USA [42], at CERN [43], and in Japan [44]. The key advantages of the NF beams (over conventional beams) are :

[4]Muon lifetime is 100 times longer than charged pions, so inorder to ensure that a large fraction of muons decay in a channel we need to have a storage ring with long straight sections. Since the decay fraction must be large we cannot use a linear muon decay channel as it is practically not feasible.

- ν_e **and** $\bar{\nu}_e$ **beams**, as well as ν_μ and $\bar{\nu}_\mu$ beams!

- **No contamination :** The decay of μ^- gives ν_μ and $\bar{\nu}_e$. Thus, we get neutrino and anti-neutrino beams of different flavours. One can look for appearance modes, $\nu_\mu \rightarrow \nu_e, \nu_\tau$ and $\bar{\nu}_e \rightarrow \bar{\nu}_\mu, \bar{\nu}_\tau$.

- **High event rates.** With 2×10^{20} muon decays per year in the beam-forming straight section of a 50 GeV neutrino factory the ν_μ event rates in a distant detector would be about a factor of 60 higher than the corresponding rates for the next generation of conventional beams (NuMI at FNAL for example). These neutrino factory rates would yield tens of thousands of events per year within a reasonable sized detector on the other side of the Earth (L $\sim$ 10000 km). In addition a near detector a few hundred meters from the end of beam-forming striaght section of a 50 GeV neutrino factory would measure of the order of a million events per year per kg ! This facilitates search for non-oscillation physics scenarios.

- **Narrow** ν **and** $\bar{\nu}$ **energy spectra :** The beam neutrino factory is essentially 'narrow band' as they have much narrower energy spectrum while those from conventional sources are 'wide band' beams.

- **Low systematic uncertainities :** The systematic uncertainties on the flux and spectrum of neutrinos at a distant experiment are expected to be significantly lower than for a conventional beam since muon decay spectrum is well known. This would improve the ultimate precision of ν_μ disappearance measurements.

- **Polarization :** The ν_e component in the beam can be controlled by changing the polarisation of the muons in the storage ring.

- **Compactness :** By injecting the muons in a storage ring with long straight sections, the muon storage ring is compact. Thus, it is possible to tilt it downwards at a large angle so

that the neutrino beam can pass through Earth and very LBL experiments ($L \sim \mathcal{O}(10^4)$ Km) can be imagined.

Now let us discuss the properties of neutrino beams produced at a NF. Consider an ensemble of polarized negatively-charged muons. When the muons decay they produce muon neutrinos with a distribution of energies and angles in the muon rest–frame described by [45]:

$$\frac{d^2N_{\nu_\mu}}{dxd\Omega_{cm}} \propto \frac{2x^2}{4\pi}\left[(3-2x)+(1-2x)P_\mu\cos\theta_{cm}\right], \tag{1.34}$$

where $x \equiv 2E_\nu/m_\mu$, θ_{cm} is the angle between the neutrino momentum vector and the muon spin direction, and P_μ is the average muon polarization along the beam direction. The electron antineutrino distribution is given by:

$$\frac{d^2N_{\bar{\nu}_e}}{dxd\Omega_{cm}} \propto \frac{12x^2}{4\pi}\left[(1-x)+(1-x)P_\mu\cos\theta_{cm}\right], \tag{1.35}$$

and the corresponding distributions for $\bar{\nu}_\mu$ and ν_e from μ^+ decay are obtained by the replacement $P_\mu \to -P_\mu$. Only neutrinos and antineutrinos emitted in the forward direction ($\cos\theta_{lab} \simeq 1$) are relevant to the neutrino flux for long-baseline experiments; in this limit $E_\nu = xE_{max}$ and at high energies the maximum E_ν in the laboratory frame is given by $E_{max} = \gamma(1+\beta\cos\theta_{cm})m_\mu/2$, where β and γ are the usual relativistic factors. The ν_μ and $\overline{\nu}_e$ distributions as a function of the laboratory frame variables are then given by:

$$\frac{d^2N_{\nu_\mu}}{dxd\Omega_{lab}} \propto \frac{1}{\gamma^2(1-\beta\cos\theta_{lab})^2}\frac{2x^2}{4\pi}\left[(3-2x)+(1-2x)P_\mu\cos\theta_{cm}\right], \tag{1.36}$$

and

$$\frac{d^2N_{\overline{\nu}_e}}{dxd\Omega_{lab}} \propto \frac{1}{\gamma^2(1-\beta\cos\theta_{lab})^2}\frac{12x^2}{4\pi}\left[(1-x)+(1-x)P_\mu\cos\theta_{cm}\right]. \tag{1.37}$$

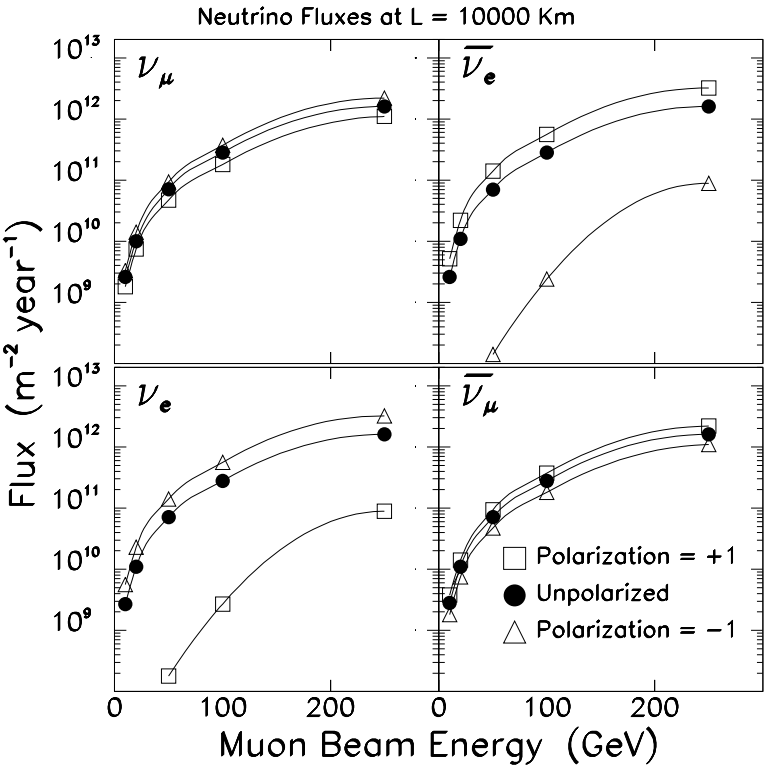

Figure 1.8: *Calculated ν and $\overline{\nu}$ fluxes in the absence of oscillations at a far site located 10000 km from a neutrino factory in which 2×10^{20} muons have decayed in the beam–forming straight section. The fluxes are shown as a function of the energy of the stored muons for negative muons (top two plots) and positive muons (bottom two plots), and for three muon polarizations as indicated. The calculated fluxes are averaged over a circular area of radius 1 km at the far site.*

Thus, for a high energy muon beam with no beam divergence, the neutrino and antineutrino energy and angular distributions depend upon the parent muon energy, the decay angle, and the direction of the muon spin vector. With the muon beam intensities that could be provided by a muon collider type muon source [46] the resulting neutrino fluxes at a distant site would be large. For example, Figure 1.8 shows as a function of muon energy and polarization, the computed fluxes per 2×10^{20} muon decays at a site on the other side of the Earth ($L =$ 10000 km). Note that the ν_e ($\overline{\nu}_e$) fluxes are suppressed when the muons have $P = +1$ (-1). This can be understood by examining equation 1.37 and noting that for $P = -1$ the two terms cancel in the forward direction for all x.

Specifications for the LBL NF detector are rather typical for an accelerator -based neutrino experiment. However, because of the need to maintain a high neutrino rate at these long distances ($\sim$ 3000 Km), the detectors considered here are 3-10 times more massive than those in current neutrino experiments.

For the far-site several detector options can be considered :

- A 50 kT steel-scintillator-proportional-drift-tube(PDT) detector.
- A large water-Cherenkov detector, similar to Super-Kamiokande but with either a magnetized water volume or toroids separating smaller water tanks [47].
- A massive liquid-argon magnetized detector [48]
- A large mass magnetized iron calorimeter, such as one proposed for India-based Neutrino Observatory (INO) [49]

Near-site detectors are crucial from the view point of flux optimization. For the near detector, a compact liquid-argon type time-projection-chamber (TPC) (similar to ICARUS [50]) could be used. An experiment with a relatively thin Pb target (1 L_{rad}), followed by a standard fixed-target spectrometer could also be considered.

1.4 Physics Goals at a Neutrino Factory

In this section we describe the important physics goals that can be addressed at a NF. Broadly speaking we can divide them into 2 classes :

- **Oscillation Physics :** Ultimately, to fully test the three-flavour mixing framework, determine all of the relevant neutrino oscillation parameters, and answer the most important neutrino-oscillation related physics questions, one would like to measure the oscillation probabilities $P(\nu_\alpha \to \nu_\beta)$ as a function of baseline L and neutrino energy E (and hence L/E) for all possible initial and final states. This requires a beam with well-known flavour content, and a detector that can identify the flavour of interacting neutrino. The neutrinos interact in the detector via CC and NC interactions to produce a lepton accompanied by a hadronic shower arising from the remnants of the struck nucleon. In CC interactions, the final-state lepton tags the flavour (β) of the interacting neutrino. To accomplish the ultimate goal, we need ν_e in addition to the ν_μ beams, and detectors that can distinguish between NC, ν_e CC, ν_μ CC and ν_τ CC interactions. The exact neutrino helicity composition of beams produced via muon decay is ideally suited for oscillation measurements. Thus one can easily select the helicities of neutrinos and anti-neutrinos by allowing either μ^- or μ^+ to decay. At a NF, with negative muons stored, the initial beam consists of 50% ν_μ and 50% $\bar{\nu}_e$ and the following transitions can occur (see Figure 1.7),

  - $\nu_\mu \to \nu_\mu$ disappearance
  - $\nu_\mu \to \nu_e$ appearance
  - $\nu_\mu \to \nu_\tau$ appearance
  - $\bar{\nu}_e \to \bar{\nu}_e$ disappearance
  - $\bar{\nu}_e \to \bar{\nu}_\mu$ appearance
  - $\bar{\nu}_e \to \bar{\nu}_\tau$ appearance

An important feature of the NF is the possibility of having opposite muon charges circulating in the ring, therefore allowing also the study of the charge-conjugated processes of those above.

The simultaneous presence of both neutrino flavours in the beam poses the problem of separating the neutrinos due to oscillations from beam background. A simple identification of the lepton produced in CC interactions is not sufficient, since muons, for instance, could come from the ν_μ component of the beam, from the oscillation $\bar{\nu}_e \rightarrow \bar{\nu}_\mu$, or even from the oscillation $\bar{\nu}_e \rightarrow \bar{\nu}_\tau$, followed by the decay $\tau \rightarrow \mu$. The obvious way to distinguish the neutrinos coming from the beam from those coming from oscillations is to measure the charge of lepton produced in CC events. The ideal case would be to measure the charge of both electrons and muons, and perhaps find a way also to identify taus. The last two requirements are quite difficult to match. We consider a case that the detector for NF will be able to identify the charge of muons and taus. If also electron identification can be performed, the detected events can be classified in six classes:

- CC electron or positron (assuming the charge cannot be measured)
- Right-sign muons
- Wrong-sign muons
- Positive tau leptons
- Negative tau leptons
- Events with no leptons

The measurements can be made with negative muons stored in the NF, and with negative muons stored. Thus there are 12 differential spectra that can be simultaneously fit to obtain the oscillation parameters.

- **Non-Oscillation Physics :** The study of utility of intense beams from a muon storage ring in determining the parameters governing non-oscillation physics started in 1997

[51]. An extensive non-oscillation physics program is planned to be carried out at a NF facilty. A high-performance 50 GeV NF can provide $10^6 - 10^7$ neutrino events per kg per year, enabling highly instrumented detectors to obtain data samples of unprecedented magnitude. Experiments that might benefit from these intense beams include

- precise neutrino cross section measurements,
- structure function measurements (with no nuclear corrections), in which individual qurak flavour parton distributions can be extracted,
- precise α_s measurements from non-singlet structure functions,
- studies of nuclear effects (*e.g.* shadowing) separately for valence and se quarks,
- spin structure functions,
- tagged single charm meson and baryon production (a 1 ton detector could yield 10^8 flavour-tagged charm hadrons per year),
- electroweak tests ($\sin\Theta_W$ and $\sigma(\nu - e)$),
- exotic interaction searches,
- neutral heavy lepton searches, and
- searches for anomalous neutrino interactions in EM fields.

Among the non-oscillation physics possibilities, NF offer the possibility of searching for **exotic processes** resulting in **production of** e^-, μ^+, **or** τ**- lepton of either charge**. These searches are also useful to rule out exotic contributions to LBL neutrino oscillation signals (discussed above). One could distinguish between exotic processes and the beginning of a neutrino oscillation by exploiting their differing dependence on energy and distance. Specifically, these exotic processes would probably have a flat or rising dependence on the neutrino energy E. In contrast, a neutrino oscillation would have a $1/E^2$ dependence. Also if the distance L of the experiment changes, the rate of exotic events would decrease with the flux as $1/L^2$. In contrast, the neutrino oscillation probability

would increase as L^2 (for L small compared to the oscillation period), and so the rate of oscillated events would be independent of L.

Current understanding of muon interactions allows for exotic processes in two forms :

- Anomalous lepton production could occur if muons decay to neutrino flavours other than those in the usual decay $\mu \rightarrow e\nu_\mu\bar{\nu}_e$, and the anomalous neutrinos then interact in the target.
- Alternatively, they could be produced if a ν_μ or $\bar{\nu}_e$ interacts with the target via an exotic process.

In order to look for exotic interactions, it is preferable to have a detector at near-site since oscillation effects are negligible at short distances.

1.5 Chapters Layout

The approach here seeks to explore how NF, a tool of the future can be used to explore non-standard interactions in the neutrino sector. In this thesis we consider SUSY and theories with LQ as possible candidates for probing beyond SM physics in the neutrino sector. The layout of various chapters is : In chapter 2 we analyze the R-parity violating SUSY interactions leading to tau and wrong sign muon production at a NF. In chapter 3 we describe interactions arising from LQ interactions that lead to tau and wrong sign muon production at near and short baselines. In chapter 4 we show how LQ can lead to an enhanced production of b($\bar{b}$) at a NF.

Chapter 2

Signals of R-parity Violating Supersymmetry

Neutrino oscillation signals at muon storage rings can be faked by SUSY interactions in an R-parity violating scenario. We investigate the τ-appearance signals for both LBL and near-site experiments, and conclude that the latter is of great use in distinguishing between oscillation and SUSY effects. On the other hand, for a wide and phenomenologically consistent choice of parameters, SUSY can cause a manifold increase in the event rate for wrong-sign muons at a LBL setting, thereby providing us with signatures of new physics. Some of the results presented in this chapter are published in Phys. Rev. **D64,** 015011 (2001).

2.1 Introduction

The increasingly strong empirical indications of neutrino oscillations from the observed solar and atmospheric neutrino deficits [52] have emphasised the need for their independent confirmation in accelerator and reactor experiments. One of the actively discussed possibilities in this connection is a muon storage ring [39–41, 53] which can act as an intense source of collimated neutrinos impinging upon a fixed target. A μ^- (μ^+) beam can thus produce both

ν_μ ($\bar{\nu}_\mu$) and $\bar{\nu}_e$ (ν_e), thereby providing an opportunity to test both ν_e-ν_μ and ν_μ-ν_τ oscillations which are the favoured solutions for the two anomalies mentioned above.

In the simplest extensions of the SM, non-degenerate masses for the different neutrino species (and consequent mixing among them) can account for the oscillation phenomena. Considering, for example, the atmospheric ν_μ deficit, the Super-Kamiokande (SK) results [52] strongly suggest ν_μ-ν_τ oscillation with $\Delta m^2 \simeq 10^{-3} - 10^{-2}\ eV^2$ and $\sin^2 2\theta \simeq 1$. Such oscillation was earlier indicated by the Irving-Michigan-Brookhaven and Kamiokande collaborations, and has been also supported more recently by the SOUDAN-II [54] and MACRO [55] experiments. At a muon storage ring, one therefore expects a certain fraction of the ν_μ's to oscillate into ν_τ, depending on the energy and the baseline length. Interaction of these ν_τ's with the target material will produce τ-leptons, the detection of which may, in the simplest case, be interpreted as additional proof of oscillation [56]. Similarly, the detection of wrong sign muons may be a vindication of the $\bar{\nu}_e$-$\bar{\nu}_\mu$ oscillation hypothesis, thereby providing one with a probe of the parameter spaces corresponding to the vacuum and matter-enhanced oscillation solutions to the solar neutrino puzzle.

However, the predicted rates of τ-appearance or wrong-sign muons in a given experimental setting can be significantly affected by non-standard interactions. In other words, it is possible for non-oscillation physics to intervene and fake oscillation phenomena. Lepton flavour violation (LFV) effects in general can mimic the neutrino oscillation signal. Such issues have been already discussed in some detail in a model-independent way in the references [57]. For example, it is possible for *un-oscillated ν_μ's* to scatter into τ's in an R-parity violating SUSY framework (with $R = (-1)^{(3B+L+2S)}$), by virtue of lepton-number violating trilinear couplings [10]. Also, such couplings can produce $\bar{\nu}_\mu$'s from μ^--decay and thus give rise to μ^+'s in the detector even in the absence of oscillation [11]. It is important to know the effects of such interactions for two reasons:

(i) to look for enhancement in τ and wrong-sign muon event rates and thus to uncover SUSY effects, and

(ii) to see to what extent the signals supposedly coming from oscillation are faked by such new physics.

In this chapter, we show that one can answer both questions by combining LBL experiments with those in which one places the neutrino detectors at a short distance from the storage ring, where the oscillation probability gets suppressed by the baseline length.

In addition, other non-standard options such as left-right symmetric models and theories with extra gauge bosons also can lead to some of the observable consequences discussed here. However, the rather stringent lower bounds (of the order of 500 GeV and above) on the masses of these bosons suppress the contributions. On the other hand, the very relaxation of lepton number conservation in a SUSY scenario introduces several additional couplings in the theory, not all of which can be excluded with a great degree of severity from currently available experimental results. It is some of these new interaction terms, coupled with the possibility of having sfermions in the mass range of 100-300 GeV, that are responsible for the remarkable enhancement of tau-and wrong-sign muon event rates at a NF. Similarly, lepton number violating couplings also occur in the theories with LQ. In R-parity violating SUSY (with λ'-type couplings), squarks behave in much the same way as scalar leptoquarks. Therefore, the results of our analysis on τ appearance are equally applicable to the interactions involving scalar LQ with charge $\pm\frac{1}{3}$. This will be discussed in detail in chapter 3.

While a LBL experiment is of advantage from the viewpoint of oscillation, a detector placed at a near site has also been considered in recent studies [40, 58]. Its merit lies in having a large event rate even when its dimensions are small. In reference [40], for example, τ detection has been investigated in the context of a detector consisting of an array of tungsten sheets with silicon tracking. Such a detector will be helpful in isolating new τ-producing interactions which can be potential contaminants of the oscillation signature.

2.2 Neutrino Oscillations

Let us first consider τ-appearance through oscillation. For a muon-neutrino with energy E_ν (in GeV) traversing a distance L (in Km), the probability of oscillation into a tau-neutrino is given by

$$\mathcal{P}_{\nu_{\mu,e}\to\nu_\tau} = \sin^2 2\theta \ \sin^2\left[1.27\,\Delta m^2\,\frac{L}{E_\nu}\right] \tag{2.1}$$

where Δm^2 is the mass-squared difference between the corresponding physical states in eV^2, and θ, the mixing angle between flavours. For a baseline length of, say, 700 Km, and a muon beam of energy 50 GeV, this probability corresponding to the solution space for the atmospheric SK data lies in the range $10^{-3} - 10^{-2}$, and is smaller for shorter baselines. In order to obtain the τ-event rate one has to fold the CC cross-section with this probability as well as the ν_μ energy distribution, and finally use the effective luminosity appropriate for the cone subtended by the detector, which depends on the area and baseline length.

2.3 R-parity Violating Supersymmetric Interactions

The presence of scalars carrying lepton (L) or baryon (B) number in a SUSY scenario makes it possible to have *one* of the above quantum numbers broken while the other is conserved. One can thus avoid undesirable consequences like fast proton decay, and can still be consistent with all other symmetries when R-parity is violated. In such a scenario with broken lepton number, the corresponding part of the superpotential is given (suppressing colour and $SU(2)$ indices) by [11],

$$W_{\not L} = \epsilon_i \hat{L}_i \hat{H}_2 + \lambda_{ijk}\hat{L}_i\hat{L}_j\hat{E}^c_k + \lambda'_{ijk}\hat{L}_i\hat{Q}_j\hat{D}^c_k \tag{2.2}$$

where i, j and k are generation indices, $\hat{L}$ and $\hat{Q}$ represent the SU(2) doublet lepton and quark superfields, and $\hat{E}$, $\hat{U}$ and $\hat{D}$ denote the right-handed charged lepton, up-type quark and down-

type quark superfields respectively. In terms of the component fields (with the sfermion fields characterised by the tilde sign), the trilinear terms above lead to interactions of the form

$$\begin{aligned}\mathcal{L} &= \lambda'_{ijk}\,[\,\tilde{d}^j_L\,\bar{d}^k_R\nu^i_L + (\tilde{d}^k_R)^*(\bar{\nu}^i_L)^c d^j_L + \tilde{\nu}^i_L\bar{d}^k_R d^j_L \\ &\qquad - \tilde{e}^i_L\bar{d}^k_R u^j_L - \tilde{u}^j_L\,\bar{d}^k_R e^i_L - (\tilde{d}^k_R)^*(\bar{e}^i_L)^c u^j_L] + h.c. \\ &\quad +\lambda_{ijk}\,[\,\tilde{e}^j_L\,\bar{e}^k_R\nu^i_L + (\tilde{e}^k_R)^*(\bar{\nu}^i_L)^c e^j_L + \tilde{\nu}^i_L\bar{e}^k_R e^j_L - (i\leftrightarrow j)] + h.c \end{aligned} \tag{2.3}$$

It should be noted that these interaction terms violate both lepton flavour and lepton number. By suitable combinations of two such terms, it is possible to achieve contributions to processes which conserve lepton number but involve transition between different generations. The implications of such interactions have been investigated earlier in the contexts of solar [59] and ultra-high energy neutrinos [60]. At a NF, they can affect the τ or wrong sign μ event rates in the following ways:

1. λ'-type interactions give rise to a τ starting from a ν_μ which is produced via standard muon decay.

2. λ-type interactions produce a $\bar{\nu}_\mu$ from muon decay, which subsequently has standard charged-current interaction with the target, leading to a wrong-sign muon.

3. A ν_τ can be produced as a result of λ-type interactions in muon decay, which produces a τ through standard interaction.

4. The $\bar{\nu}_e$ from μ^- decay may scatter into a μ^+ via λ'-type interactions with the target.

Here we present results for cases 1 and 2 above. The Feynman diagrams for these two cases are shown in Figure 2.1, where we have chosen those λ'-and λ-interactions which make $\tilde{b}$ and $\tilde{\tau}$ the mediators in the corresponding diagrams. Predictions for cases 3 and 4 are qualitatively similar to those for 1 and 2 respectively.

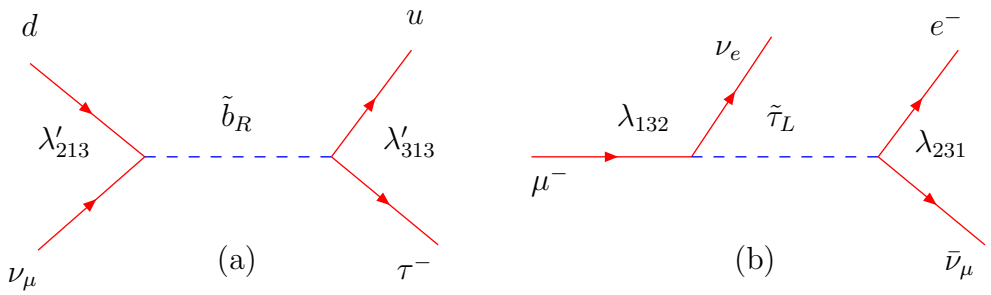

Figure 2.1: *Feynman diagrams for processes producing (a) a τ or (b) a wrong sign muon in R-parity violating SUSY.*

The SM CC cross-section for $\nu_\tau N \longrightarrow \tau^- X$ can be found, for example, in references [40, 56]. In R-parity violating SUSY, a ν_μ can give rise to the same final state through the couplings λ'_{213} and λ'_{313} when the tree-level process is mediated by a b-squark. From considerations of phase-space availability as well as parton densities in a nucleon, the most favourable τ-producing processes at the quark level are $\nu_\mu d \longrightarrow \tau^- u$ and $\nu_\mu \bar{u} \longrightarrow \tau^- \bar{d}$. On performing Fierz transformations (see Appendix A) on the SUSY amplitudes for these processes, one obtains

$$\begin{aligned} \mathcal{M}_{SUSY}(\nu_\mu\, d \longrightarrow \tau^-\, u) &= \frac{\lambda'_{213}\lambda'_{313}}{2(\hat{s} - m^2_{\tilde{b}_R})} \left[\bar{u}_\tau \gamma_\mu P_L u_{\nu_\mu}\right] \left[\bar{u}_u \gamma^\mu P_L u_d\right] \\ \mathcal{M}_{SUSY}(\nu_\mu\, \bar{u} \longrightarrow \tau^-\, \bar{d}) &= \frac{\lambda'_{213}\lambda'_{313}}{2(\hat{t} - m^2_{\tilde{b}_R})} \left[\bar{u}_\tau \gamma_\mu P_L u_{\nu_\mu}\right] \left[\bar{v}_u \gamma^\mu P_L v_d\right] \end{aligned} \tag{2.4}$$

where $m_{\tilde{b}}$ is the b-squark mass. Left-right mixing in the squark sector has been neglected here. No consequence of the phases of the λ'-type couplings has been considered. It should be noted that the $(\nu_\mu \leftrightarrow \nu_\tau)$ oscillation amplitude (arising from neutrino mass splitting) is purely imaginary in a two level analysis [61]. Hence, there is no interference between the oscillation and R-parity violating amplitudes as long as the product of two λ' couplings is real. We have worked under such an assumption here.

There are phenomenological bounds on the L-violating couplings [62]; however, most of

these bounds are derived on the assumption that only a single coupling at a time is non-zero (we call them the 'stand-alone' bounds). Thus, although there are individual limits on λ'_{213} and λ'_{313}, obtained from the universality of charged-current decays of π^- and τ [62], such limits are not necessarily applicable in the most general case. At any rate, no conclusive limit has been obtained for the product $(\lambda'_{213}\ \lambda'_{313})$. Hence this product can be treated as a *free parameter when it comes to looking for experimental signals*. We have also checked that the values of the *effective LFV coupling* used here do not contradict any limits on such couplings available in the literature.

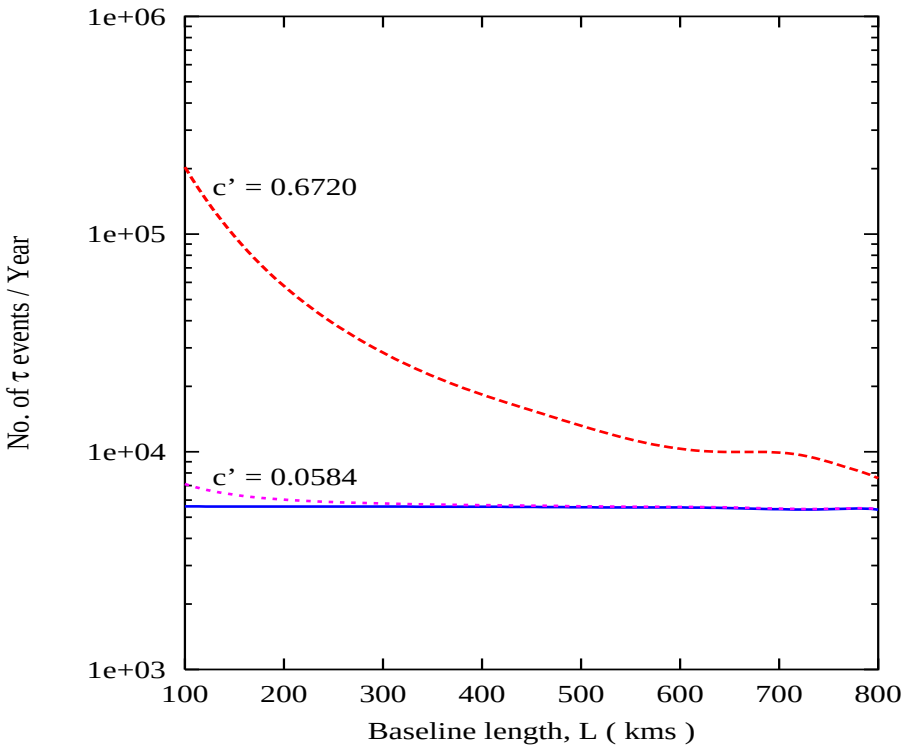

Figure 2.2: *The τ-event rate as a function of the baseline length (L) for $E_\mu = 50$ GeV. The solid line corresponds to the contribution from $\nu_\mu - \nu_\tau$ oscillation, using SK parameters (see text). The two dashed lines refer to cases where the SUSY contributions are included, taking different values of c' $(\equiv \lambda'_{213}\lambda'_{313})$.*

In Figure 2.2 we show the event rates for tau production for long-baseline experiments, as functions of the baseline length, for a 50 GeV muon beam. When calculating the total τ appearance rate, we add the R-parity violating contribution with the SM contribution (from $\nu_\tau\ N \to \tau^-\ X$) after folding the latter with oscillation probability. The results presented here correspond to a sample detector of mass 10 kT, with a circular cross-section of 100 m^2. Such a specification is similar to that of the ICANOE experiment [63]. A muon source producing 10^{20} muons per year has been assumed. The expected event rates for both standard CC and SUSY contributions added to them are displayed. We have used CTEQ4LQ [9] parton distributions to calculate the event rates. The SM contribution to the τ-production rates has been calculated assuming an oscillation probability corresponding to $\Delta m^2_{23} \simeq 5.0 \times 10^{-3}\ eV^2$ and $\sin^2\theta_{23} = 1$, which is within solution space for the atmospheric ν_μ deficit. An average τ-detection efficiency of 30% [40, 63] has been used here. Different values of the products of the R-violating couplings have been used, with a bottom-squark mass of 300 GeV, which is consistent with current experimental limits. The lower one of these corresponds to the product of the stand-alone bounds of the individual couplings; we also display the results with a value of c' which is 10 times greater, and is close to the product of the perturbative limits of the individual couplings. As can be seen from the figure, for baselines of length $\geq$ 200 km, R-parity violating effects make a serious difference only when the couplings are close to their perturbative limits, while for shorter baselines ($\simeq$ 100 km), they can be competitive even with values on the order of the stand-alone bounds.

However, new physics effects are quite clearly separated when one comes to a near-site detector setting. Here the SM contribution is suppressed due to the paucity of τ's produced in oscillation. In Figure 2.3 we show some plots of τ-event rates with a 1 kT, 2500 cm^2 detector placed at a distance of 40 m from the storage ring [40]. The two sets of values for the product of the λ'-type couplings already used in the previous figure are also used here; in addition, we show the predictions for two considerably smaller values of this product. One notices a substantial enhancement in the number of τ-events (calculated again with an assumed average

detection efficiency of 30%) to a level considerably higher than what the SM predicts. This is the case even when the relevant coupling strengths are much smaller than the limits given in reference [64]. Combining Figure 2.2 and Figure 2.3, the conclusion, therefore, is that *even when the couplings are well within the bounds for the stand-alone situation*, near-site effects arising from them lead to overwhelmingly large τ-production, while for LBL experiments, contamination of the oscillation signals through R-violating interactions is appreciable when one goes beyond the limits derived on the assumption that only one coupling is non-vanishing at a time.

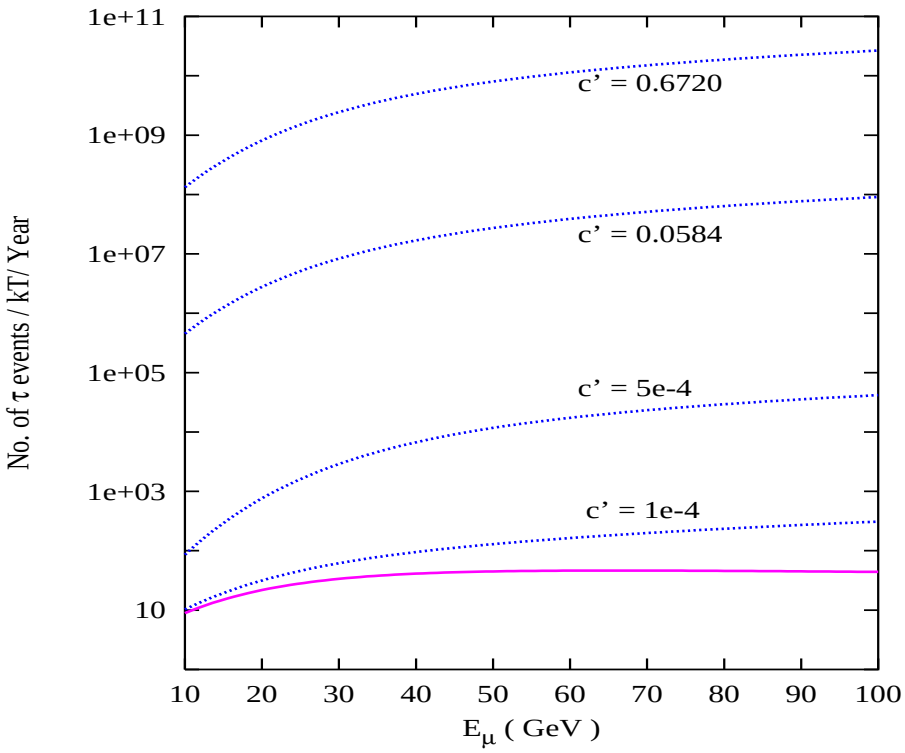

Figure 2.3: *The τ-event rate as function of the muon beam energy for a near-site detector. The solid line shows the oscillation contribution, while the SUSY contributions are included to the dashed lines, using different values of c' ($\equiv \lambda'_{213}\lambda'_{313}$).*

Similarly, a ν_τ can also be produced in the decay of the μ^- via diagrams of the kind shown

in Figure 2.1. It can consequently produce a τ at the detector even without oscillation. In such a case, the event rates are suppressed by the branching ratio of the R-parity violating decay, to an extent depending on the product of the corresponding λ-couplings. The predictions are similar to the ones discussed above.

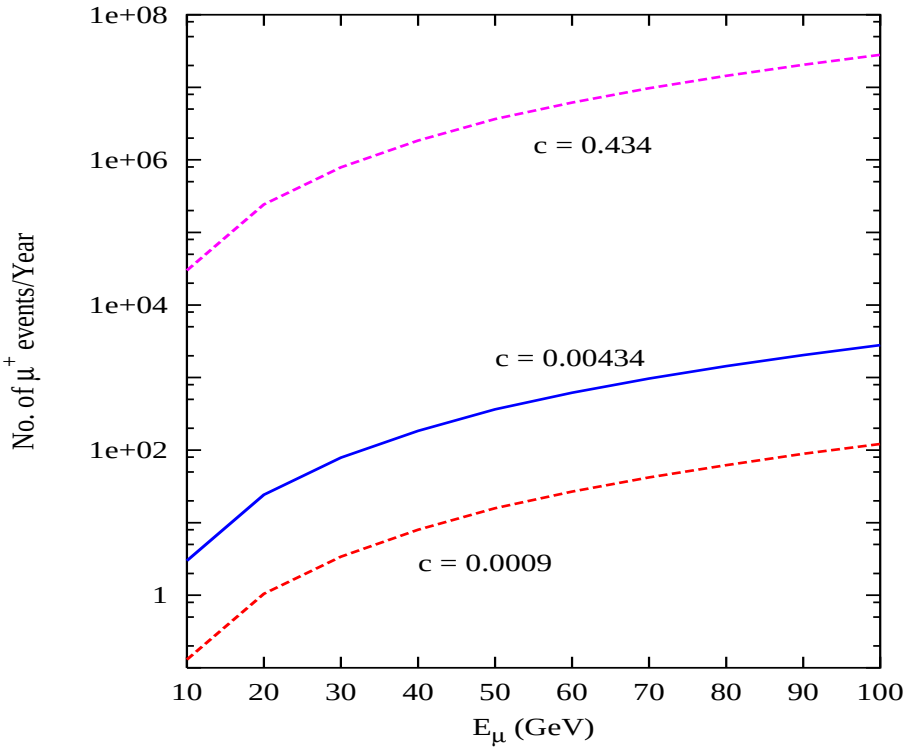

Figure 2.4: *The event rates for wrong-sign muons as functions of muon energy, for a baseline length of 250 km and a 10 kT detector of area 100 m^2. Different values of c ($\equiv \lambda_{231}\lambda_{132}$) have been used, with $m_{\tilde{\tau}} = 100$ GeV*

Next, we consider wrong-sign muons produced due to R-parity violating effects in *muon decays*. The Mikhyev-Smirnov-Wolfenstein (MSW) solution to the solar neutrino problem with matter-enhanced ν_e-ν_μ oscillation requires a mass-splitting of $\simeq 10^{-5}\ eV^2$ between the mass eigenstates [65]. It has been found earlier [56] that with a muon beam energy of upto 50 GeV, and with standard charged current interactions, one can hardly expect to see any events given this kind of mass-splitting, for any realistic baseline length. The situation is even worse

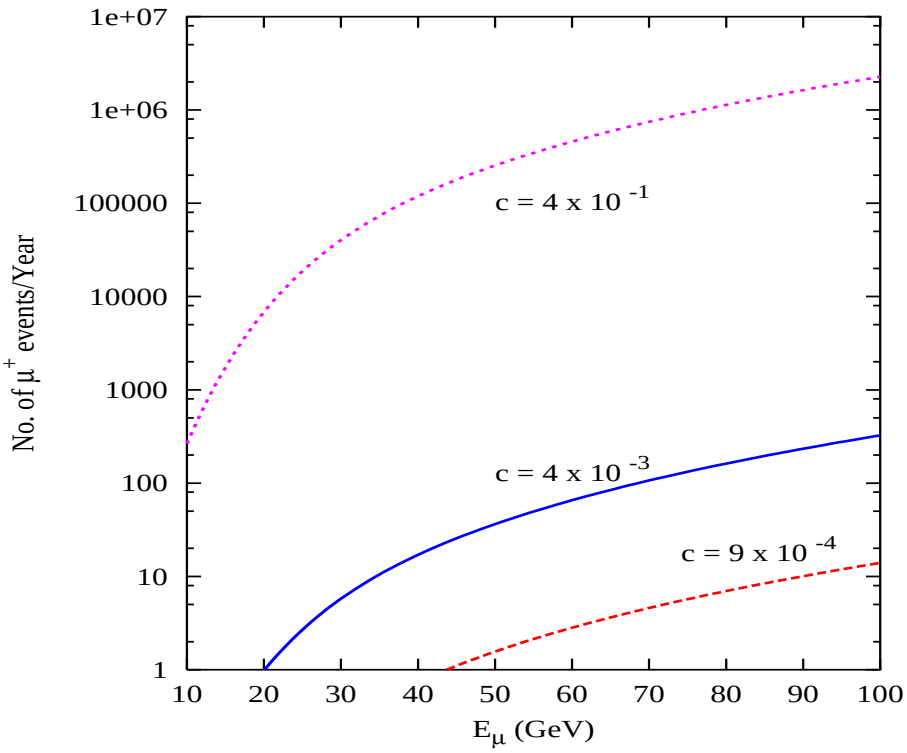

Figure 2.5: *The event rates for wrong-sign muons as functions of muon energy, for a baseline length of 732 km and a 10 kT detector of area 100 m^2. Different values of c ($\equiv \lambda_{231}\lambda_{132}$) have been used, with $m_{\tilde{\tau}} = 100$ GeV*

for the vacuum oscillation solution which requires $\Delta m^2 \simeq 10^{-10}\ eV^2$. Thus a sizable event rate for wrong-sign muons at a LBL experiment should be interpreted as a signal of some new effect, unless ν_e-ν_μ oscillation is *not* the solution to the solar neutrino puzzle. In the latter situation, however, the predicted wrong-sign muon rates allow one to probe the solution space to, for example, the LSND results [66]. In such a case, it becomes even more important to understand the potential contributions coming from new physics effects such as R-parity violating SUSY. In the discussion below, we have tried to demonstrate our main point by confining ourselves to solar neutrino solution space, and showing the visibility of the events through SUSY interactions.

Equation 2.3 tells us that the ν_μ produced in μ-decays cannot give rise to a μ^+ through R-

parity-violating interactions unless there is substantial left-right mixing in the (D-type) squark sector. On the other hand, diagrams of the kind shown in Figure 2.1(b) can lead to decays like $\mu^- \longrightarrow \nu_e e \bar{\nu}_\mu$. This decay is governed, for example, by the product $\lambda_{231}\lambda_{132}$ when the process is mediated by a stau. The decay amplitude, as obtained from Figure 2.1, is

$$\mathcal{M}_{SUSY}(\mu \longrightarrow \nu_e\, e\, \bar{\nu_\mu}) \;=\; \frac{\lambda_{132}\lambda_{231}}{(s_1 - m^2_{\tilde{\tau}_L})}\,[\bar{u}_{\nu_e} P_R u_\mu]\,[\bar{u}_e P_L u_{\nu_\mu}] \tag{2.5}$$

where $s_1 \;=\; (p_\mu \;-\; p_{\nu_e})^2$

In Figure 2.4 and Figure 2.5 we show the event rates for a typical ICANOE-type detector as functions of the muon beam energy, using different values of the above product. Predictions are made for two different baseline lengths, one corresponding to the K2K proposal (Figure 2.4) and the other, to the Fermilab-SOUDAN or CERN-Gran Sasso LBL experiment. Again, the value 0.004 corresponds to the product of the stand-alone bounds. In addition, two other values, one close to the perturbative limit and the other one considerably smaller, have been used. It may be noted that the only limit on the relevant product c, attempted from the absence of muonium-antimuonium conversion [67], is about 6.3×10^{-3}. Two of the three values of c taken here are consistent with these limits. Substantial event rates are produced even with such values. In addition, a general limit on the parameter, g^s_{RR} [1] denoting the scalar coupling of a muon leading to its decay into a right-handed electron exists in the literature. Such a limit translates to $c < 0.022$, with which a large part of the parameter space covered in the figures is consistent.

Even with conservative choices of the interaction strengths, a clear prediction of ten to several hundred events can be observed for $E_\mu \;\simeq\; 50$ GeV, in the R-parity violating case, while no events are expected so long as the masses and mixing in the ν_μ-ν_ϵ sector offer a solution to the solar deficit. Clearly, a shorter baseline such as the one shown in Figure

[1] The most general scalar interaction leading to the decay of a muon to a right-handed electron can be written as: $\mathcal{L} = \frac{4G_F}{\sqrt{2}}\,\left[g^S_{RR}\,\langle \bar{e}_R|\Gamma^S|(\nu_e)_L\rangle\,\langle(\bar{\nu}_\mu)_L|\Gamma^S|\mu_R\rangle\right]$. The current experimental limit on g^S_{RR} constrains it to be less than 0.066 [73].

2.4 is of greater advantage. Furthermore, a near-site detector should be able to detect a huge abundance of events, although backgrounds caused by muons produced upstream of the detector pose additional problems there. Taking everything into account, we conclude that a far-site detector with modest baseline length like the one studied in Figure 2.4 is probably the optimal answer to questions on possible contributions to wrong-sign muon signals. This statement, however, ceases to be valid if the mass-squared splitting corresponding to ν_e-ν_μ oscillation belongs, for example, to the solution space for the LSND results. A confirmation (or otherwise) of the LSND claim is expected to come from the MiniBooNE experiment. In case of a reaffirmation of such kind of ν_e-ν_μ oscillation, for which substantial wrong-sign muon rates are predicted in LBL experiments, one has to worry about possible faking by SUSY processes discussed here. Under such circumstances, one has to combine the observed data with those obtained from a near-site detector to separate the two types of effects.

2.4 Conclusions

In conclusion, we have investigated the effects of the R-parity violating trilinear couplings on the suggested signals of neutrino oscillations at a muon storage ring. We find that, while the new couplings have to be on the higher side to show a detectable enhancement in the τ-appearance rate with LBL, even tiny R-violating couplings can lead to very large number of τ's at a near-site detector, much in excess of what is expected via oscillation. Near-site experiments can thus be recommended for isolating new physics effects that fake signals of neutrino oscillation. On the other hand, a class of R-violating interactions, with strengths well within their current experimental limits, can be responsible for an enhanced rate of wrong sign muons at a LBL experiment. Since the solution space for the solar neutrino puzzle does not permit such event rates, such muons, if observed at a NF, can therefore be greeted as harbingers of some new physics, of which R-parity violating SUSY is a favoured example.

Chapter 3

Leptoquark Signals in Neutrino Scattering

The accurate prediction of neutrino beam produced in muon decays and the absence of opposite helicity contamination for a particular neutrino flavour makes a future NF based on a MSR, the ideal place to look for the LFV effects. In this chapter, we address the contribution of mediating LFV LQ in $\nu(\bar{\nu}) - \mathrm{N}$ interactions leading to production of τ's and wrong sign μ's at MSR and investigate the region where LQ interactions are significant in the near-site and short baseline experiments. Some of the results presented in this chapter are published in Phys. Lett. **B535,** 219 (2002).

3.1 Introduction

Recent results from Super-Kamiokande and other experiments [52] strongly suggest ν_μ-ν_τ oscillation as the dominant oscillation mode, in order to explain the atmospheric ν_μ deficit. Similarly, the results for solar neutrino problem point towards ν_e-ν_μ oscillation as the favoured solution [65]. In fact, the prime goal of next generation neutrino physics experimental studies (*e.g.* NF based on MSR) is to explore the physics beyond SM to unfold the mystery of the

neutrino mass hierarchy and confirm the nature of neutrino flavour conversion [53]. At MSR with a μ^- (μ^+) beam, roughly $\simeq 10^{20}$ muons are allowed to decay per year giving rise to nearly equal number of ν_μ ($\bar{\nu}_\mu$) and $\bar{\nu}_e$ (ν_e). These ν ($\bar{\nu}$)'s at the detector, may or may not have changed their flavour due to oscillation of neutrino mass eigenstates, which on interaction with matter produce associated charged leptons [56]. However, as mentioned in chapter 1 and chapter 2, there can be effective LFV interactions motivated from new physics which may give rise to charged leptons in the final state as expected through $\nu(\bar{\nu})$-oscillations [68].

In this backdrop, it is worthwhile to study the production of τ and wrong sign μ via LQ as mediators which occur naturally in grand unified theories, tecnicolour models and E_6 inspired superstring theories [69]. There have been numerous phenomenological studies to put constraints on LQ from low energy flavour changing NC processes which are generated by both the scalar and vector LQ interactions, since there is no reason why the quark-lepton couplings with LQ have to be simultaneously diagonal in quark and lepton mass matrices. Direct experimental searches for LQ have also been carried out at the e p collider and bounds obtained [70]. In this work, we compute and analyse the contribution of mediating LFV LQ in $\nu(\bar{\nu})$-N CC interactions.

3.2 Expression for Event Rate

The most general expression for the event rate per kilo Ton (kT) of the target per year for any charged lepton flavour l_k, obtained via CC interaction of ν_j beam[1] produced as a result of oscillation from an initial ν_i beam can be written as :

$$\mathcal{N}_{l_k^-,l_k^+} = \mathcal{N}_n \int \frac{d^2\sigma^{\nu,\bar{\nu}}\left(\nu_j(\bar{\nu}_j)q \longrightarrow l_k^-(l_k^+)q'\right)}{dx\ dy} \left[\frac{dN_{\nu,\bar{\nu}}}{dE_{\nu_i,\bar{\nu}_i}}\right] \mathcal{P}_{osc}(\nu_i(\bar{\nu}_i) \longrightarrow \nu_j(\bar{\nu}_j)) dE_{\nu_i(\bar{\nu}_i)}\ dx\ dy \tag{3.1}$$

[1] $k = j$ for the SM Lepton Flavour Conserving situation

where, $\mathcal{N}_n$ is the number of nucleons present kT of the target material, x and y are the Bjorken scaling variables, q and q' are the quarks in the initial and final states, respectively and $\mathcal{P}_{osc}$ is the oscillation probability. The differential parton level cross-section is given by

$$\frac{d^2\sigma^{\nu,\bar{\nu}}}{dx\ dy} = \left[\frac{|\mathcal{M}(x,y)|^2}{32\pi\hat{s}}\right]\left[2\lambda^{-1/2}(1,0,\frac{m_l^2}{\hat{s}})\right]$$

where , $\hat{s}$ is the parton level CM energy, m_l is the mass of the final-state lepton and

$$\lambda^{1/2}(x,y,z) = x^2+y^2+z^2-2xy-2xz-2yz$$

is the Michael parameter and $\left[\frac{dN_{\nu,\bar{\nu}}}{dE_{\nu_i,\bar{\nu}_i}}\right]$ is the differential ν ($\bar{\nu}$) flux.

For the two flavour oscillation scenario[2], the probability

$$\mathcal{P}_{osc}(\nu_i \rightarrow \nu_j) = \sin^2 2\theta_m\ \sin^2\left[1.27\,\Delta m^2[eV^2]\,\frac{L[km]}{E_\nu[GeV]}\right]$$

where, L is the baseline length, E_ν is the neutrino energy, Δm^2 is the mass-squared difference between the corresponding physical states, and θ_m is mixing angle between flavours. The general characteristics of τ and wrong sign μ production in the oscillation scenario (OS), for example are given by Dutta *et al.* [56].

3.3 Leptoquark Lagrangian

The effective Lagrangian with the most general dimensionless, $SU(3)_c \times SU(2)_L \times U(1)_Y$ invariant couplings of *scalar* and *vector* LQ satisfying baryon (B) and lepton number (L) conservation (suppressing colour, weak isospin and generation (flavour) indices) is given [13] by:

$$\mathcal{L} \;=\; \mathcal{L}_{|F|=2} + \mathcal{L}_{|F|=0} \qquad \text{where}$$

[2]For the present case, it is sufficient to illustrate the main ideas by considering only the two flavour oscillations in vacuum.

$$\begin{aligned}\mathcal{L}_{|F|=2} &= [g_{1L}\,\bar{q}_L^c\,i\,\tau_2\,l_L + g_{1R}\,\bar{u}_R^c\,e_R]\;S_1 + \tilde{g}_{1R}\,\bar{d}_R^c\,e_R\,\tilde{S}_1 + g_{3L}\,\bar{q}_L^c\,i\,\tau_2\,\vec{\tau}\,l_L\,\vec{S}_3 \\ &+ \left[g_{2L}\,\bar{d}_R^c\,\gamma^\mu\,l_L + g_{2R}\,\bar{q}_L^c\;\gamma^\mu\,e_R\right]\;V_{2\mu} + \tilde{g}_{2L}\,\bar{u}_R^c\,\gamma^\mu\,l_L\,\tilde{V}_{2\mu} + h.c., \\ \\ \mathcal{L}_{|F|=0} &= [h_{2L}\,\bar{u}_R\,l_L + h_{2R}\,\bar{q}_L\,i\,\tau_2\,e_R]\;R_2 + \tilde{h}_{2L}\,\bar{d}_R\,l_L\,\tilde{R}_2 + \tilde{h}_{1R}\,\bar{u}_R\,\gamma^\mu\,e_R\,\tilde{U}_{1\mu} \\ &+ \left[h_{1L}\,\bar{q}_L\,\gamma^\mu\,l_L + h_{1R}\,\bar{d}_R\,\gamma^\mu\,e_R\right]\;U_{1\mu} + h_{3L}\,\bar{q}_L\,\vec{\tau}\,\gamma^\mu\,l_L\,U_{3\mu} + h.c. \qquad (3.2)\end{aligned}$$

where q_L, l_L are the LH quarks and lepton doublets and e_R, d_R, u_R are the RH charged leptons, down- and up-quark singlets respectively. The scalar (*i.e.* S_1, $\tilde{S}_1$, S_3) and vector (*i.e.* V_2, $\tilde{V}_2$) LQ carry fermion number F=3B+L= -2, while the scalar (*i.e.* R_2, $\tilde{R}_2$) and vector (*i.e.* U_1, $\tilde{U}_1$, U_3) LQ have F=0. Using this Lagrangian we discuss below the production of τ's and wrong sign μ's along with the standard Mass-Mixing solution of neutrino oscillation case.

3.4 Tau Production

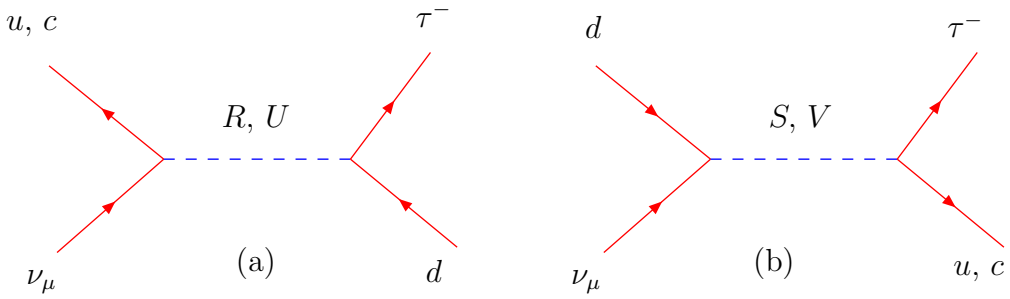

Figure 3.1: *τ^- from scalar & vector LQ: (a) u-channel process corresponding to* |F| *= 0 LQ and (b) s-channel process corresponding to* $|F| = 2$ *LQ.*

We consider the production of τ^- from unoscillated ν_μ (obtained from μ^- decay) through LFV interactions with nucleon via u-channel processes for $|F| = 0$ case (Figure 3.1(a)) and s-channel processes for $|F| = 2$ case (Figure 3.1(b)) LQ unlike OS where τ^- are produced

through ν_τ (oscillated from ν_μ with $\Delta m^2 = 0.0023$ eV^2 and $\sin^2(2\theta_m) = 1.0$) nucleon interaction. There are four processes contributing to τ^- production in the u-channel (Figure 3.1(a)), one mediated by the charge 2/3, scalar LQ (R_2) with $T_3 = -1/2$ and three by the vector LQ ($U_1, U_1, U3$) with $T_3 = 0$ each, where T_3 is the weak isospin. The matrix element squared for all the u-channel processes is

$$\left|\mathcal{M}_{LQ}^{u-chann}(\nu_\mu d \longrightarrow \tau^- u)\right|^2 = \left[\hat{u}(\hat{u} - m_\tau^2)\right]\left[\frac{h_{2L}^2 h_{2R}^2}{(\hat{u} - M_{R_2^a}^2)^2}\right] + \left[4\hat{s}(\hat{s} - m_\tau^2)\right]\left[\frac{h_{1L}^4}{(\hat{u} - M_{U_{1\mu}}^2)^2}\right.$$
$$\left. + \frac{h_{3L}^4}{(\hat{u} - M_{U_{3\mu}^0}^2)^2} - 2\frac{h_{1L}^2 h_{3L}^2}{(\hat{u} - M_{U_{1\mu}}^2)^2(\hat{u} - M_{U_{3\mu}^0}^2)^2}\right] + \left[4\hat{t}(\hat{t} - m_\tau^2)\right]\left[\frac{h_{1L}^2 h_{1R}^2}{(\hat{u} - M_{U_{1\mu}}^2)^2}\right] \tag{3.3}$$

where, the Mandelstam variables at the parton level are given by $\hat{s} = (p_{\nu_\mu} + p_d)^2$, $\hat{t} = (p_{\nu_\mu} - p_{\tau^-})^2$ and $\hat{u} = (p_{\nu_\mu} - p_{u,c})^2$, with p_i denoting the four momemtum of the i^{th} particle. In the s-channel, three processes are mediated by charge -1/3, scalar LQ (S_1, S_1, S_3) with $T_3 = 0$ and fourth by vector LQ (V_2) with $T_3 = -1/2$ (Figure 3.1(b)). The matrix element squared for s-channel processes is

$$\left|\mathcal{M}_{LQ}^{s-chann}(\nu_\mu d \longrightarrow \tau^- u)\right|^2 = \left[\hat{s}(\hat{s} - m_\tau^2)\right]\left[\frac{g_{1L}^4}{(\hat{s} - M_{S_1}^2)^2} + \frac{g_{1L}^2 g_{1R}^2}{(\hat{s} - M_{S_1}^2)^2} + \frac{g_{3L}^4}{(\hat{s} - M_{S_3^0}^2)^2}\right.$$
$$\left. - 2\frac{g_{1L}^2 g_{3L}^2}{(\hat{s} - M_{S_1}^2)^2(\hat{s} - M_{S_3^0}^2)^2}\right] + \left[4\hat{t}(\hat{t} - m_\tau^2)\right]\left[\frac{g_{2L}^2 g_{2R}^2}{(\hat{s} - M_{V_{2\mu}^a}^2)^2}\right] \tag{3.4}$$

In order to demonstrate the behaviour of the τ production rate, we consider the contribution from LQ carrying different fermion numbers separately, which implies that *either* the $h's$ *or* the $g's$ (contributing to a given process) are non-zero at a time. For simplicity, we have taken the masses of scalar and vector LQ and couplings $h's$ ($g's$) for |F| = 0 (|F|=2) to be

equal. We have used CTEQ4LQ parton distribution functions [9] to compute the event rates. To study the variation of τ events w.r.t E_μ and baseline length L, we have plotted the events for two different LQ masses 250 GeV & 500 GeV respectively using the product of couplings to be equal to α_{em}. As also mentioned earlier, there exist bounds on lepton number violating couplings from rare τ-decays, specifically from $\tau^- \rightarrow \mu^-\pi^0$ [70]. These bounds however are derived on the assumption that only a single coupling at a time is non-zero and either a scalar or a vector LQ contributes to the process. Thus, though there are individual limits on h's and g's, it would be the *weaker bound* that will mainly contribute to the processes considered here. If such bounds, whatever there applicability are to be used, the cross section will decrease by roughly a factor of 40 in comparison to what has been presented here for the purpose of illustration.

In Figure 3.2(a), we plot the net contribution (from LQ and oscillation) to tau events for a near-site experimental set-up w.r.t E_μ. We have considered a detector with a sample area of .025 m^2 [40] and placed at 40 mts from the storage ring. It is worthwhile to mention that the contribution is predominantly from LQ as the oscillation is suppressed at such baseline length. We give similar curves in Figure 3.2(c) with the detector placed at a baseline length of 250 kms (K2K Proposal, *from KEK to Kamioka*) and sample detector area of 100 m^2 [40]. Here the contribution of LQ is comparable to that of the oscillation. Figure 3.2(b) shows the variation of events w.r.t. the baseline length, $1\,m$ to 100 m (appropriate for near-site experiment) for E_μ fixed at 50 GeV. The graph clearly shows the independence of the tau events with baseline length in this range, while in Figure 3.2(d) the behaviour of tau event rate is markedly different for short and medium baselines ($1 - 1000$ kms). Here, the LQ event rate falls off as $1/L^2$ to zero and hence the combined event rate for τ essentially merges with that due to oscillation alone.

The background for the signal of τ and the ways to eliminate them have been already discussed in detail in the existing literature (see for example, reference [71]) and it is found out that the missing-p_T and isolation cuts taken together can remove the entire set of backgrounds

due to charmed particle production, from unoscillated CC events and from the neutral current background. Recently, there have been theories that propose the existence of an extra neutral boson in many extensions of SM which lead to ν_μ associated charm production [72], which also acts as a source of background and need to be eliminated as far as detection of τ events are concerned. The τ-detection efficiency factor of 30% [40, 68, 71] taken in the present calculation, adequately accounts for all the selection cuts (including the cuts for missing p_T, isolation cut and the branching ratio) required to eliminate the backgrounds.

Sensitivity Limits : An estimate of the sensitivity limits on product of couplings and LQ masses can be based on the total number of events. Here we determine the range of LQ masses and product of LFV couplings, for which the number of signal events is equal to two and five times the square root of the OS events. Accepting this requirement of 2σ and 5σ effect as a sensible discovery criterion, we plot the corresponding contours in Figure 3.3 for baseline length=40 m. Thus, non compliance of these estimate with experimental observation would mean that the lower region enclosed by the curve are ruled out at 2σ and 5σ level, respectively.

3.5 Wrong Sign Muon Production

In the OS, $\bar{\nu}_e$ from the parent μ^- beam can oscillate to either $\bar{\nu}_\mu$ or to $\bar{\nu}_\tau$ which give rise to μ^+ and τ^+, respectively. The τ^+ furthur decay muonically ($BR = 17\%$ [73]) and thus contribute to the μ^+ events. However, it is worthwhile to mention here that one can hardly expect any μ^+ events from oscillations since the neutrino mass-slitting required for the Mikheyev-Smirnov-Wolfenstein (MSW) solution to the solar neutrino problem [65] with matter-enhanced ν_e-ν_μ oscillation is $\Delta m^2 \simeq 10^{-5} eV^2$. The situation is even worse for the case of Vacuum Oscillation solution which requires $\Delta m^2 \simeq 10^{-10} eV^2$. For the ν_e-ν_τ oscillation , there exists no experimental support and so, the region of parameter space to be explored for such oscillation mode is not known at all. Thus, a significant event rate for wrong sign muons cannot be attributed to ν-oscillation effects alone.

Here, we consider the production of μ^+ from parent μ^- beam via *unoscillated* $\bar{\nu}_e$ through LFV interactions with nucleon mediated by LQ in two different ways:

(i) Direct Production of μ^+ as well as

(ii) Production of τ^+, which further decays leptonically to μ^+.

Both of these involve s-channel processes corresponding to F=0 & charge=2/3 (Figure 3.4(a)) LQ and u-channel processes corresponding to |F| =2 & charge = -1/3 (Figure 3.4(b)) LQ. In Figure 3.4(a) out of four s-channel diagrams, one is mediated by scalar LQ (R_2^a) with $T_3 = -1/2$, while the other three are mediated by vector LQ ($U_{1\mu}; U_{1\mu}; U_{3\mu}^0$) with $T_3 = 0$. The matrix element squared for all the four s-channel processes is

$$\left|\mathcal{M}_{LQ}^{s-chann}(\bar{\nu_e}u \longrightarrow \mu^+ d)\right|^2 = \left[\hat{s}(\hat{s}-m_\mu^2)\right]\left[\frac{h_{2L}^2 h_{2R}^2}{(\hat{s}-M_{R_2^a}^2)^2}\right] + \left[4(\hat{s}+\hat{t})(\hat{s}+\hat{t}-m_\mu^2)\right]\left[\frac{h_{1L}^4}{(\hat{s}-M_{U_{1\mu}}^2)^2}\right.$$
$$\left. + \frac{h_{3L}^4}{(\hat{s}-M_{U_{3\mu}^0}^2)^2} - 2\frac{h_{1L}^2 h_{3L}^2}{(\hat{s}-M_{U_{1\mu}}^2)^2(\hat{s}-M_{U_{3\mu}^0}^2)^2}\right] + \left[4\hat{t}(\hat{t}-m_\mu^2)\right]\left[\frac{h_{1L}^2 h_{1R}^2}{(\hat{s}-M_{U_{1\mu}}^2)^2}\right] \tag{3.5}$$

where, $\hat{s} = (p_{\bar{\nu_e}} + p_{u,c})^2$, $\hat{t} = (p_{\bar{\nu_e}} - p_{\mu^+})^2$ and $\hat{u} = (p_{\bar{\nu_e}} - p_d)^2$, with p_i denoting the four momemtum of the i^{th} particle. In Figure 3.4(b) out of four u-channel diagrams three are mediated by scalar LQ (S_1; S_1; S_3^0) with $T_3 = 0$ and the fourth diagram is mediated by vector LQ ($V_{2\mu}^a$) with $T_3 = -1/2$. The matrix element squared for all the four u-channel processes corresponding to |F|=2 is

$$\left|\mathcal{M}_{LQ}^{u-chann}(\bar{\nu_e}u \longrightarrow \mu^+ d)\right|^2 = \left[\hat{u}(\hat{u}-m_\mu^2)\right]\left[\frac{g_{1L}^4}{(\hat{u}-M_{S_1}^2)^2} + \frac{g_{1L}^2 g_{1R}^2}{(\hat{u}-M_{S_1}^2)^2} + \frac{g_{3L}^4}{(\hat{u}-M_{S_3^0}^2)^2}\right.$$
$$\left. - 2\frac{g_{1L}^2 g_{3L}^2}{(\hat{u}-M_{S_1}^2)^2(\hat{u}-M_{S_3^0}^2)^2}\right] + \left[4\hat{t}(\hat{t}-m_\mu^2)\right]\left[\frac{g_{2L}^2 g_{2R}^2}{(\hat{u}-M_{V_{2\mu}^a}^2)^2}\right] \tag{3.6}$$

Similar expressions of matrix element squared for s- and u- channel diagrams corresponding to the process $\bar{\nu_e}u \longrightarrow \tau^+ d$ can be obtained just by substituting m_μ^2 by m_τ^2 and p_{μ^+} by p_{τ^+} in equation 3.5 and equation 3.6.

In order to study the behaviour of wrong sign muon events w.r.t E_μ and baseline lengths, we have used the same coupling strengths and masses as mentioned in section 3.4. For the indirect production of μ^+ via decay of τ^+ we have taken the efficiency factor for τ detection (in leptonic channel) to be 30% [40, 68]. Predictions for wrong sign muon production rate w.r.t E_μ and baseline length are plotted in Figure 3.5. The features of the plots for both near-site and short baseline experiments are same as that for τ production case discussed in the previous section.

In our calculation, we have not put any specific selection cut for the production of wrong sign μ. However, the muons from charm decay which forms a significant background for the production of wrong sign muons, can be eliminated by incorporating stringent cuts on the transverse momentum of muons , missing p_T and isolation cut as mentioned in [40, 68, 71].

Sensitivity Limits : Accepting the requirement of 2σ and 5σ effect as a sensible discovery criterion, we plot the corresponding contours for the wrong sign muons at a baseline length=40 m in Figure 3.6.

3.6 Low Energy Bounds

In last two sections, for the purpose of illustration, we considered |F| = 0 and |F| = 2 couplings separately and took all couplings to be equal to the electromagnetic coupling, α_{em}. But as also discussed in the introduction, strong constraints on the LQ couplings and masses have been obtained in the literature from FCNC processes [14]. In particular, bounds obtained from rare τ decay $\tau \rightarrow \pi^0\mu$ and from $\mu \leftrightarrow e$ conversion in nuclei would have a direct bearing on the processes considered here. This is because low energy limits put stringent bounds on effective

four-fermion interactions involving two leptons and two quarks and since at a NF the centre of mass energy in collisions is low enough, we can consider the neutrino-quark interactions as four-fermion interactions. These bounds on the effective couplings given as LQ couplings over mass squared of the LQ are derived on the assumption that individual LQ coupling contribution to the branching ratio does not exceed the experimental upper limits and in the branching ratios only one LQ coupling contribution is considered by *switching off* all the other couplings. The couplings are taken to be real but in these studies combinations of left and right chirality couplings are not considered.

Based on these studies, we make some simplified assumptions like obtaining the product of couplings of different chirality from the square of couplings of individual chirality. We extract the coupling products relevant to $(\nu_\mu\, d)\ (\tau\, u)$ vertex from rare τ decay bounds as quoted in the reference [14] and we get the following

$$\begin{aligned}
|h_{1L}|^2 = |h_{1R}|^2 &= 1.9\times10^{-3}\ \left(\frac{M_{LQ}}{100\ \text{GeV}}\right)^2, \quad |h_{2L}|^2 = 3.9\times10^{-3}\ \left(\frac{M_{LQ}}{100\ \text{GeV}}\right)^2,\\
|h_{3L}|^2 &= 6.4\times10^{-4}\ \left(\frac{M_{LQ}}{100\ \text{GeV}}\right)^2, \quad |h_{2R}|^2 = 1.9\times10^{-3}\ \left(\frac{M_{LQ}}{100\ \text{GeV}}\right)^2,\\
|g_{1L}|^2 = |g_{1R}|^2 &= 3.9\times10^{-3}\ \left(\frac{M_{LQ}}{100\ \text{GeV}}\right)^2, \quad |g_{3L}|^2 = 1.3\times10^{-3}\ \left(\frac{M_{LQ}}{100\ \text{GeV}}\right)^2,\\
|g_{2L}|^2 &= 1.9\times10^{-3}\ \left(\frac{M_{LQ}}{100\ \text{GeV}}\right)^2, \quad |g_{2R}|^2 = 9.7\times10^{-4}\ \left(\frac{M_{LQ}}{100\ \text{GeV}}\right)^2. \quad (3.7)
\end{aligned}$$

In case of wrong sign μ, the bounds on the couplings for $(\bar{\nu}_e u)(\mu^+ d)$ vertex arising from $\mu \leftrightarrow e$ conversion are so stringent, being typically 2-3 orders of magnitude lower compared to bounds on couplings involving third generation of quarks and leptons, that the direct production of μ^+ is highly suppressed. The relevant coupling constants extracted from [14] are

$$\begin{aligned}
|h_{1L}|^2 = |h_{1R}|^2 &= 2.6\times10^{-7}\ \left(\frac{M_{LQ}}{100\ \text{GeV}}\right)^2, \quad |h_{2L}|^2 = 5.2\times10^{-7}\ \left(\frac{M_{LQ}}{100\ \text{GeV}}\right)^2,\\
|h_{3L}|^2 &= 8.5\times10^{-8}\ \left(\frac{M_{LQ}}{100\ \text{GeV}}\right)^2, \quad |h_{2R}|^2 = 2.6\times10^{-7}\ \left(\frac{M_{LQ}}{100\ \text{GeV}}\right)^2,\\
|g_{1L}|^2 = |g_{1R}|^2 &= 5.2\times10^{-7}\ \left(\frac{M_{LQ}}{100\ \text{GeV}}\right)^2, \quad |g_{3L}|^2 = 1.7\times10^{-7}\ \left(\frac{M_{LQ}}{100\ \text{GeV}}\right)^2,\\
|g_{2L}|^2 &= 2.6\times10^{-7}\ \left(\frac{M_{LQ}}{100\ \text{GeV}}\right)^2, \quad |g_{2R}|^2 = 1.3\times10^{-7}\ \left(\frac{M_{LQ}}{100\ \text{GeV}}\right)^2. \quad (3.8)
\end{aligned}$$

In this situation, wrong sign muons mainly arise through the production of τ^+'s, which subsequently decay via leptonic channel. The bounds on coupling constants for the $(\bar{\nu}_e u)(\tau^+ d)$ vertex come from the decay $\tau \to \pi^0 e$ and are essentially the same as that for the case of τ production [14]. In Figure 3.7 we show the variation of τ events with muon beam energy and in Figure 3.8, the variation of wrong sign muons with muon energy for the baseline lengths of 40 m and 250 km respectively. The graphs clearly show that number of tau and wrong sign muon events is independent of LQ masses, as expected. On comparing Figure 3.7 & Figure 3.8 with Figure 3.2 & Figure 3.5 respectively, we find considerable suppression in event rates. We should however bear in mind that rare decay bounds in LQ interactions with a charm quark are comparatively weak and therefore these bounds can be evaded if we can tag the charm production.

3.7 Conclusions

Neutrino factory will open up unprecendented opportunities to investigate neutrino physics, bearing not only on neutrino oscillation phenomenon but also providing physical laboratory for testing physics beyond the SM. In this chapter, we investigated the LFV effect in theories with LQ on the production of τ's and wrong sign μ's in the near-site and short baseline experiments. It is clear that with the increase in baseline length, the LQ event rate falls off and neutrino oscillations are the main source events examined here. At near-site experiments, on the other hand, the events mainly arise from *new interactions* and can thus be used to constrain the theory. In particular one can obtain constraints on LFV couplings between the first and third generation, the bounds on which are generally not available. At near-site experiments, the event rate is practically independent of baseline length.

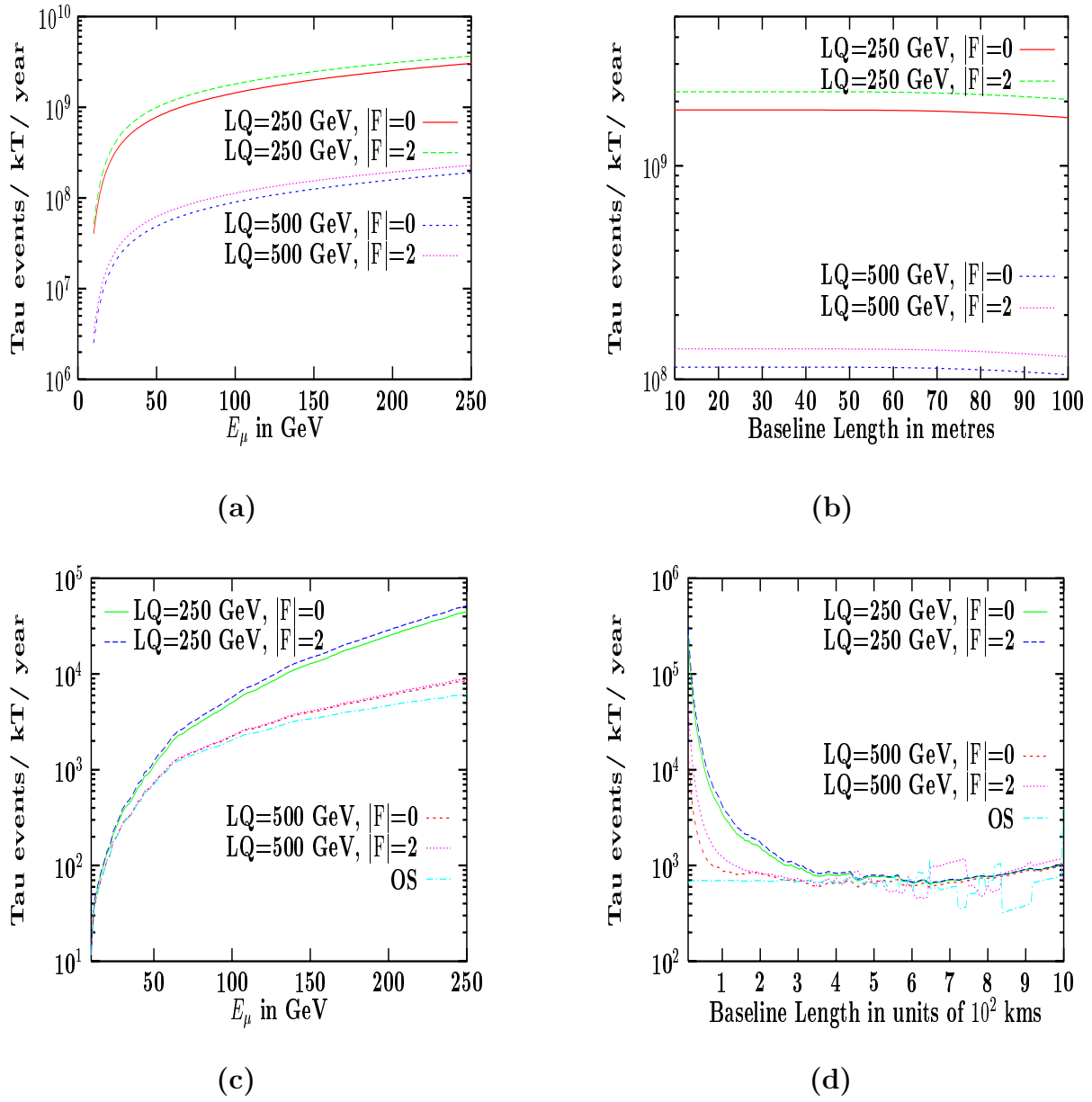

Figure 3.2: *Variation τ-events (from oscillation and LQ) for a 1 kT detector, LQ mass 250 & 500 GeV and product of LQ coulings = 0.089 with : (a) muon beam energy for a baseline length 40 m and sample detector area 0.025 m^2, (b) baseline length for muon beam energy 50 GeV and detector area 0.025 m^2, (c) muon beam energy for a baseline length 250 kms and sample detector area 100 m^2, (d) baseline length for muon beam energy 50 GeV and detector area 100 m^2.*

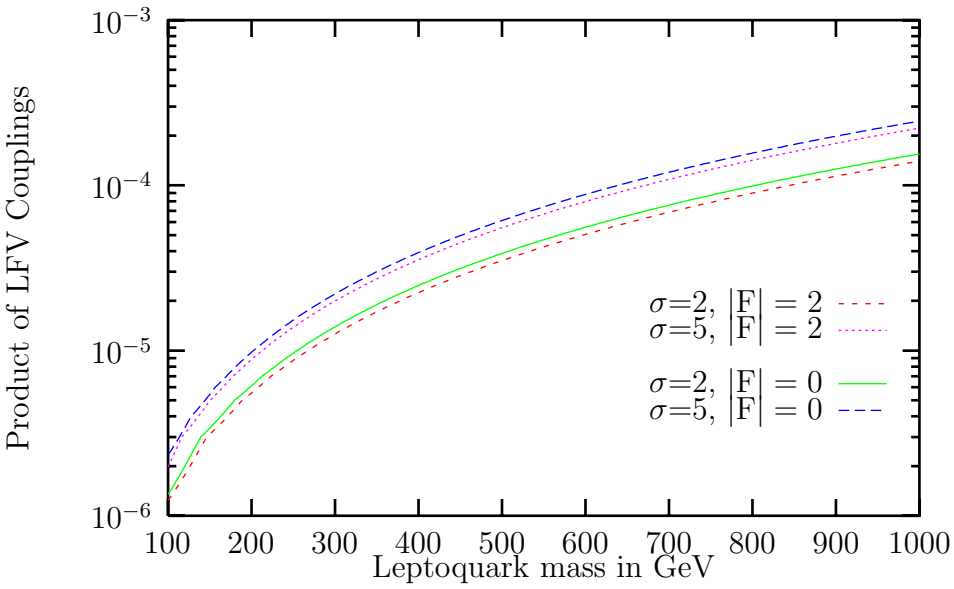

Figure 3.3: *Contours for 2σ and 5σ effect for E_μ = 50 GeV, baseline length = 40 m and sample detector of area 2500 cm^2 and mass 1 kT.*

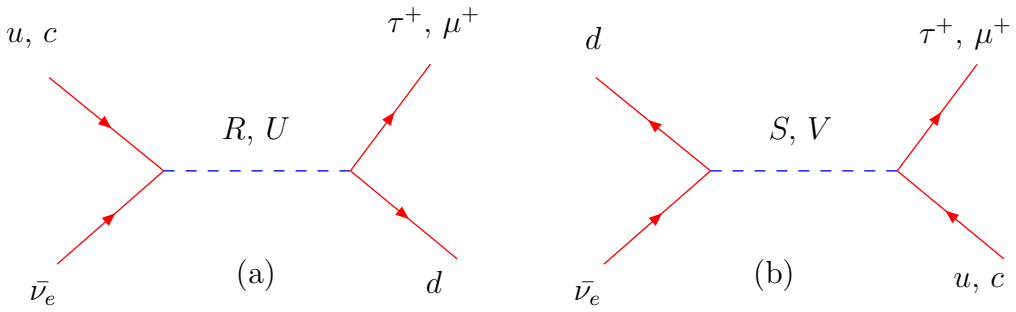

Figure 3.4: *τ^+ and μ^+ from scalar & vector LQ: (a) s-channel process corresponding to |F|=0 LQ and (b) u-channel process corresponding to |F|=2 LQ.*

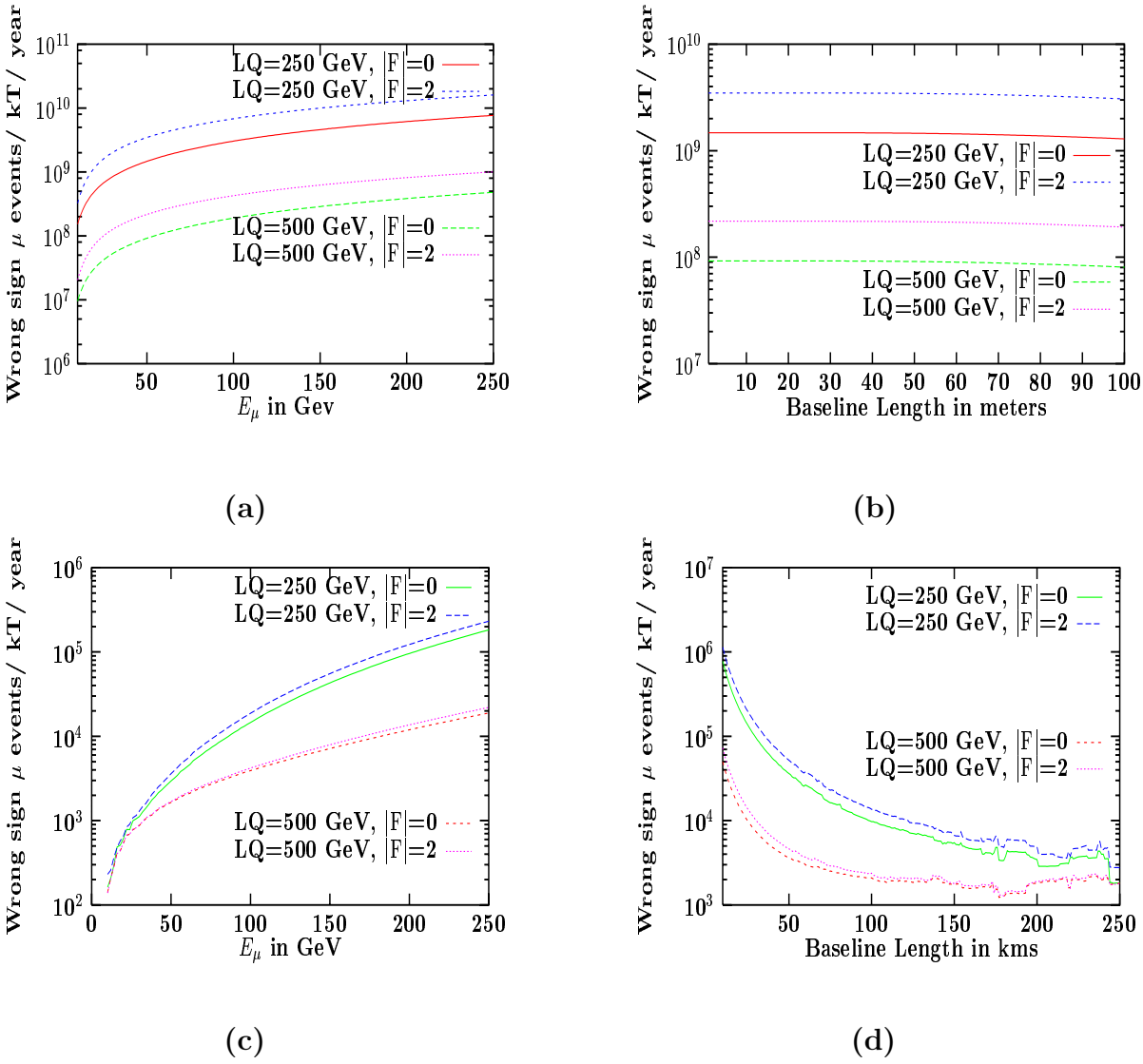

Figure 3.5: *Variation of wrong sign μ-events (from oscillation and LQ) coulings = 0.089 with : (a) muon beam energy for a baseline length 40 m, (b) baseline length for near-site detector configuration, (c) muon beam energy for a baseline length 250 kms, (d) baseline length for short baseline situation. All the parameters used here are as mentioned in the caption of Figure 3.2.*

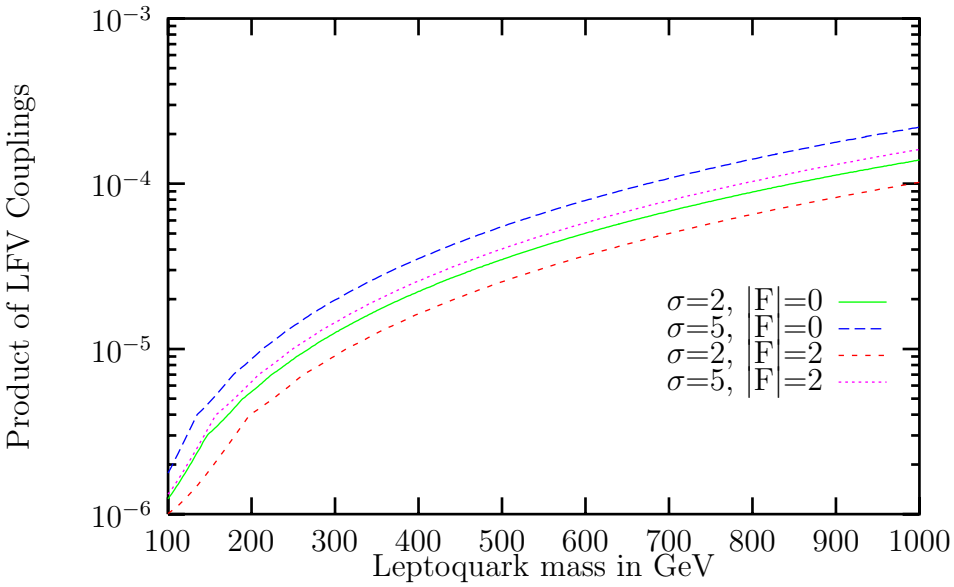

Figure 3.6: *Contour plot for Wrong sign muons at 2σ and 5σ effect for E_μ = 50 GeV, baseline length = 40 m and sample detector of area 2500 cm^2 and mass 1 kT.*

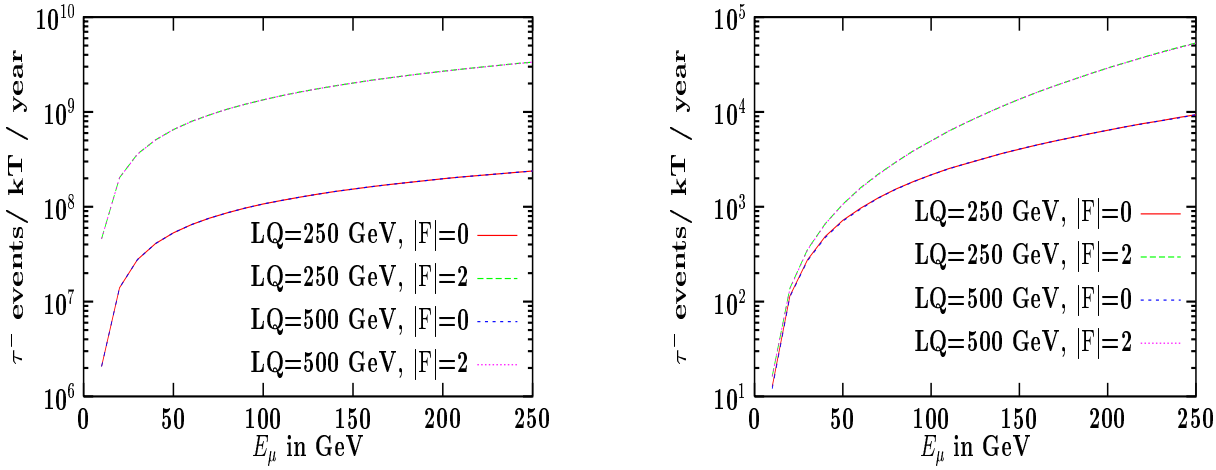

(a) **(b)**

Figure 3.7: *Variation of τ-events (from oscillation and LQ) with : (a) muon beam energy for a baseline length 40 m, (b) muon beam energy for a baseline length 250 kms. All the parameters used here except for the couplings are as mentioned in the caption of Figure 3.2.*

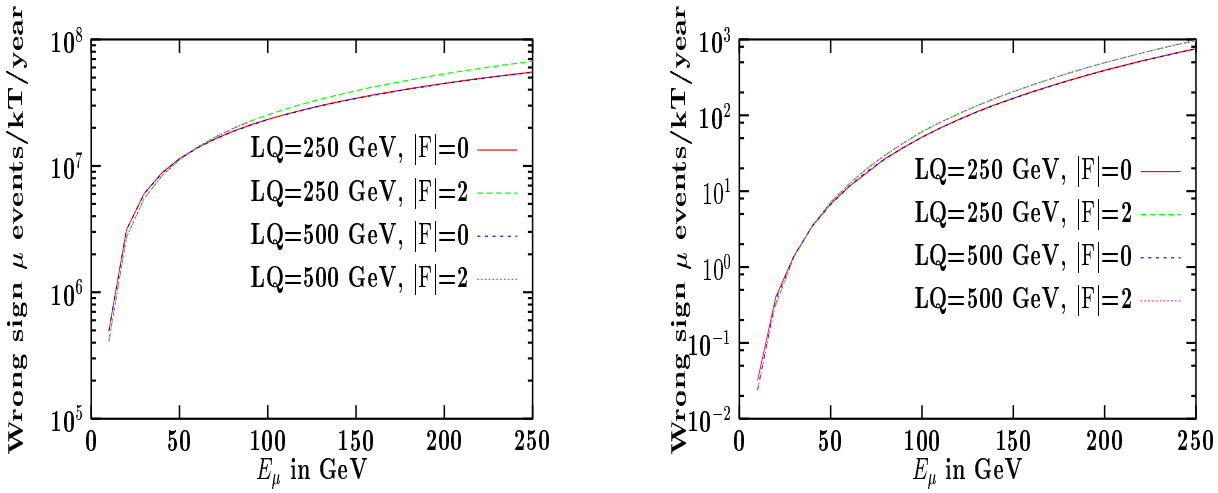

(a) **(b)**

Figure 3.8: *Variation of wrong sign μ-events (from oscillation and LQ) with : (a) muon beam energy for a baseline length 40 m, (b) muon beam energy for a baseline length 250 kms. All parameters used here for plotting except for couplings are as quoted in the caption of Figure 3.5.*

Chapter 4

Heavy Quark Production via Leptoquarks

The proposed NF based on a MSR is an ideal place to look for heavy quark production via NC and CC interactions. In this chapter, we address the issue of contribution coming from mediating LQ in $\nu_\mu(\bar{\nu}_e) - \mathrm{N}$ scattering leading to the production of $b(\bar{b})$ at a MSR and investigate the region where LQ interactions are significant in the near-site experiments. Some of the results presented in this chapter are published in Phys. Rev. **D67,** 053006 (2003).

4.1 Introduction

It is being frequently suggested nowadays that a NF, cashing on the intense and well-calibrated supply of ν_μ and ν_e coming out of a MSR, can go a long way in investigating the world of neutrinos where numerous puzzles are still in store for us [53, 74]. In addition to its usefulness in probing neutrino oscillations, such high precision neutrino experiments can have several other interesting physics goals. One of these is the possible investigation of physics beyond the SM, something which becomes a necessity once one accepts the existence of neutrino mass and mixing. Thus it is natural to ask whether there are observables rising above the threshold

of detectability in a NF, which will unequivocally imply the existence of such new physics interactions involving the neutrino sector.

Recent strong indications of atmospheric neutrino oscillation ($\nu_\mu \longrightarrow \nu_x$, where x is not e) [75] have rekindled the interest in accelerator experiments that could study the same range of parameter space. The solar neutrino deficit is interpreted either as matter enhanced Mikhyev−Smirnov−Wolfenstein (MSW) oscillations [76] or as vacuum oscillations [77] that deplete the original ν_e's, presumably in favour of ν_μ's.

The role of a NF in determining masses and mixing angles for $\nu_\mu \leftrightarrow \nu_\tau$ and $\bar{\nu}_e \leftrightarrow \bar{\nu}_\mu$ oscillations both at short and long baseline experiments has been extensively discussed in the literature. Investigation of physics beyond the SM through certain novel interactions in the neutrino sector, in particular the appearance of τ and wrong sign μ signals in new physics scenarios like SUSY theories with broken R-parity [68] and theories that allow LQ mediated LFV interactions [78] have been dealt with in chapter 2 and chapter 3.

With the same motivation to look for the role played by the non-standard interactions at a NF the production of heavy quarks through ν_μ-N scattering (particularly in NC events) in an R-parity violating SUSY theory was investigated recently [79] and it was shown that it is possible to have significant event rates for b ($\bar{b}$) production via both NC and CC interactions. We should emphasize here that in SM the production of b ($\bar{b}$) is severely suppressed at tree level. Thus a considerable number of b ($\bar{b}$) or an excess well above the SM rate at a NF would unequivocally imply the existence of non-standard physics in the neutrino sector. In contrast to SM, b quark production via non-standard $\nu - N$ scattering processes can take place at the tree level itself via the CC interactions, $\nu_\mu\,\bar{u} \longrightarrow \mu^-\,\bar{b}$, $\nu_\mu\,\bar{c} \longrightarrow \mu^-\,\bar{b}$ and $\bar{\nu}_e\,u \longrightarrow e^+\,b$, all of which are suppressed in the SM either due to the Cabibbo−Kobayashi−Masakawa (CKM) matrix elements V_{ub} or due to the interaction of ν_μ with sea quarks present inside the nucleon. The corresponding NC processes $\nu_\mu\,d \longrightarrow \nu_\mu\,b$ and $\bar{\nu}_e\,d \longrightarrow \bar{\nu}_e\,b$ can occur only at one loop level in the SM.

One can conclude from above that if there is any observation of excess in CC b-production

over the SM rate, or if NC events are observed with a b in final state, it will clearly signal some kind of new physics. The question is, given other kinds of constraints (specially those from b-decays) on the same operators that give rise to such events, is it possible at a NF to have any observable excess of events, or to use the absence of such excess to impose useful bounds on the new interactions.

In this context, it is worthwhile to consider theories with leptoquarks which occur naturally in Grand Unified Theories, Superstring inspired E_6 models and in Technicolor models [69] and study heavy flavour $(b, \bar{b})$ production in scattering of neutrinos on a fixed isonucleon target with LQ as mediators of the interaction. In our earlier work (chapter 3), we have studied the contribution of mediating lepton flavor violating LQ in $\nu_\mu\,(\bar{\nu}_e)$-N scattering leading to an enhanced production of τ's and wrong sign μ's at MSR and investigated the region where LQ interactions are significant in the near-site and short baseline experiments and we found that one can constrain LFV couplings between the first and third generation, the bounds on which are not generally available. With the same spirit in this present work, we investigate the b quark production in both NC and CC channels through $\nu_\mu(\bar{\nu}_e)$-N scattering at the NF, mediated by scalar and vector leptoquarks. It is worth mentioning that we consider $\bar{\nu}_e$ beam also for production of $b, \bar{b}$ in both the NC and CC channels unlike reference [79]. In order to observe new physics effects in the DIS of these neutrinos, it is preferable to have a near-site detector, where the neutrino detectors are placed at a very short distance (typically $\simeq$ 40m from the straight section of storage ring) rather than a long baseline one, so that oscillation effects do not dominate. Here we do not consider the LFV processes. The processes that we consider in this chapter for the $b, \bar{b}$ production via NC and CC channels are :

$$\text{NC}: \ \nu_\mu\, d \longrightarrow \nu_\mu\, b, \qquad \bar{\nu}_e\, d \longrightarrow \bar{\nu}_e\, b \tag{4.1}$$

$$\text{CC}: \ \nu_\mu\, \bar{u} \longrightarrow \mu^-\, \bar{b}, \qquad \bar{\nu}_e\, u \longrightarrow e^+\, b \tag{4.2}$$

At near-site experiments, the incoherent scattering effects dominate over oscillation effects. The total number of $b, \bar{b}$ quark production events per year via either CC or NC interactions

can be obtained by folding the relevant cross section by a survival probability and the neutrino flux and it can be written as

$$\mathcal{N}_{b,\,\bar{b}} = \mathcal{N}_n \int \frac{d^2\sigma^{\nu,\bar{\nu}}_{NC/CC}}{dx\ dy} \left[\frac{dN_{\nu,\bar{\nu}}}{dE_{\nu_i,\bar{\nu}_i}}\right] \mathcal{P}_{surv}(\nu_i(\bar{\nu}_i) \longrightarrow \nu_i(\bar{\nu}_i)) dE_{\nu_i(\bar{\nu}_i)}\, q(x)\ \ dx\ dy \tag{4.3}$$

where, $\mathcal{N}_n$ is the number of nucleons per kT of the target material [1] , x and y are the Bjorken scaling variables, q and q' are the quarks in the initial and final states, respectively and $q(x)$ is the quark distribution function. The differential parton level cross-section can be expressed as

$$\frac{d^2\sigma^{\nu,\bar{\nu}}_{NC/CC}}{dx\ dy} = \left[\frac{d^2\sigma^{\nu,\bar{\nu}}_{NC/CC}}{dx'\ dy'}\right] \times \frac{\partial\,(x',\,y')}{\partial\,(x,\,y)} = \left[\frac{|\mathcal{M}\,(\,x',\,y'\,)|^2_{NC/CC}}{32\pi\hat{S}}\right] \tag{4.4}$$

where $y' = -\,\hat{t}/\hat{S} = Q^2/(2\,M\,E_\nu\,x')$, x' is the *slow rescaling* variable[2] that arises due to the mass shell constraint of the heavy quark produced in the final state,

$$x' = \frac{Q^2 + m_Q^2}{2\,M\,\nu} = x\ +\ \frac{m_Q^2}{2\,M\,E_\nu\,y} \qquad \text{Therefore} \quad \frac{\partial\,(x',\,y')}{\partial\,(x,\,y)} = 1. \tag{4.5}$$

with M being the nucleon mass, E_ν being the neutrino energy and $\nu = E_{\nu_l} - E_{l^-}$ $(E_{\bar{\nu}_l} - E_{l^+})$. $\hat{S}$ is the parton level CM energy and $\left[\frac{dN_{\nu,\bar{\nu}}}{dE_{\nu_i,\bar{\nu}_i}}\right]$ is the differential ν $(\bar{\nu})$ flux. The survival probability of a particular neutrino flavour 'i' is given by $\mathcal{P}_{surv}(\nu_i \to \nu_i) = 1 - \mathcal{P}_{osc}(\nu_i \to \nu_j)$ where j takes all possible values, $j = e, \mu, \tau$ but $j \neq i$[3]. The predictions on b-production have no perceptible dependence on the precise values of the oscillation parameters, at near-site setting.

The effective Lagrangian with the most general dimensionless, $SU(3)_c \times SU(2)_L \times U(1)_Y$ invariant couplings of *scalar* and *vector* LQ satisfying baryon (B) and lepton number (L) conservation (suppressing colour, weak isospin and generation (flavour) indices) is given [13] by:

[1] $\mathcal{N}_n = 6.023\,\mathrm{X}\,10^{32}$ for a target of mass 1 kT.

[2] For production of a heavy quark from a light quark, the heavy quark mass modifies the scaling variable of the quark distribution. x' is the quark momentum fraction appropriate to absorb the virtual W described by ν and Q^2.

[3] For two flavour oscillation case, $\mathcal{P}_{osc}(\nu_i \to \nu_j) = \sin^2 2\theta_m\ \sin^2\left[1.27\,\Delta m^2[eV^2]\,\frac{L[km]}{E_\nu[GeV]}\right]$, where, L is the baseline length, E_ν is the neutrino energy, Δm^2 is the mass-squared difference between the corresponding physical states, and θ_m is mixing angle between flavours.

$$
\begin{aligned}
\mathcal{L} &= \mathcal{L}_{|F|=2} + \mathcal{L}_{|F|=0} \qquad \text{where} \\
\mathcal{L}_{|F|=2} &= \left[g_{1L}\,\bar{q}_L^c\, i\,\tau_2\, l_L + g_{1R}\,\bar{u}_R^c\, e_R\right]\, S_1 + \tilde{g}_{1R}\,\bar{d}_R^c\, e_R\,\tilde{S}_1 + g_{3L}\,\bar{q}_L^c\, i\,\tau_2\,\vec{\tau}\, l_L\,\vec{S}_3 \\
&+ \left[g_{2L}\,\bar{d}_R^c\,\gamma^\mu\, l_L + g_{2R}\,\bar{q}_L^c\;\gamma^\mu\, e_R\right]\, V_{2\mu} + \tilde{g}_{2L}\,\bar{u}_R^c\,\gamma^\mu\, l_L\,\tilde{V}_{2\mu} + \textbf{c.c.}, \\
\mathcal{L}_{|F|=0} &= \left[h_{2L}\,\bar{u}_R\, l_L + h_{2R}\,\bar{q}_L\, i\,\tau_2\, e_R\right]\, R_2 + \tilde{h}_{2L}\,\bar{d}_R\, l_L\,\tilde{R}_2 + \tilde{h}_{1R}\,\bar{u}_R\,\gamma^\mu\, e_R\,\tilde{U}_{1\mu} \\
&+ \left[h_{1L}\,\bar{q}_L\,\gamma^\mu\, l_L + h_{1R}\,\bar{d}_R\,\gamma^\mu\, e_R\right]\, U_{1\mu} + h_{3L}\,\bar{q}_L\,\vec{\tau}\,\gamma^\mu\, l_L\, U_{3\mu} + \textbf{c.c.}
\end{aligned}
\tag{4.6}
$$

where q_L, l_L are the LH quarks and lepton doublets and e_R, d_R, u_R are the RH charged leptons, down- and up-quark singlets respectively . The Scalar (i.e. S_1, $\tilde{S}_1$, S_3) and Vector (i.e. V_2, $\tilde{V}_2$) LQ carry fermion number F = 3B + L = −2, while the Scalar (i.e. R_2, $\tilde{R}_2$) and Vector (i.e. U_1, $\tilde{U}_1$, U_3) LQ have F = 0.

Numerous phenomenological studies have been made in order to derive bounds and put stringent constraints on LQ couplings particularly from low energy FCNC processes [14] that are generated by scalar and vector LQ interactions. Direct experimental searches for leptoquarks have also been carried out at the e-p collider and bounds obtained [70] and in particular bounds obtained from B meson decays ($B \longrightarrow l^+l^-X$, where $l^+l^- = \mu^+\mu^-,\ e^+e^-$) and also bounds derived from meson-antimeson ($B\bar{B}$) mixing would have direct bearing on the processes considered here. This is because low energy limit puts stringent bound on effective four-fermion interactions involving two leptons and two quarks and since at the NF the centre of mass energy in collision is low enough, we can consider the neutrino-quark interaction as an effective four-fermion interaction. The bounds on effective couplings used in this chapter are the LQ couplings over mass squared of the LQ and are derived on the assumption that individual leptoquark coupling contribution to the branching ratio does not exceed the experimental upper limits and in the branching ratios only one leptoquark coupling is considered by switching off all the other couplings. All couplings are considered to be real and combinations of left and right chirality coupling are not considered. We discuss the $b(\bar{b})$ production through

$\nu(\bar{\nu})$-N interactions via NC and CC channels in section 4.2 and 4.3 respectively and give the plots of event rate versus muon beam energy. In the last section we outline the conclusions drawn from our results.

4.2 $b(\bar{b})$ production via neutral current processes

Let us first consider the possible NC processes that can lead to $b/\bar{b}$ in the final state. There is no SM tree level process in the NC channel as NC processes leading to $b/\bar{b}$ can only occur at one loop level in the SM. However, there can be two possible non-standard tree level NC processes that can lead to the production of $b/\bar{b}$ in the final state, due to the presence of both ν and $\bar{\nu}$ of different flavors from μ decay, *viz* $\mu^- \longrightarrow e^- \nu_\mu \bar{\nu_e}$

1. $\nu_\mu + d \longrightarrow \nu_\mu + b$

2. $\bar{\nu}_e + d \longrightarrow \bar{\nu}_e + b$

For the two NC processes mentioned above, we have both s- and u-channel diagrams arising from the relevant interaction terms in the effective LQ lagrangian. For the first process, $\nu_\mu + d \longrightarrow \nu_\mu + b$ (shown in Figure 4.1), there are two possible u-channel diagrams mediated by LQs $(\tilde{R}^\dagger, U^\dagger)$ carrying |F| = 0 and charge = 1/3, while there are three possible s-channel diagrams that are mediated by LQs $(S^\dagger, V^\dagger)$ carrying |F| = 2 and charge = $-1/3$. For the second process, $\bar{\nu}_e + d \longrightarrow \bar{\nu}_e + b$ (shown in Figure 4.2), the two possible s-channel diagrams are mediated by LQs $(\tilde{R}, U)$ carrying |F| = 0 and charge = $-1/3$, while the three possible u-channel diagrams are mediated by LQs (S, V) carrying |F| = 2 and charge = 1/3.

We first consider the production of "b" from ν_μ (obtained from μ^- decay) interactions with nucleon via NC u-channel processes for $|F| = 0$ case (Figure 4.1(a)) and NC s-channel processes for $|F| = 2$ case (Figure 4.1(b)). There are in all two diagrams contributing to production of b via $(\nu_\mu + d \longrightarrow \nu_\mu + b)$ in the u-channel (Figure 4.1(a)), one mediated by the charge = 1/3, scalar LQ $(\tilde{R_2^{-1/2}}^\dagger)$ carrying $T_3 = -1/2$ and the other one by a vector LQ

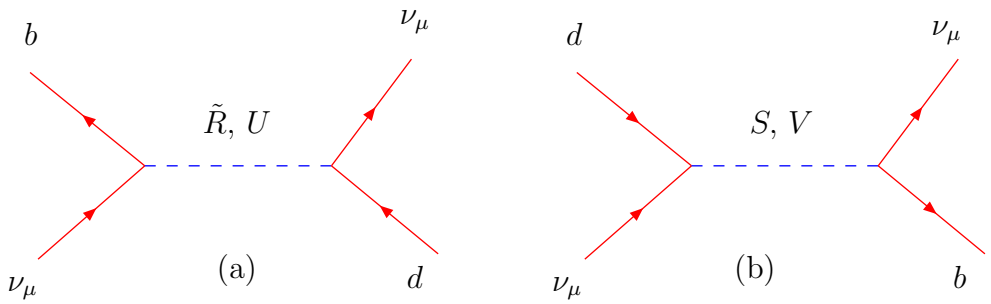

Figure 4.1: *b production via NC process ($\nu_\mu + d \longrightarrow \nu_\mu + b$) from scalar & vector LQ: (a) u-channel process corresponding to* |F| = 0 *LQ and (b) s-channel process corresponding to* $|F| = 2$ *LQ.*

$(U_{3\mu}^{-\,\dagger})$ with $T_3 = -1$, where T_3 is the weak isospin. The matrix element squared for 2 diagrams contributing to the u-channel NC process is

$$\left|\mathcal{M}_{LQ}^{u-chann}(\nu_\mu d \longrightarrow \nu_\mu b)\right|^2 = \left[\hat{u}(\hat{u}-m_b^2)\right]\left[\frac{\left|\tilde{h_{2L}}\,\tilde{h_{2L}}\right|^2}{(\hat{u}-M^2_{\tilde{R_2^{-1/2}}})^2}\right] + \left[4\hat{s}(\hat{s}-m_b^2)\right]\left[\frac{\left|\sqrt{2}h_{3L}\,\sqrt{2}h_{3L}\right|^2}{(\hat{u}-M^2_{U_{3\mu}^-})^2}\right] \tag{4.7}$$

where, the Mandelstam variables at the parton level are given by $\hat{s} = (p_{\nu_\mu} + p_d)^2$, $\hat{t} = (p_{\nu_\mu}(initial) - p_{\nu_\mu}(final))^2$ and $\hat{u} = (p_{\nu_\mu} - p_b)^2$, with p_i denoting the four momentum of the i^{th} particle.

In the s-channel, two diagrams are mediated by charge $= -1/3$, scalar LQs $(S_1{}^\dagger, S_3^{0\dagger})$ with $T_3 = 0$, while one is mediated by a vector LQ $(V_{2\mu}^{-1/2\,\dagger})$ with $T_3 = -1/2$ (Figure 4.1(b)). The matrix element squared for all the 3 diagrams contributing to the NC s-channel process is

$$\left|\mathcal{M}_{LQ}^{s-chann}(\nu_\mu d \longrightarrow \nu_\mu b)\right|^2 = \left[\hat{s}(\hat{s}-m_b^2)\right]\left[\frac{\left|g_{1L}\,g_{1L}\right|^2}{(\hat{s}-M^2_{S_1})^2} + \frac{\left|g_{3L}\,g_{3L}\right|^2}{(\hat{s}-M^2_{S_3^0})^2}\right.$$

$$+\ 2\frac{|g_{1L}\, g_{3L}|^2}{(\hat{s}-M^2_{S_1})(\hat{s}-M^2_{S_3^0})}\Big] \ +\ \Big[4\hat{u}(\hat{u}-m_b^2)\Big]\Big[\frac{|g_{2L}\, g_{2L}|^2}{(\hat{s}-M^2_{V_{2\mu}^{-1/2}})^2}\Big] \tag{4.8}$$

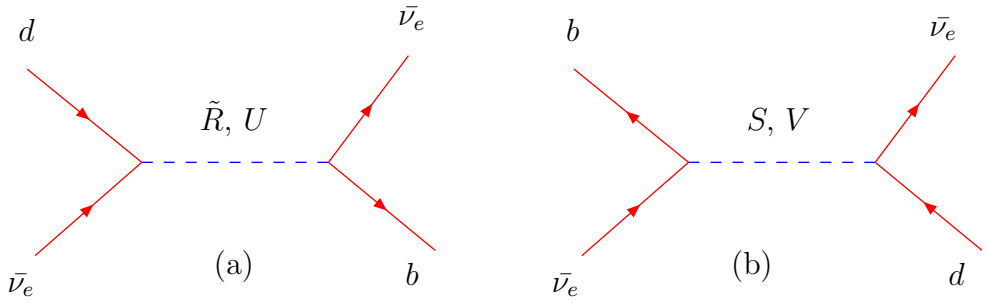

Figure 4.2: *b production via NC process ($\bar{\nu}_e + d \longrightarrow \bar{\nu}_e + b$) from scalar & vector LQ: (a) s-channel process corresponding to* |F| = 0 *LQ and (b) u-channel process corresponding to* $|F| = 2$ *LQ.*

Next we consider the production of "b" from $\bar{\nu}_e$ (also obtained from the μ^- decay) through interactions with nucleon via NC s-channel process for $|F| = 0$ case (Figure 4.2(a)) and NC u-channel process for $|F| = 2$ case (Figure 4.2(b)). There are in all two diagrams contributing to production of b via ($\bar{\nu}_e + d \longrightarrow \bar{\nu}_e + b$) in the s-channel (Figure 4.2(a)), one mediated by the charge $= -1/3$, scalar LQ ($\tilde{R}_2^{-1/2}$) with $T_3 = -1/2$ and while the other one by a vector LQ ($U_{3\mu}^-$) with $T_3 = -1$. The matrix element squared for the 2 diagrams contributing to the NC s-channel process is

$$\Big|\mathcal{M}_{LQ}^{s-chann}(\bar{\nu_e}d \longrightarrow \bar{\nu_e}b)\Big|^2 = \Big[\hat{s}(\hat{s}-m_b^2)\Big]\Big[\frac{\Big|\tilde{h_{2L}}\,\tilde{h_{2L}}\Big|^2}{(\hat{s}-M^2_{\tilde{R_2}^{-1/2}})^2}\Big] \ +\ \Big[4\hat{u}(\hat{u}-m_b^2)\Big]\Big[\frac{\Big|\sqrt{2}h_{3L}\,\sqrt{2}h_{3L}\Big|^2}{(\hat{s}-M^2_{U_{3\mu}^-})^2}\Big] \tag{4.9}$$

where, the Mandelstam variables at the parton level are given by $\hat{s} = (p_{\bar{\nu_e}} + p_d)^2$, $\hat{t} = (p_{\bar{\nu_e}}(initial) - p_{\bar{\nu_e}}(final))^2$ and $\hat{u} = (p_{\bar{\nu_e}} - p_b)^2$.

In the u-channel, two diagrams are mediated by the charge = 1/3, scalar LQs (S_1, S_3^0) with $T_3 = 0$ and one is mediated by a vector LQ $(V_{2\mu}^{-1/2})$ with $T_3 = -1/2$ (Figure 4.2(b)). The matrix element squared for all 3 diagrams contributing to the NC u-channel process is

$$\left|\mathcal{M}_{LQ}^{u-chann}(\bar{\nu}_e d \longrightarrow \bar{\nu}_e b)\right|^2 = \left[\hat{u}(\hat{u}-m_b^2)\right]\left[\frac{|g_{1L}\, g_{1L}|^2}{(\hat{u}-M_{S_1}^2)^2} + \frac{|g_{3L}\, g_{3L}|^2}{(\hat{u}-M_{S_3^0}^2)^2} + 2\frac{|g_{1L}\, g_{3L}|^2}{(\hat{u}-M_{S_1}^2)(\hat{u}-M_{S_3^0}^2)}\right] + \left[4\hat{s}(\hat{s}-m_b^2)\right]\left[\frac{|g_{2L}\, g_{2L}|^2}{(\hat{u}-M_{V_{2\mu}^{-1/2}}^2)^2}\right] \tag{4.10}$$

Having said all about the relevant NC diagrams leading to b-production, we now focus on

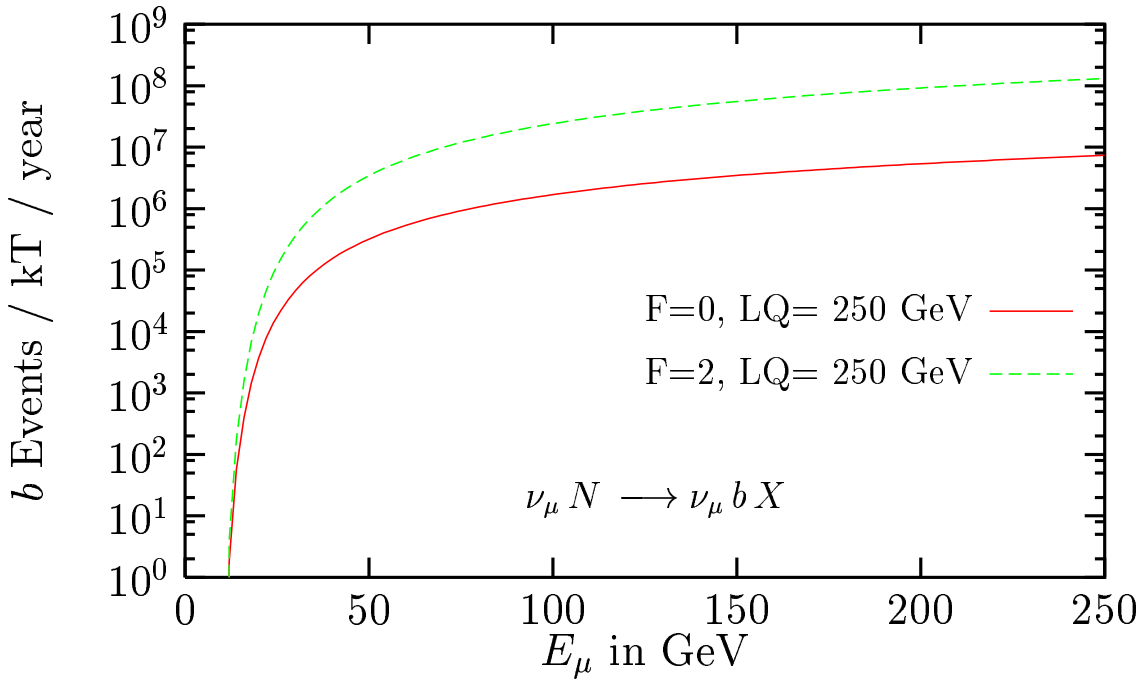

Figure 4.3: *Variation of b-events (from LQ) for a 1kT detector and LQ mass 250 GeV with muon beam energy for a baseline length 40 meters and sample detector area 0.025 m^2*

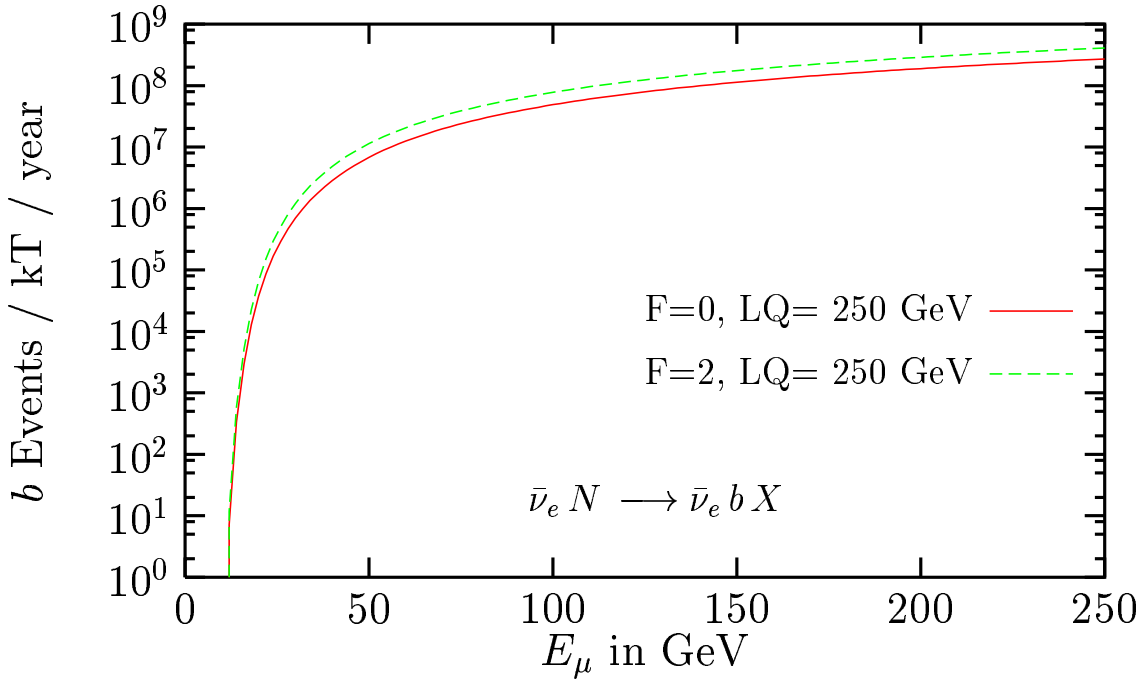

Figure 4.4: *Variation of b-events (from LQ) for a 1kT detector and LQ mass 250 GeV with muon beam energy for a baseline length 40 meters and sample detector area 0.025 m^2*

the details that we use in order to compute the number of events for $b/\bar{b}$ via NC channel and demonstrate their behaviour as a function of muon energy ranging from 0 upto 250 GeV. We consider the contribution from LQ carrying different fermion numbers separately, which essentially means that *either all the h's or all the g's* contributing to a given process, are non-zero at a time. For simplicity, we take the masses of scalar and vector LQs for both F = 0 and |F| = 2 to be equal (= 250 GeV). As in our earlier works ([68], [78]), we have used CTEQ4LQ Parton Distribution Functions [9] in order to compute the events. There is however significant suppression in phase space due to the production of massive 'b' quark. In our calculation we have not imposed any event selection cuts. Using events selection cuts for

detail analysis as given in reference [74] will further scale down the contribution. We have considered a detector with a sample area of 0.025 m^2 [40] and placed at 40 m from the storage ring. Regarding the bounds on LQ couplings, we have used model independent constraints on the couplings to b quarks of B and L conserving LQs as discussed in [14] where it is shown that one can constrain the generation dependent LQ couplings to b quarks from the upper bounds on the flavour-changing decays $B \longrightarrow l^+l^-X$ (where $l^+l^- = \mu^+\mu^-, e^+e^-$), the CKM matrix element V_{ub} and from meson - antimeson ($B\bar{B}$) mixing and obtain some of the best bounds for the processes of our interest. All the bounds on couplings that we have used for calculation of event rates are listed in Table 4.1. Since the bounds on the couplings h_{2L} & g_{1R} are not available from reference [14], we take them to be the same as bounds on couplings h_{2R} & g_{1L} (which are the opposite chirality counterparts of h_{2L} & g_{1R} respectively). We make some simplifying assumptions like the product of couplings of different chirality is obtained from the squares of the couplings of individual chiralities. We extract bounds relevant to $(\nu_\mu d)(\nu_\mu b)$ vertex from the bounds for (21)(23) generation of quark-lepton pair, while for the vertex $(\bar{\nu}_e d)(\bar{\nu}_e b)$, we use the bounds for the (11)(13) generation indices relevant to the process. These bounds are derived from semileptonic inclusive B decays. The latest bounds coming from BABAR and BELLE experiments [80] however are not relevant for the processes considered here except for the bound on V_{ub} which does not make any significant change in the couplings. In Figure 4.3 and Figure 4.4, we have plotted the b-quark production rate as a function of muon beam energy for $\nu_\mu - \mathrm{N}$ and $\bar{\nu}_e - \mathrm{N}$ scattering processes respectively.

4.3 $b(\bar{b})$ production via charged current processes

As discussed above the production of $\bar{b}$ or b in the final state through CC interaction can also occur in the SM at the tree level in contrast to the NC case where SM contributes only at the one loop level. The SM cross-sections for the CC processes $\nu_\mu + \bar{u} \longrightarrow \mu^- + \bar{b}$ and

(lq)(lq)	h_{1L}	h_{1R}	h_{2L}	h_{2R}	h_{3L}	g_{1L}	g_{1R}	g_{2L}	g_{2R}	g_{3L}
(11)(13)	.002	.003	–	.006	.002	.004	–	.003	.003	.004
(21)(23)	.0004	.0004	–	.0008	.0004	.004	–	.0004	.0004	.0004

Table 4.1: The best bounds on all relevant products of couplings (from B decays and $B\bar{B}$ mixing) taken from Table 15 of the reference [14] by S. Davidson *et al.*). All the bounds are multiplied by $(m_{LQ}/[100\ \text{GeV}])^2$.

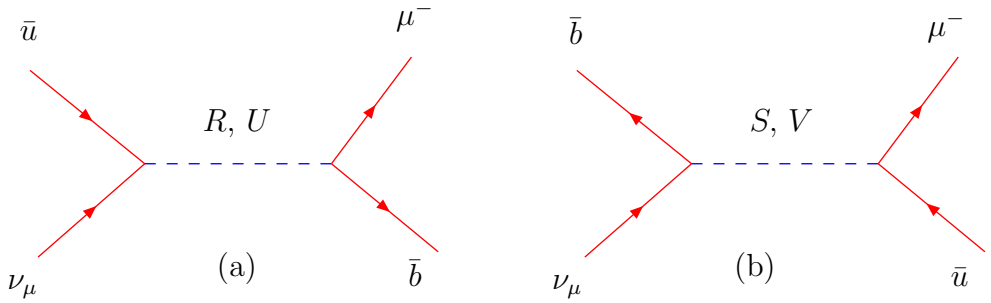

Figure 4.5: *b production via CC process* ($\nu_\mu + \bar{u} \longrightarrow \mu^- + \bar{b}$) *from scalar & vector LQ: (a) s-channel diagram corresponding to* $|\mathrm{F}| = 0$ *LQ and (b) u-channel diagram corresponding to* $|\mathrm{F}| = 2$ *LQ.*

$\bar{\nu}_e + u \longrightarrow e^+ + b$ are given by

$$\begin{aligned}
\frac{d^2\sigma}{dx\ dy}\left(\nu_\mu\, N \longrightarrow \mu^-\, \bar{b}\, X\right) &= \frac{G_F^2\, S}{\pi}\left(\frac{M_W^2}{M_W^2+Q^2}\right)^2\left(x' - x'\,y' - \frac{m_b^2}{S}\right)(1-y')\,\bar{u}(x')\,|V_{ub}|^2 \\
\frac{d^2\sigma}{dx\ dy}\left(\bar{\nu}_e\, N \longrightarrow e^+\, b\, X\right) &= \frac{G_F^2\, S}{\pi}\left(\frac{M_W^2}{M_W^2+Q^2}\right)^2\left(x' - x'\,y' - \frac{m_b^2}{S}\right)(1-y')\,u(x')\,|V_{ub}|^2
\end{aligned} \tag{4.11}$$

Here we have the advantage of having the SM rates as benchmark against which to the compare the rates obtained via LQ. $\bar{u}(x')$ and $u(x')$ are the distribution functions of up-type antiquark and quark respectively.

For the CC processes mentioned above, we can have both s- and u-channel diagrams arising

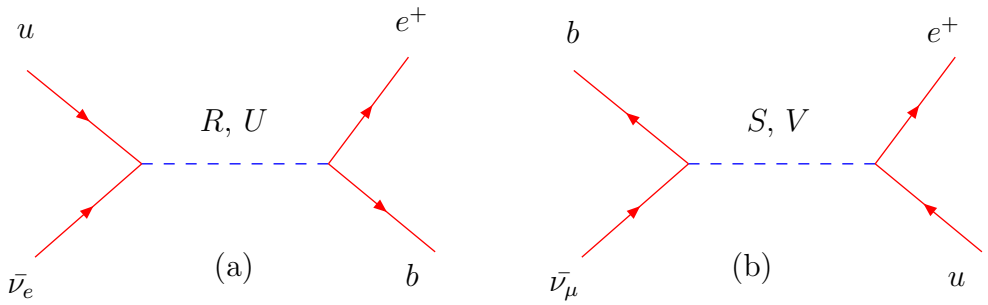

Figure 4.6: *b production via CC process ($\bar{\nu}_e + u \longrightarrow e^+ + b$) from scalar & vector LQ: (a) s-channel diagram corresponding to* $|\mathrm{F}| = 0$ *LQ and (b) u-channel diagram corresponding to* $|\mathrm{F}| = 2$ *LQ.*

from the relevant interaction terms in the effective LQ Lagrangian, as for the case of NC processes. For the first process, $\nu_\mu + \bar{u} \longrightarrow \mu^- + \bar{b}$ (as shown in Figure 4.5), there are 4 possible s-channel diagrams mediated by LQs $(R^\dagger, U^\dagger)$ carrying $|\mathrm{F}| = 0$ and charge $= -2/3$. Also there are 4 possible u-channel diagrams that are mediated by LQs $(S^\dagger, V^\dagger)$ carrying $|\mathrm{F}| = 2$ and charge $= -1/3$. For the second process, $\bar{\nu}_e + u \longrightarrow e^+ + b$ (as shown in Figure 4.6), the 4 possible s-channel diagrams are mediated by LQs (R, U) carrying $|\mathrm{F}| = 0$ and charge $= 2/3$, while the 4 possible u-channel diagrams are mediated by LQs (S, V) carrying $|\mathrm{F}| = 2$ and charge $= 1/3$, respectively. We first consider the production of "$\bar{b}$" from ν_μ (obtained from μ^- decay) through interactions with nucleon via CC s-channel process for the $|F| = 0$ case (Figure 4.5(a)) and CC u-channel process for the $|F| = 2$ case (Figure 4.5(b)).

There are in all 4 diagrams contributing to production of $\bar{b}$ via $(\nu_\mu + \bar{u} \longrightarrow \mu^- + \bar{b})$ in the s-channel (Figure 4.5(a)), one mediated by the charge $= -2/3$, scalar LQ $(R_2^{-1/2\dagger})$ with $T_3 = -1/2$ and the other three by vector LQs $({U_{1\mu}}^\dagger, {U_{1\mu}}^\dagger, {U_{3\mu}^0}^\dagger)$ with $T_3 = -1$. The matrix element squared for all 4 diagrams contributing to the CC s-channel process is

$$\left|\mathcal{M}_{LQ}^{s-chann}(\nu_\mu \bar{u} \longrightarrow \mu^- \bar{b})\right|^2 = \left[\hat{s}(\hat{s} - m_b^2)\right]\left[\frac{|h_{2L}\, h_{2R}|^2}{(\hat{s} - M^2_{R_2^{-1/2}})^2}\right] + \left[4\hat{u}(\hat{u} - m_b^2)\right]\left[\frac{|h_{1L}\, h_{1L}|^2}{(\hat{s} - M^2_{U_{1\mu}})^2}\right.$$

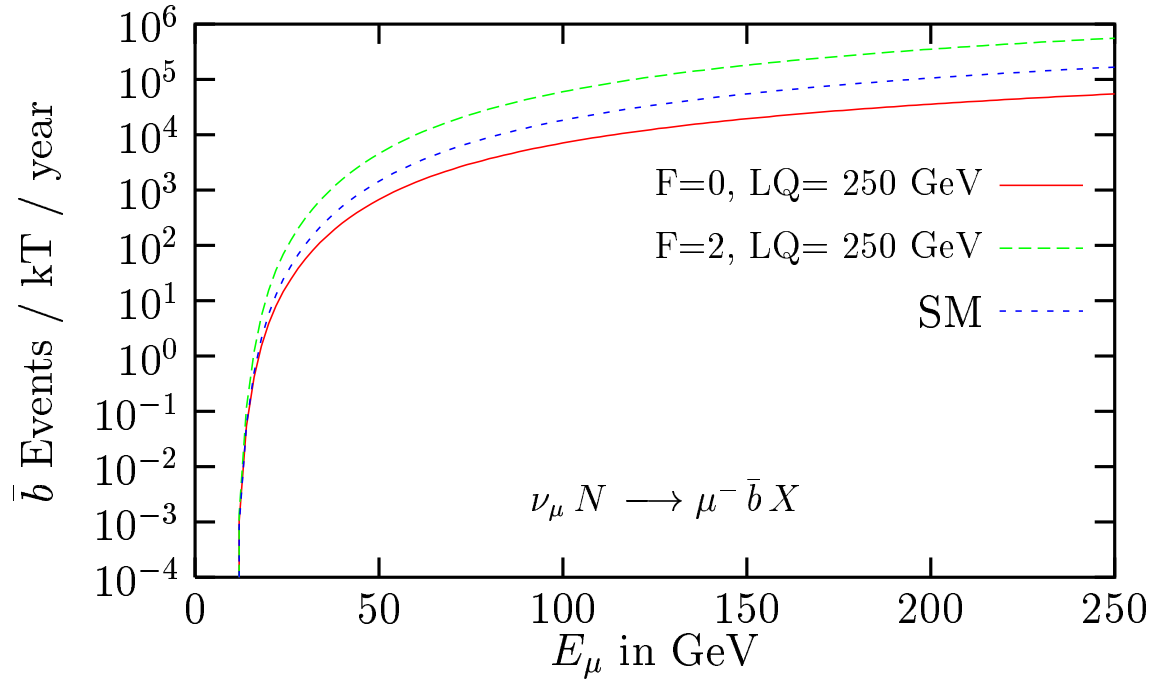

Figure 4.7: *Variation of $\bar{b}$-events (from SM and LQ) for a 1kT detector and LQ mass 250 GeV with muon beam energy for a baseline length 40 meters and sample detector area 0.025 m^2*

$$+ \frac{|h_{3L}\, h_{3L}|^2}{(\hat{s} - M^2_{U^0_{3\mu}})^2} - 2\frac{|h_{1L}\, h_{3L}|^2}{(\hat{s} - M^2_{U_{1\mu}})\,(\hat{s} - M^2_{U^0_{3\mu}})}\Big] + \Big[4(\hat{s}+\hat{u})(\hat{s}+\hat{u}-m_b^2)\Big]\Big[\frac{|h_{1L}\, h_{1R}|^2}{(\hat{s} - M^2_{U_{1\mu}})^2}\Big] \tag{4.12}$$

where, the Mandelstam variables at the parton level are given by $\hat{s} = (p_{\nu_\mu}+p_{\bar{u}})^2$, $\hat{t} = (p_{\nu_\mu}-p_{\mu^-})^2$ and $\hat{u} = (p_{\nu_\mu} - p_{\bar{b}})^2$.

In the u-channel, 3 diagrams are mediated by the charge $= -1/3$, scalar LQs $({S_1}^\dagger, {S_1}^\dagger, {S_3^0}^\dagger)$ with $T_3 = 0$ and one is mediated by a vector LQ $({V_{2\mu}^{-1/2}}^\dagger)$ with $T_3 = -1/2$ (Figure 4.5(b)).

The matrix element squared for all 4 diagrams contributing to the CC u-channel process is

$$\left|\mathcal{M}_{LQ}^{u-chann}(\nu_\mu \bar{u} \longrightarrow \mu^- \bar{b})\right|^2 = \left[\hat{u}(\hat{u}-m_b^2)\right]\left[\frac{|g_{1L}\, g_{1L}|^2}{(\hat{u}-M_{S_1}^2)^2} + \frac{|g_{1L}\, g_{1R}|^2}{(\hat{u}-M_{S_1}^2)^2} + \frac{|g_{3L}\, g_{3L}|^2}{(\hat{u}-M_{S_3^0}^2)^2} - 2\frac{|g_{1L}\, g_{3L}|^2}{(\hat{u}-M_{S_1}^2)(\hat{u}-M_{S_3^0}^2)}\right] + \left[4(\hat{s}+\hat{u})(\hat{s}+\hat{u}-m_b^2)\right]\left[\frac{|g_{2L}\, g_{2L}|^2}{(\hat{u}-M_{V_{2\mu}^{-1/2}}^2)^2}\right] \tag{4.13}$$

Next we consider the production of "b" from $\bar{\nu_e}$ (also obtained from the μ^- decay) through interactions with nucleon via CC s-channel process for $|F| = 0$ case (Figure 4.6(a)) and CC u-channel process for $|F| = 2$ case (figure 4.6(b)). There are in all 4 diagrams contributing to production of b via ($\bar{\nu_e} + u \longrightarrow e^+ + b$) in the s-channel (Figure 4.6(a)), one mediated by the charge = 2/3, scalar LQ ($R_2^{-1/2}$) with $T_3 = -1/2$ and while the other three mediated by vector LQs ($U_{1\mu}, U_{1\mu}, U_{3\mu}^0$) having $T_3 = 0$ each. The matrix element squared for the 4 diagrams contributing to the CC s-channel process is

$$\left|\mathcal{M}_{LQ}^{s-chann}(\bar{\nu_e} u \longrightarrow e^+ b)\right|^2 = \left[\hat{s}(\hat{s}-m_b^2)\right]\left[\frac{|h_{2L}\, h_{2R}|^2}{(\hat{s}-M_{R_2^{-1/2}}^2)^2}\right] + \left[4\hat{u}(\hat{u}-m_b^2)\right]\left[\frac{|h_{1L}\, h_{1L}|^2}{(\hat{s}-M_{U_{1\mu}}^2)^2} + \frac{|h_{3L}\, h_{3L}|^2}{(\hat{s}-M_{U_{3\mu}^0}^2)^2} - 2\frac{|h_{1L}\, h_{3L}|^2}{(\hat{s}-M_{U_{1\mu}}^2)\,(\hat{s}-M_{U_{3\mu}^0}^2)}\right] + \left[4(\hat{s}+\hat{u})(\hat{s}+\hat{u}-m_b^2)\right]\left[\frac{|h_{1L}\, h_{1R}|^2}{(\hat{s}-M_{U_{1\mu}}^2)^2}\right] \tag{4.14}$$

where, the Mandelstam variables at the parton level are given by $\hat{s} = (p_{\bar{\nu_e}} + p_u)^2$, $\hat{t} = (p_{\bar{\nu_e}} - p_{e^+})^2$ and $\hat{u} = (p_{\bar{\nu_e}} - p_b)^2$.

In the u-channel, three diagrams are mediated by the charge = 1/3, scalar LQs (S_1, S_1, S_3^0) with $T_3 = 0$ and one is mediated by a vector LQ ($V_{2\mu}^{-1/2}$) with $T_3 = -1/2$ (Figure 4.6(b)). The matrix element squared for all 4 diagrams contributing to the CC u-channel process is

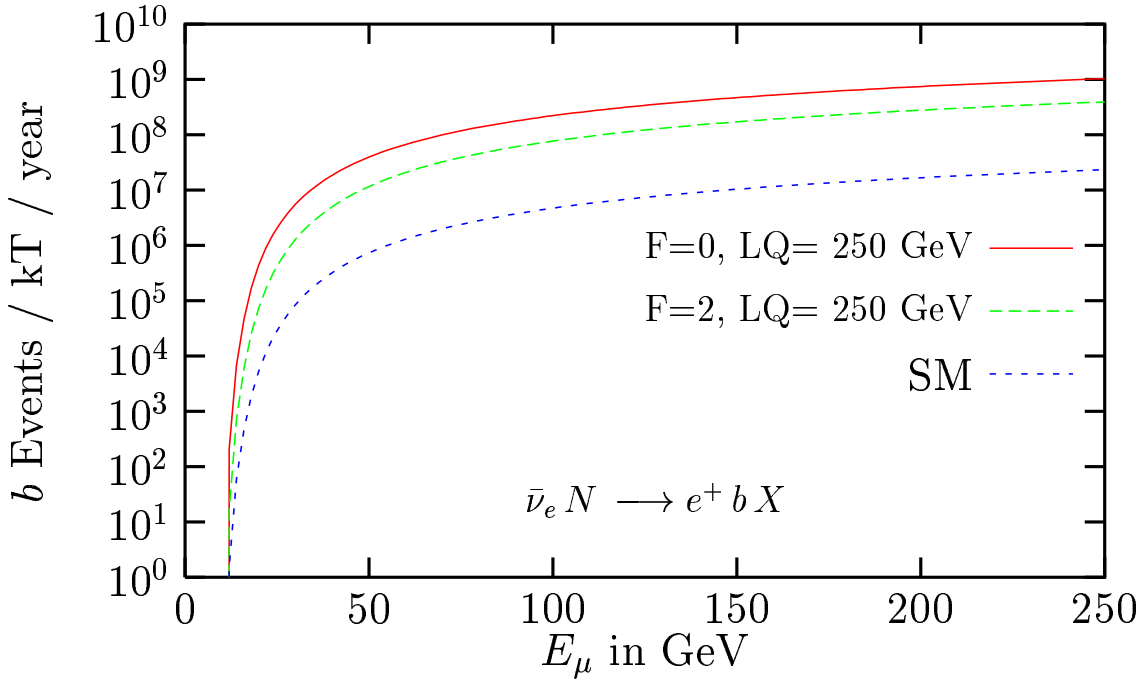

Figure 4.8: *Variation of b-events (from SM and LQ) for a 1kT detector and LQ mass 250 GeV with muon beam energy for a baseline length 40 meters and sample detector area 0.025 m^2*

$$\left|\mathcal{M}_{LQ}^{u-chann}(\bar{\nu_e}u \longrightarrow e^+b)\right|^2 = \left[\hat{u}(\hat{u}-m_b^2)\right]\left[\frac{|g_{1L}\,g_{1L}|^2}{(\hat{u}-M_{S_1}^2)^2} + \frac{|g_{1L}\,g_{1R}|^2}{(\hat{u}-M_{S_1}^2)^2} + \frac{|g_{3L}\,g_{3L}|^2}{(\hat{u}-M_{S_3^0}^2)^2} - 2\frac{|g_{1L}\,g_{3L}|^2}{(\hat{u}-M_{S_1}^2)(\hat{u}-M_{S_3^0}^2)}\right] + \left[4(\hat{s}+\hat{u})(\hat{s}+\hat{u}-m_b^2)\right]\left[\frac{|g_{2L}\,g_{2L}|^2}{(\hat{u}-M_{V_{2\mu}^{-1/2}}^2)^2}\right] \tag{4.15}$$

As discussed in the previous section, we have used the model independent bounds on couplings from [14] and the relevant bounds for the processes listed above are listed in Table 4.1. We

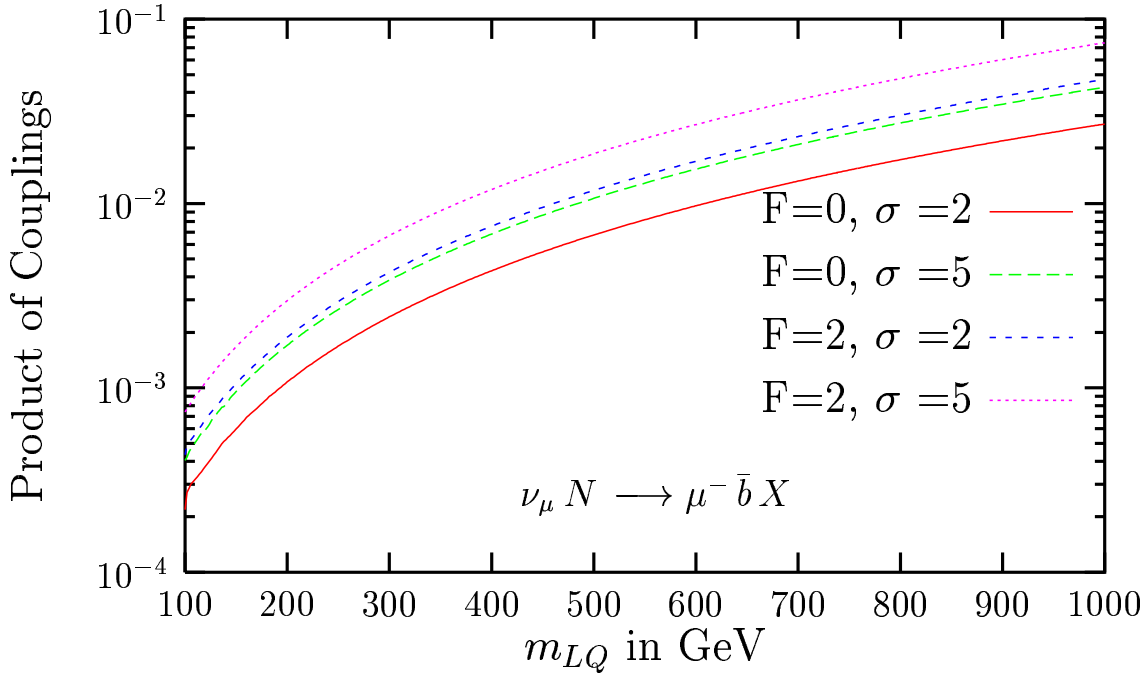

Figure 4.9: *Contour plot for $\bar{b}$ production at 2σ and 5σ effect for E_μ=50 GeV, baseline length=40 meters and sample detector of area 2500 cm^2 and mass 1kT.*

extract bounds relevant to $(\nu_\mu \bar{u})(\mu^- \bar{b})$ vertex from the bounds for (21)(23) generation of quark-lepton pair, while for the vertex $(\bar{\nu}_e u)(e^+ b)$, we use the bounds for the (11)(13) generation indices relevant for the process $\bar{\nu}_e u \longrightarrow e^+ b$. The other inputs to compute the event rates are the same as for the NC diagrams. In Figure 4.7 and Figure 4.8, we have plotted the $\bar{b}$ and b event rates as a function of muon beam energy for $\nu_\mu - N$ and $\bar{\nu}_e - N$ scattering processes respectively. For these processes we have also plotted the SM contribution to $\bar{b}$ and b events. To determine the allowed range of LQ masses and products of couplings, we have used the criterion that the number of signal events is equal to two or five times the square root of events in the SM. Accepting this requirement of 2σ and 5σ effect as a sensible discovery criterion the

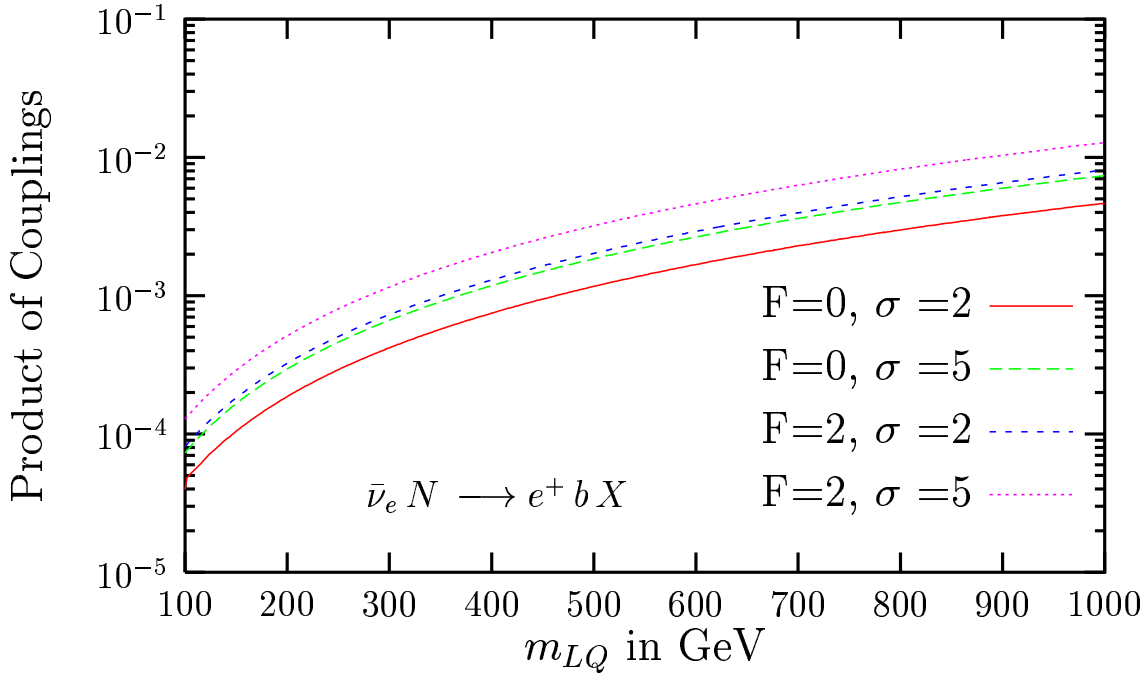

Figure 4.10: *Contour plot for b production at 2σ and 5σ effect for E_μ=50 GeV, baseline length=40 meters and sample detector of area 2500 cm^2 and mass 1kT.*

contour in Figure 4.9 and Figure 4.10 are drawn for a baseline length of 40 m and thus the non-compliance of these estimates with experimental observation would mean that the region above these curves is ruled out.

4.4 Discussions and Results

Heavy quark $(b, \bar{b})$ production from ν_μ – N and $\bar{\nu}_e - N$ scattering via both the CC and NC interactions at a NF provides an exciting possibility to detect signals of new physics. This comes about because in these processes the SM contribution is heavily suppressed either due

to CKM matrix element or due to interaction of neutrinos with the sea quarks present inside the nucleon. The NC processes in SM are further suppressed as they can take place only at one loop level. We have computed here the $b(\bar{b})$ event rates in theories with LQ and confined ourselves to the near-site experiments where the oscillation effects are negligible. From Figure 4.7, it is clear that the contribution coming from the SM to the $\bar{b}$ production rate in the CC channel is higher than that of LQ's with $|\mathrm{F}| = 0$, while it is lower than the contribution from LQ's with $|\mathrm{F}| = 2$ for our choice of the couplings obtained from low energy experiments. We typically find (Figure 4.8) that the SM contribution to b production rate is 2 to 3 orders of magnitude smaller than LQ contribution in CC channel even after using the most severe constraints on LQ couplings and masses from low energy FCNC processes. Further the b production rate in the NC channel (Figure 4.3 and Figure 4.4) is comparable to that for the CC case. We have investigated the region in coupling - mass space for LQ which can provide a reasonable signal for the discovery of new physics involving LQ. It may be noted that this region can be even more restrictive than that implied by the low energy bounds obtained from B meson decays. Also the inclusion of LFV interactions via LQ's could further squeeze the allowed region of LFV Couplings and masses.

Chapter 5

Summary and Final Comments

In this thesis we have studied the effects of non-standard interactions in the neutrino sector at a NF set-up. In particular we have looked at the production of tau and wrong sign muon production in a SUSY scenario with broken R-parity and in theories with LQ. We infer that non-standard interactions both at muon decay level and at interaction level in new physics scenarios discussed above, can give signals that mimic the standard oscillation signals. One can have a clean detection of the presence of non-standard interactions at a near site set-up where the effects due to oscillations are suppressed. We have also looked at heavy quark production in DIS of neutrinos (ν_μ and $\bar{\nu}_e$) via LQ as mediators of interactions in both CC and NC channels. In case of heavy quark production, our findings are that a clear signal of new physics can emerge. This is due to the fact that in SM, b quark production is heavily suppressed. In this chapter we will summarize our inferences and will discuss the future aspects.

5.1 Summary

In chapter 2 we have investigated the effects of the R-parity violating trilinear couplings on the suggested signals of neutrino oscillations. LFV can in general mimic the neutrino oscillation signal. We consider two illustrative cases in the framework of R-parity violating SUSY : In the

first case, by virtue of lepton number violating trilinear couplings ($\lambda'-$type), the unoscillated ν_μ can scatter into τ. In the second case, such couplings ($\lambda-$type) can produce a $\bar{\nu}_\mu$ from μ^- decay, which subsequently has standard CC interactions and gives rise to μ^+ in the detector. We find that, even tiny R-violating couplings can lead to very large number of τ's at a near-detector setting, much in excess of what is expected via oscillation. Thus, near-site experiments are recommended for isolating new physics effects that fake the signals of oscillation. On the other hand, a class of R-violating interactions, with strengths well within their current experimental limits, can be responsible for an enhanced rate of μ^+ at a LBL experiment.

In chapter 3 we addressed the contribution of mediating LFV LQ in $\nu(\bar{\nu}) - N$ interactions leading to the production of τ and wrong sign μ at a NF. We also investigated the region where LQ interactions are significant in the near-site and short baseline experiments. As the baseline length increases, the LQ event rate falls off and neutrino oscillation effects take over. At near-site experiments, on the other hand, the events mainly arise from new interactions and can thus be used to constrain the theory. We also find that the event rates at near-site experiment are independent of the baseline length.

In the last chapter (chapter 4) we discussed the heavy quark production ($b/\bar{b}$) via LQ in $\nu_\mu - N$ and $\bar{\nu}_e - N$ scattering via both CC and NC channels at a NF. Given the fact that these processes are heavily suppressed in SM, the detection of heavy quarks at NF allows us to probe signals of new physics.

5.2 Experimental Status

In the context of R-parity violating SUSY theories, we have looked at tau and wrong sign muon production. We consider two representative processes to illustrate the main ideas. In the case for tau production, the couplings, $\lambda'_{213}, \lambda'_{313}$ are involved and the interaction is mediated by $\tilde{b}$ squark. For wrong sign muon production, the interaction is mediated by $\tilde{\tau}$ slepton and the couplings $\lambda_{132}, \lambda_{231}$ are involved.

Indirect bounds : The R-violating interactions can contribute to various (low-energy) processes through the virtual exchange of SUSY particles. To data all data are in good agreement with the SM. This leads directly to bounds on R-violating operators. When determining such bounds one makes simplifying assumptions due to large number of operators present. We assume that only one R-violating operator at a time is dominant, while others are negligible. Thus, although there are individual limits on λ'_{213} and λ'_{313} couplings from CC decays of π^- and τ, such limits are not necessarily applicable in the most general case. At any rate no conclusive limit has been obtained for the product $\lambda'_{213}\lambda'_{313}$. Hence this product can be treated as a free parameter when it comes to looking for experimental signals. The first systematic study of low-energy bounds on R-parity violating Yukawa couplings was performed in [11]. More recently, a very nice thorough update of all the bounds on lepton number violating couplings is listed in [81]. Below we have listed the latest 2σ [64] limits on the magnitudes of weak scale trilinear R-parity violating couplings from indirect decays and perturbativity. The dependence of the relevant superparticle mass is explicitly shown. When perturbativity bounds are more stringent than the empirical bounds for masses $m_{\tilde{l},\tilde{q}} = 1TeV$, then those are displayed in paranthesis.

$$\lambda'_{213} < 0.059 \times \frac{m_{\tilde{b}_R}}{100GeV}$$
$$\lambda'_{313} < 0.11 \times \frac{m_{\tilde{b}_R}}{100GeV} (1.12)$$

$$\lambda_{132} < 0.0062 \times \frac{m_{\tilde{\mu}_R}}{100GeV}$$
$$\lambda_{231} < 0.070 \times \frac{m_{\tilde{e}_R}}{100GeV}$$

We have used $m_{\tilde{b}_R} = 300GeV$ and $m_{\tilde{\tau}_L} = 100GeV$, which are consistent with current limits.

In case of LQ, we first consider the production of τ and wrong sign μ from unoscillated ν_μ and $\bar{\nu}_e$ through LFV interactions with the nucleon via the u-channel and the s-channel processes. At a neutrino factory, the center of mass energy in collisions is sufficiently low that the neutrino-quark interaction can be approximated as a four-fermion vertex. So, the

low energy limits on the LQ couplings obtained from μ and τ rare processes are applicable here [14]. The low energy limits are bounds on bounds on an effective four-fermion operator involving two charged leptons and two quarks. In the case of tau production $\nu_\mu d \to \tau^- u$, the u-channel process is mediated by LQ $R_2^a, U_{1\mu}, U_{3\mu}^0$ and the coupling products that are involved are : (h_{2L}, h_{2R}), (h_{1L}, h_{1L}), (h_{3L}, h_{3L}), (h_{1L}, h_{1R}) and (h_{1L}, h_{3L}) while the s-channel process is mediated by the LQ $S_1, S_3^0, V_{2\mu}^a$ and the coupling products that are involved are : (g_{1L}, g_{1L}), (g_{1L}, g_{1R}), (g_{3L}, g_{3L}), (g_{2L}, g_{2R}) and (g_{1L}, g_{3L}). For the case of wrong sign muon production $\bar{\nu}_e u \to \mu^+ d$, the s-channel process is mediated by $R_2^a, U_{1\mu}, U_{3\mu}^0$ and the coupling products that are involved are : (h_{2L}, h_{2R}), (h_{1L}, h_{1L}), (h_{3L}, h_{3L}), (h_{1L}, h_{1R}) and (h_{1L}, h_{3L}) while the u-channel process is mediated by the LQ $S_1, S_3^0, V_{2\mu}^a$ and the coupling products that are involved are : (g_{1L}, g_{1L}), (g_{1L}, g_{1R}), (g_{3L}, g_{3L}), (g_{2L}, g_{2R}) and (g_{1L}, g_{3L}).

Low energy bounds : There exist bounds on lepton number violating couplings from rare τ decays, specifically from $\tau^- \to \pi^0 \mu^-$ (involves couplings of generations (13)(12)) and from $\mu \leftrightarrow e$ conversion in nuclei. The bounds are available for coupling products of same chirality only. In order to obtain the constraints on the coupling product of mixed chirality, we use the assumption that the LQ couplings (all the h's and g's) are generation blind and extract the "individual bounds" on couplings of any chirality and then take the product of these bounds to get the relevant products for the processes considered. Otherwise these coupling products of mixed chirality will have to be treated as a free parameters. These individual bounds are derived from the existing bounds on the coupling products of same chirality and same LQ type from the tau decays. These bounds are however derived on the assumption that only a single coupling at a time is non-zero. Considering only the effects of the same kind of coupling constant at a time while "switching off" all the others, leads to more conservative bounds. We extract coupling products relevant to $(\nu_\mu d)(\tau u)$ vertex from rare τ decay bounds as quoted in reference [14] and get

$$|h_{1L}|^2 = |h_{1R}|^2 = 1.9 \times 10^{-3} \left(\frac{M_{LQ}}{100 \text{ GeV}}\right)^2, \qquad |h_{2L}|^2 = 3.9 \times 10^{-3} \left(\frac{M_{LQ}}{100 \text{ GeV}}\right)^2,$$

$$|h_{3L}|^2 = 6.4 \times 10^{-4} \left(\frac{M_{LQ}}{100\ \text{GeV}}\right)^2, \quad |h_{2R}|^2 = 1.9 \times 10^{-3} \left(\frac{M_{LQ}}{100\ \text{GeV}}\right)^2,$$
$$|g_{1L}|^2 = |g_{1R}|^2 = 3.9 \times 10^{-3} \left(\frac{M_{LQ}}{100\ \text{GeV}}\right)^2, \quad |g_{3L}|^2 = 1.3 \times 10^{-3} \left(\frac{M_{LQ}}{100\ \text{GeV}}\right)^2,$$
$$|g_{2L}|^2 = 1.9 \times 10^{-3} \left(\frac{M_{LQ}}{100\ \text{GeV}}\right)^2, \quad |g_{2R}|^2 = 9.7 \times 10^{-4} \left(\frac{M_{LQ}}{100\ \text{GeV}}\right)^2. \quad (5.1)$$

In case of wrong sign μ, the bounds on the couplings for $(\bar{\nu}_e u)(\mu^+ d)$ vertex arising from $\mu \leftrightarrow e$ conversion are so stringent, being typically 2-3 orders of magnitude lower compared to bounds on couplings involving third generation of quarks and leptons, that the direct production of μ^+ is highly suppressed. The relevant coupling constants extracted from [14] are

$$|h_{1L}|^2 = |h_{1R}|^2 = 2.6 \times 10^{-7} \left(\frac{M_{LQ}}{100\ \text{GeV}}\right)^2, \quad |h_{2L}|^2 = 5.2 \times 10^{-7} \left(\frac{M_{LQ}}{100\ \text{GeV}}\right)^2,$$
$$|h_{3L}|^2 = 8.5 \times 10^{-8} \left(\frac{M_{LQ}}{100\ \text{GeV}}\right)^2, \quad |h_{2R}|^2 = 2.6 \times 10^{-7} \left(\frac{M_{LQ}}{100\ \text{GeV}}\right)^2,$$
$$|g_{1L}|^2 = |g_{1R}|^2 = 5.2 \times 10^{-7} \left(\frac{M_{LQ}}{100\ \text{GeV}}\right)^2, \quad |g_{3L}|^2 = 1.7 \times 10^{-7} \left(\frac{M_{LQ}}{100\ \text{GeV}}\right)^2,$$
$$|g_{2L}|^2 = 2.6 \times 10^{-7} \left(\frac{M_{LQ}}{100\ \text{GeV}}\right)^2, \quad |g_{2R}|^2 = 1.3 \times 10^{-7} \left(\frac{M_{LQ}}{100\ \text{GeV}}\right)^2. \quad (5.2)$$

In this situation, wrong sign muons mainly arise through the production of τ^+'s, which subsequently decay via leptonic channel. The bounds on coupling constants for the $(\bar{\nu}_e u)(\tau^+ d)$ vertex come from the decay $\tau \to \pi^0 e$ and are essentially the same as that for the case of τ production [14].

Next we discuss the heavy quark production via LQ. The bounds on relevant couplings generally come from electroweak tests. Regarding the bounds on LQ couplings, we have used model independent constraints on the couplings to b quarks of B and L conserving LQs as discussed in [14] where it is shown that one can constrain the generation dependent LQ couplings to b quarks from the upper bounds on the flavour-changing decays $B \longrightarrow l^+ l^- X$ (where $l^+ l^- = \mu^+\mu^-, e^+e^-$), the CKM matrix element V_{ub} and from meson - antimeson ($B\bar{B}$) mixing and obtain some of the best bounds for the processes of our interest. All the bounds on couplings that we have used for calculation of event rates are listed in Table 5.1. Since the bounds on the couplings h_{2L} & g_{1R} are not available from reference [14], we take them to be the same

as bounds on couplings h_{2R} & g_{1L} (which are the opposite chirality counterparts of h_{2L} & g_{1R} respectively). We make some simplifying assumptions like the product of couplings of different chirality is obtained from the squares of the couplings of individual chiralities. We extract bounds relevant to $(\nu_\mu d)(\nu_\mu b)$ vertex from the bounds for (21)(23) generation of quark-lepton pair, while for the vertex $(\bar{\nu}_e d)(\bar{\nu}_e b)$, we use the bounds for the (11)(13) generation indices relevant to the process. These bounds are derived from semileptonic inclusive B decays. The latest bounds coming from BABAR and BELLE experiments [80] however are not relevant for the processes considered here except for the bound on V_{ub} which does not make any significant change in the couplings.

(lq)(lq)	h_{1L}	h_{1R}	h_{2L}	h_{2R}	h_{3L}	g_{1L}	g_{1R}	g_{2L}	g_{2R}	g_{3L}
(11)(13)	.002	.003	–	.006	.002	.004	–	.003	.003	.004
(21)(23)	.0004	.0004	–	.0008	.0004	.004	–	.0004	.0004	.0004

Table 5.1: The best bounds on all relevant products of couplings (from B decays and $B\bar{B}$ mixing) taken from Table 15 of the reference [14] by S. Davidson *et al.*). All the bounds are multiplied by $(m_{LQ}/[100\text{ GeV}])^2$.

5.3 Future Prospects

Future prospects for all the processes which we have considered in this report are promising. With the kind of enhancement we have for tau and wrong sign muon production, neutrino factories when coupled with detectors that are able to detect τ and wrong sign muons should be able to observe such effects easily. The non-standard eventrate falls off with the increase in baseline length and neutrino oscillations are the main source of events examined at LBL. At near-site experiments, on the other hand, the events mainly arise from new interactions and

thus can be used to constrain the theory. Thus, near site experiments are recommended for isolating new physics signals that fake signals of neutrino oscillation. A class of non-standard interactions (R-violating), with strengths well below their current experimental limits, can be responsible for an enhanced rate of wrong sign muons at a LBL setting. Since the solution space of solar neutrino puzzle doesnot permit such event rates, such muons if observed at a neutrino factory, can therefore be greeted as harbingers of new physics, of which both R-parity violating SUSY and LQ are favoured examples. In particular, one can obtain constraints on LFV couplings between the first and third generation, the bounds on which are generally not available.

Heavy quark $(b, \bar{b})$ production from $\nu_\mu - \mathrm{N}$ and $\bar{\nu}_e - N$ scattering via both the CC and NC interactions at a NF provides an exciting possibility to detect signals of new physics. This comes about because in these processes the SM contribution is heavily suppressed either due to CKM matrix element or due to interaction of neutrinos with the sea quarks present inside the nucleon. The NC processes in SM are further suppressed as they can take place only at one loop level. We have computed here the $b(\bar{b})$ event rates in theories with LQ and confined ourselves to the near-site experiments where the oscillation effects are negligible. We have investigated the region in coupling - mass space for LQ which can provide a reasonable signal for the discovery of new physics involving LQ. It may be noted that this region can be even more restrictive than that implied by the low energy bounds obtained from B meson decays. Also the inclusion of LFV interactions via LQ could further squeeze the allowed region of LFV Couplings and masses. Detection of $b/\bar{b}$ in final state are very important as far as the indirect signatures of new physics are concerned.

Bibliography

[1] S. L. Glashow, Nucl. Phys. **22**, 579 (1961); S. Weinberg, Phys. Rev. Lett. **19**, 1264 (1967); A. Salam, Proceedings of the Nobel symposium held 1968 at Lerum, Sweden, Stockholm 1968, 367-377 (Nobel prize 1979 for physics).

[2] Some reference texts : L. B. Okun, "Leptons and quarks," Amsterdam, Netherlands : North-Holland (1982) and F. Halzen and A. D. Martin, "Quarks and leptons : An introductory course in modern particle physics," New York, USA : Wiley (1984) they are complemented well by L.H. Ryder, "Quantum Field Theory," Cambridge, UK:Univ. Press (1985). A recent useful review : Zoltan Kunszt, "Bread and butter standard model," hep-ph/0004103.

[3] Peter Renton, "Electroweak interactions : An introduction to the physics of quarks and leptons," Cambridge, UK:Univ. Press (1985).

[4] S. J. Barish *et al.*, Phys. Rev. D **16**, 3103 (1977); Nucl. Phys. B **343** (1990) 285; V. V. Ammosov *et al.*, Sov. J. Part. Nucl. **23** (1992) 283; N. J. Baker *et al.*, Phys. Rev. D **23**, 2499 (1981); N. J. Baker *et al.*, Phys. Rev. D **28**, 2900 (1983).

[5] C. H. Llewellyn Smith, Phys. Rept. **3**, 261 (1972).

[6] R. P. Feynman and M. Gell-mann, Phys. Rev. D **109**, 193 (1958).

[7] A. Bodek, H. Budd and J. Arrington, AIP Conf. Proc. **698**, 148 (2004) [arXiv:hep-ex/0309024]; A. Bodek, H. Budd and J. Arrington, AIP Conf. Proc. **698**, 148 (2004) [arXiv:hep-ex/0309024].

[8] R. Blair *et al.*, Phys. Rev. Lett. **51**, 343 (1983); M. Jonker *et al.* [CHARM Collaboration], Phys. Lett. B **99**, 265 (1981) [Erratum-ibid. B **100**, 520 (1981 ERRAT,B103,469.1981)]; J. P. Berge *et al.*, Z. Phys. C **38**, 403 (1988).

[9] H. Lai *et al.*, Phys. Rev. **D55,** 1280 (1997).

[10] P. Fayet, Phys. Lett. **B69,** 489 (1977); G. Farrar and P. Fayet, Phys. Lett. **B76,** 575 (1978).

[11] V. Barger, G.F. Giudice, and T. Han, Phys. Rev. **D40,** 2987 (1989).

[12] J. C. Pati and A. Salam, Phys. Rev. D **10**, 275 (1974); E. Eichten, K. D. Lane and M. E. Peskin, Phys. Rev. Lett. **50**, 811 (1983); J. L. Hewett and T. G. Rizzo, Phys. Rept. **183**, 193 (1989) ; P. Langacker, M. Luo and A. K. Mann, Rev. Mod. Phys. **64**, 87 (1992).

[13] J. Blumlein and R. Ruckl, Phys. Lett. **B304,** 337 (1993); W. Buchmuller and D. Wyler, Phys. Lett. **B177,** 377 (1986); W. Buchmuller, R. Rückl and D. Wyler, Phys. Lett. **B191** (1987) 442; Errata, it ibid **B448** (1999) 320.

[14] S. Davidson, D. Bailey and B. A. Campbell, Z. Phys. **C61**, (1994) 613, and references therein.

[15] A. Dobado, M.J. Herrero and C. Muñoz, Phys. Lett. **B191** (1987) 449.

[16] For a review on leptoquarks at HERA see: R.J. Cashmore *et al.*, Phys. Rep. **122** (1985) 275.

[17] O. Shanker, Nucl. Phys. **B204** (1982) 375; R. Mohapatra, G. Segré and L. Wolfenstein, Phys. Lett. **B145**(1984) 433; I. Bigi, G. Köpp, and P.M. Zerwas, Phys. Lett. **B166**(1986) 238; B. A. Campbell *et al.*, Int. J. Mod. Phys. **A2** (1987) 831; A. J. Davies and X. He, Phys. Rev. **D43** (1991) 225.

[18] G. Altarelli, J. Ellis, G.F. Giudice, S. Lola and M.L. Mangano, Nucl. Phys. **B506** (1997) 3; G. Altarelli, G.F. Giudice, and M.L. Mangano, Nucl.Phys. **B506** (1997) 29; K.S. Babu, C. Kolda, J. March-Russell, and F. Wilczek, Phys. Lett. **B402** (1997) 367: C. Friberg, E. Norrbin and T. Sjostrand, Phys. Lett. **B403** (1997) 329; M. Heyssler and W.J. Stirling, Phys. Lett. **B407** (1997) 259; J.L. Hewett and T.G. Rizzo, Phys. Rev. **D56** (1997) 5709; E. Keith and E. Ma, Phys. Rev. Lett. **79** (1997) 4318; T.K. Kuo and T. Lee, Mod. Phys. Lett. **A12** (1997) 2367; T. Plehn, H. Spiesberger, M. Spira, and P.M. Zerwas, Z. Phys. **C74** (1997) 611; Z. Kunszt and W.J. Stirling, Z. Phys. **C75** (1997) 453; N.G. Deshpande and B. Dutta, Phys. Lett. **B424** (1998) 313; J.K. Elwood and A.E. Faraggi Nucl. Phys. **B512** (1998) 42; M. Sekiguchi, H. Wada and S. Ishida, Prog. Theor. Phys. **99** (1998) 707.

[19] H1 Collaboration, C. Adloff *et al.*, Z. Phys. **C74** (1997) 191.

[20] ZEUS Collaboration, J. Breitweg *et al.*, Z. Phys. **C74** (1997) 207.

[21] H1 Collaboration, C. Adloff *et al.*, Eur. Phys. J. **C11** (1999) 447.

[22] Y. Fukuda *et al.* [Super-Kamiokande Collaboration], Phys. Rev. Lett. **81**, 1562 (1998) [arXiv:hep-ex/9807003].

[23] Y. Fukuda *et al.* [Super-Kamiokande Collaboration], Phys. Rev. Lett. **82**, 2644 (1999) [arXiv:hep-ex/9812014].

[24] E. Kearns, talk at XXIst International Conference on Neutrino Physics and Astrophysics (Neutrino-2004), Paris, June 14-19, 2004, see http://neutrino2004.in2p3.fr/

[25] M. Ambrosio *et al.* [MACRO Collaboration], Phys. Lett. B **566**, 35 (2003) [arXiv:hep-ex/0304037].

[26] M. H. Ahn *et al.* [K2K Collaboration], Phys. Rev. Lett. **90**, 041801 (2003) [arXiv:hep-ex/0212007].

[27] B. T. Cleveland *et al.*, Astrophys. J. **496**, 505 (1998).

[28] J. N. Abdurashitov *et al.* [SAGE Collaboration], "Measurement of the solar neutrino capture rate by the Russian-American J. Exp. Theor. Phys. **95**, 181 (2002) [Zh. Eksp. Teor. Fiz. **122**, 211 (2002)] [arXiv:astro-ph/0204245].

[29] W. Hampel *et al.* [GALLEX Collaboration], Phys. Lett. B **447**, 127 (1999).

[30] M. Altmann *et al.* [GNO Collaboration], Phys. Lett. B **490**, 16 (2000) [arXiv:hep-ex/0006034].

[31] S. Fukuda *et al.* [Super-Kamiokande Collaboration], Phys. Lett. B **539**, 179 (2002) [arXiv:hep-ex/0205075].

[32] Q. R. Ahmad *et al.* [SNO Collaboration], Phys. Rev. Lett. **89**, 011301 (2002) [arXiv:nucl-ex/0204008].

[33] S. N. Ahmed *et al.* [SNO Collaboration], Phys. Rev. Lett. **92**, 181301 (2004) [arXiv:nucl-ex/0309004].

[34] K. Eguchi *et al.* [KamLAND Collaboration], Phys. Rev. Lett. **90**, 021802 (2003) [arXiv:hep-ex/0212021].

[35] L. Wolfenstein, Phys. Rev. D **17**, 2369 (1978); S. P. Mikheev and A. Y. Smirnov, Sov. J. Nucl. Phys. **42**, 913 (1985) [Yad. Fiz. **42**, 1441 (1985)].

[36] Y. Itow *et al.*, arXiv:hep-ex/0106019.

[37] D. Ayres *et al.* [Nova Collaboration], arXiv:hep-ex/0210005.

[38] D. G. Koshkarev, CERN/ISR-DI/74-62.

[39] S. Geer, Phys. Rev. D **57**, 6989 (1998) [Erratum-ibid. D **59**, 039903 (1999)] [arXiv:hep-ph/9712290]; S. Geer, Comments Nucl. Part. Phys. A **2**, 284 (2002) [arXiv:hep-ph/0008155].

[40] C. Albright *et al.*, arXiv:hep-ex/0008064.

[41] C. Quigg, AIP Conf. Proc. **435**, 242 (1998) [arXiv:hep-ph/9803326].

[42] M. M. Alsharo'a *et. al*, Phys. ReV. st Accel. Bemas 6, 081001 (2003).

[43] B. Autin, A. Blondel, J. Ellis (Eds.), CERN yellow report 99-02.

[44] NufactJ Working Group (Ed. Y. Kuno and Y. Mori) "A Feasibilty Study of Neutrino Factory in Japan", see http://www-prism.kek.jp/nufactj/index.html "

[45] See for example, T.K. Gaisser, "Cosmic Rays and Particle Physics", Cambridge University Press 1990.

[46] C. M. Ankenbrandt *et al.*, Phys. Rev. ST Accel. Beams **2**, 081001 (1999) [arXiv:physics/9901022].

[47] See UNO official homepage, http://superk.physics.sunysb.edu/uno/.

[48] D. B. Cline, F. Sergiampietri, J. G. Learned and K. McDonald, Nucl. Instrum. Meth. A **503**, 136 (2003) [arXiv:astro-ph/0105442]; K. T. McDonald, arXiv:hep-ex/0204037; D. Ayres *et al.* [Neutrino Factory and Muon Collider Collaboration], arXiv:physics/9911009; An early proposal for a liquid argon detector, AGRONAUT, may be found in G. Harigel *et. al*, Fermilab Proposal no. 601D, 1978.

[49] For recent talks and working group reports, see INO offical homepage, http://www.imsc.res.in/∼ino

[50] F. Arneodo *et al.*, Nucl. Instrum. Meth. A **455**, 376 (2000).

[51] Proceedings of the Fermilab Workshop on Physics at a Muon Collider and the Front End of a Muon Collider, eds.-S. Geer, R. Raja (Nov. 1997), AIP Conf. Proc. 435; S. Geer, Physics Potential of Neutrino Beams from Muon Storage Rings, AIP Conf. Proc. 435, 384 (1998).

[52] Y. Suzuki, talk given at the XIX International Conference on Neutrino Physics & Astrophysics, see, *http://nu2000.sno.laurentian.ca/Y. Suzuki*; H. Sobel, talk given at the same conference, see, *http://nu2000.sno.laurentian.ca/H.Sobel*, S. Rigolin, (hep–ph/0002108).

[53] D. Ayres *et al.*, (electronic archive: physics/9911009); A. Cervera *et al.*,(hep–ph/0002108); A. Blondel *et al.*, CERN-EP-2000-05; M. L. Mangano *et al.*, (hep–ph/0105155), CERN-TH/2001-131.

[54] T. Mann, talk given at the XIX International Conference on Neutrino Physics & Astrophysics, see, *http://nu2000.sno. laurentian.ca/T. Mann.*

[55] B. Barish, talk given at the XIX International Conference on Neutrino Physics & Astrophysics, see, *http://nu2000.sno. laurentian.ca/B. Barish.*

[56] A. De Rujula, M.B. Gavela, P. Hernandez, Nucl. Phys. **B547,** 21 (1999); S. Dutta, R. Gandhi and B. Mukhopadhyaya, Eur. Phys. J. C **18**, 405 (2000) [arXiv:hep-ph/9905475]; V. Barger, S. Geer, R. Raja, K. Whisnant, Phys. Lett. **B485,** 379 (2000); Phys. Rev. **D62,** 013004 (2000); I. Mocioiu and Robert Shrock, Phys. Rev. **D62,** 053017 (2000).

[57] S. Bergmann, Y. Grossman, D. Pierce, Phys. Rev. **D61,** 053005 (2000); L. Jhonson, D. Mckay, Phys. Rev. **D61,** 113007 (2000); S. Bergmann et al., Phys. Rev. **D62,** 073001

(2000); S. Bergmann, H. Klapdor-Kleingrothaus, H. Pass, Phys. Rev. **D62,** 113002 (2000).

[58] V. D. Barger, S. Geer, R. Raja and K. Whisnant, Phys. Rev. D **63**, 033002 (2001) [arXiv:hep-ph/0007181].

[59] V. Barger, R. Phillips, K. Whisnant, Phys. Rev. **D44,** 1629 (1991).

[60] M. Carena *et al.*, Phys. Rev. **D58,** 095003 (1998).

[61] P. B. Pal, Int. J. Mod. Phys. **A7**, 5387 (1992).

[62] R. Barbier et al., (hep–ph/9810232) and references therein; C. Allanach, A. Dedes and H. Dreiner, Phys. Rev. **D60,** 075014 (1999).

[63] ICANOE Proposal, LNGS-P21/99, see, *http://pcnometh4.cern.ch*; A. Rubbia, talk given at International Conference on Next Generation Nucleon Decay and Neutrino Detector (NNN '99), (hep–ex/0001052).

[64] C. Allanach, A. Dedes and H. Dreiner, Phys. Rev. **D60,** 075014 (1999).

[65] J. J. Bahcall, P. I. Krastev, A. Yu. Smirnov, Phys. Rev. **D58,** 096016 (1998); Phys. Rev. **D60,** 093991 (1999); M. Gonzalez-Garcia, Talk given at the XIX International Conference on Neutrino Physics & Astrophysics, see, *http://nu2000.sno.laurentian.ca/M. Gonzalez-Garcia*; J. Bachall, P. Krastev and A. Smirnov, (hep–ex/0103179).

[66] *LSND Collab.*, C. Athanassopoulos et al., Phys. Rev. Lett. **75,** 2650 (1995); ibid. **77,** 3082 (1996); Phys. Rev. **C58,** 2489 (1998).

[67] J. E. Kim, P. Ko, D. Lee, Phys. Rev. **D56,** 100 (1997).

[68] A. Datta, R. Gandhi, B. Mukhopadhayaya, P. Mehta, Phys. Rev. **D64,** 015011 (2001).

[69] See the references in [12, 13]; O. Shankar, Nucl. Phys. **B206,** 253 (1982); M. A. Doncheski and R. W. Robinett, Phys. Rev. **D56,** 7412 (1997); U. Mahanta, Phys. Rev. **D62,** 073009 (2000).

[70] See the reference in [14]; E. Gabrielli, (hep–ph/9911539); S. Aid *et al.* Phys. Lett. **B353,** 578 (1995); Derrick *et al.*, Z. Phys. C**73,** 613 (1997); C. Adloff *et al.*, (hep–ex/9907002).

[71] See the second reference in [56] and references therein.

[72] P. Migliozzi *et al.*, (hep–ph/0011051)

[73] Particle Data Group, D. E. Groom *et al.*, The European Phys. Jr. **C15**, 1 (2000)

[74] M.L. Mangano *et. al.*, (hep–ph/0105155).

[75] Y. Fukuda et. al., Phys. Lett. **B433,** 9 (1998), Phys. Rev. Lett. **81,** 1562 (1998); T. Kagita, in proceedings of the XVIIIth International Conference on Neutrino Physics and Astrophysics, Takayama, Japan (June 1998).

[76] L. Wolfenstein, Phys. Rev. **D17,** 2369 (1978), Phys. Rev. **D20,** 2634 (1979); S. P. Mikheyev and A. Yu Smirnov, Sov. J. Nucl. Phys.**42** (1986) 913.

[77] B. Pontecorvo, Sov. Phys. JETP **26** (1968) 984.

[78] P. Mehta, A. Goyal, S. Dutta, Phys. Lett. **B535,** 219 (2002).

[79] D. Chakraverty, A. Dutta, B. Mukhopadhayaya, Phys. Lett. **B503,** 74 (2001).

[80] K. Abe *et. al.* (The Belle Collaboration), (hep–ex/0204002), to appear in Phys. Rev. Lett.; B. Aubert *et. al.* (BABAR Collaboration), (hep–ex/0207080); A. Roodman, (hep–ex/0112019); V. Halyo, (hep–ex/0207010); J. Nam *et. al.* (The Belle Collaboration), IJMPA Vol. 16, Suppl. 1B: 625-627, 2001.

[81] All bounds on λ and λ' have been updated by F. Ledroit and G. Sajot, GDR-S-008(ISN, Grenoble, 1998). This can be obtained at : http://qcd.th.u-psud.fr/GDR_SUSY/GDR_SUSY_PUBLIC/entete_note_publique.

Appendix A

A.1 Dirac Matrices

$$\{\gamma^\mu, \gamma^\nu\} = \gamma^\mu\gamma^\nu + \gamma^\nu\gamma^\mu = 2g^{\mu\nu}, \qquad \{\gamma^5, \gamma^\mu\} = 0 \tag{A.1}$$

$$\gamma^5 \equiv \gamma_5 = -i\gamma_0\gamma_1\gamma_2\gamma_3 = i\gamma^0\gamma^1\gamma^2\gamma^3 \tag{A.2}$$

$$\gamma^\mu = (\gamma^0, \vec{\gamma}) \tag{A.3}$$

$$(\gamma^0)^2 = -(\gamma^k)^2 = (\gamma^5)^2 = I \qquad (k = 1, 2, 3) \tag{A.4}$$

$$\gamma_\mu = g_{\mu\nu}\gamma^\nu = (\gamma_0, -\vec{\gamma}) \tag{A.5}$$

$$\sigma_{\mu\nu} = \frac{i}{2}[\gamma_\mu, \gamma_\nu] \tag{A.6}$$

In Dirac Representation,

$$\gamma^0 = \begin{pmatrix} I & 0 \\ 0 & I \end{pmatrix} \qquad \vec{\gamma} = \begin{pmatrix} 0 & \vec{\sigma} \\ -\vec{\sigma} & 0 \end{pmatrix} \qquad \gamma_5 = \begin{pmatrix} 0 & I \\ I & 0 \end{pmatrix} \tag{A.7}$$

where, I is the 2×2 identity matrix. The 2×2 Pauli matrices $\vec{\sigma} = (\sigma_x, \sigma_y, \sigma_z)$ are given by

$$\sigma_x = \begin{pmatrix} 0 & 1 \\ 1 & 0 \end{pmatrix} \qquad \sigma_y = \begin{pmatrix} 0 & -i \\ i & 0 \end{pmatrix} \qquad \sigma_z = \begin{pmatrix} 1 & 0 \\ 0 & -1 \end{pmatrix} \tag{A.8}$$

which satisfy

$$[\sigma_i, \sigma_j] = 2i\epsilon^{ijk}\sigma_k \tag{A.9}$$

$$\{\sigma_i, \sigma_j\} = 2\delta_{ij} \tag{A.10}$$

$$Tr(\sigma_i \sigma_j) = 2\delta_{ij} \tag{A.11}$$

where, ϵ^{ijk} is totally antisymmetric : $\epsilon^{ijk} = \epsilon_{ijk} = 1$ for an even permutation of x, y, z.

Hermitian Conjugate :

$$(\gamma^\mu)^\dagger = \gamma^0 \gamma^\mu \gamma^0$$

$$(\gamma^0)^\dagger = \gamma^0, \qquad (\gamma^k)^\dagger = -\gamma^k, \quad (k = 1, 2, 3) \qquad (\gamma^5)^\dagger = \gamma^5 \tag{A.12}$$

A.2 Particle-Antiparticle Conjugation Operator ($\hat{C}$)

The action of $\hat{C}$ on a fermionic field ψ is defined through

$$\hat{C} : \psi \rightarrow \psi^c = C\bar{\psi}^T \quad \text{where} \quad C = i\gamma_2\gamma_0. \tag{A.13}$$

The matrix C has the following properties :

$$C^\dagger = C^T = C^{-1} = -C$$

$$C\gamma_\mu C^{-1} = -{\gamma_\mu}^T \tag{A.14}$$

Some useful relations based on these properties are :

- $(\psi^c)^c = \psi$
- $\bar{\psi}^c = \psi^T C$
- $\bar{\psi}_1 {\psi_2}^c = \bar{\psi}_2^c \psi_1$
- $\bar{\psi}_1 A \psi_2 = \bar{\psi}_2^c (C A^T C^{-1}) {\psi_1}^c$

where ψ, ψ_1, ψ_2 are four component fermion fields and A is any arbitrary 4×4 matrix.

Using the commutation properties of the Dirac γ-matrices, we can see that, acting on a **chiral field**, $\hat{C}$ flips its chirality;

$$\begin{aligned} \hat{C} : \psi_L &\longrightarrow (\psi_L)^c = (\psi^c)_R \\ \hat{C} : \psi_R &\longrightarrow (\psi_R)^c = (\psi^c)_L \end{aligned} \tag{A.15}$$

i.e. the antiparticle of a LH fermion is RH.

Note : The particle-antiparticle conjugation operator $\hat{C}$ should not be confused with the charge conjugation operator C which, by definition flips all the charge-like quantum numbers of a field (*e.g.* electric charge, baryon number, lepton number, etc.) but leaves all the other quantum numbers (*e.g.* chirality) intact. Inparticular, C will take a LH neutrino to a RH antineutrino (which does not exist). This is a *consequence of C-noninvariance of weak interactions*. At the sametime, particle-antiparticle conjugation $\hat{C}$ converts a LH neutrino into a RH antineutrino which does exist and is the antiparticle of LH neutrino.
For massive fermions, $\hat{C}$ coincides with the usual charge conjugation operator, C.
For **Dirac fermions**,

$$\begin{aligned} \hat{C} : \psi = \psi_L + \psi_R &\longrightarrow \psi^c = (\psi_L)^c + (\psi_R)^c = (\psi^c)_R + (\psi^c)_L \\ C : \psi = \psi_L + \psi_R &\longrightarrow \tilde{\psi} = \tilde{\psi_L} + \tilde{\psi_R} = (\psi^c)_L + (\psi^c)_R \end{aligned} \tag{A.16}$$

For **Majorana neutrinos**, both $\hat{C}$ and C leave the field unchanged, since it does not have any charges. However, there may be some difference in phase factors.

Note that for a massive fermion, the mass term in Lagrangian has the form

$$-\mathcal{L}_m = m\bar{\psi}\psi = \overline{(\psi_L + \psi_R)}(\psi_L + \psi_R) = \bar{\psi}_L\psi_R + \bar{\psi}_R\psi_L \tag{A.17}$$

Thus the mass terms couple the LH and RH components of the fermion field and therefore a massive field must have both components : $\psi = \psi_L + \psi_R$
There are 2 possibilities :

(1) ψ_R is independent of $\psi_L \longrightarrow$ **Dirac Field**.

(2) $\psi_R \longrightarrow \hat{C}$-conjugate of the LH field $\psi_L \longrightarrow$ **Majorana Field**

$$\psi_R = (\psi_L)^c = (\psi^c)_R$$

$$\psi = \psi_L + \psi_R = \psi_L + \eta\,(\psi^c)_R = \psi_L + \eta\,(\psi_L)^c \quad (\ \eta = e^{\iota\phi},\ \text{arbitrary phase factor}\ )$$

Therefore just one Weyl field is required to construct the Majorana field. $\hat{C}$ - conjugate field and therefore coincides with itself upto a phase factor.

$$\psi^c \;=\; \eta^\star \psi$$

$\Longrightarrow$ Particles described by Majorana fields are genuinely neutral, *i.e.* , coincide with their antiparticles.

Examples

Consider the expression $[\bar{\nu}^c \gamma_\mu P_R e^c]$ and express it interms of SM current

Using the properties of particle-antiparticle conjugation operator (equation A.13 and equation A.14),

$$\begin{aligned}
C = i\gamma_2\gamma_0\ ;\ C^\dagger = -C \\
\hat{C} : e \longrightarrow e^c = C\bar{e}^T = i\gamma_2 e^* \\
\hat{C} : \nu \longrightarrow \nu^c = C\bar{\nu}^T = i\gamma_2 \nu^* \\
\bar{\nu}^c = \overline{(C\bar{\nu}^T)} = \nu^T C \\
C\gamma_\mu C^{-1} = -\gamma_\mu^T \\
\Longrightarrow \gamma_\mu = -C^{-1}\gamma_\mu^T C
\end{aligned} \tag{A.18}$$

Therefore we have

$$\begin{aligned}
\bar{\nu}^c\,\gamma_\mu\,P_R\,e^c &= \bar{\nu}^c\,\gamma_\mu\left(\frac{1+\gamma_5}{2}\right)e^c \\
&= \frac{1}{2}\left[\nu^T\,C\,\gamma_\mu\,(1+\gamma_5)\,C\,\bar{e}^T\right] \\
&= \frac{1}{2}\left[\nu^T\,C\,(\,-C^{-1}\,\gamma_\mu^T\,C\,)\,(1+\gamma_5)\,(-C^{-1})\,\bar{e}^T\right] \\
&= \frac{1}{2}\left[\nu^T\,(C\,C^{-1})\,\gamma_\mu^T\,C\,(1+\gamma_5)\,(C^{-1})\,\bar{e}^T\right] \\
&= \frac{1}{2}\left[\nu^T\,\gamma_\mu^T\,(C\,C^{-1})\,\bar{e}^T\;+\;\nu^T\,\gamma_\mu^T\,C\,\gamma_5\,C^{-1}\,\bar{e}^T\right] \\
&= \frac{1}{2}\left[\nu^T\,\gamma_\mu^T\,\bar{e}^T\;+\;\nu^T\,\gamma_\mu^T\,\gamma_5\,(C\,C^{-1})\,\bar{e}^T\right] \\
&= \frac{1}{2}\left[\nu^T\,\gamma_\mu^T\,\bar{e}^T\;+\;\nu^T\,\gamma_\mu^T\,\gamma_5^T\,\bar{e}^T\right] \\
&= \frac{1}{2}\left[(\bar{e}\,\gamma_\mu\,\nu)^T\;+\;(\bar{e}\,\gamma_5\,\gamma_\mu\,\nu)^T\right] \\
&= \frac{1}{2}\left[(\bar{e}\,\gamma_\mu\,\nu)\;+\;(\bar{e}\,\gamma_5\,\gamma_\mu\,\nu)\right] \\
&= \frac{1}{2}\left[\bar{e}\,\gamma_\mu\,(1\;-\;\gamma_5)\,\nu\right] \\
&= \left[\,\bar{e}\,\gamma_\mu\,P_L\,\nu\,\right] \qquad \text{(A.19)}
\end{aligned}$$

Figure A.1: *Diagrammatic depiction of the equivalence between charge-conjugated current term with (V+A) interaction term interms of charge-conjugated fields and the SM (V-A) current term in terms of usual fields denoted by the particles.*

The above equality (equation A.19) of the two currents in terms of charge-conjugated fields and the usual SM fields respectively is shown diagramatically in Figure A.1.

A.3 Fierz Transformations

As the 16 Γ^i matrices with $i = S, V, T, A, P$ form a complete set of N=4 matrices, any product of bilinear covariants of the form $(\bar{u}_1\Gamma^i u_2)\,(\bar{u}_3\Gamma^j u_4)$ can be expressed as a linear combination of similar products written with a different sequence of spinors

$$(\bar{u}_1\Gamma^i u_2)\,(\bar{u}_3\Gamma^j u_4) \;=\; \sum_{mn} \mathcal{C}^{ij}_{mn}(\bar{u}_1\Gamma^m u_4)\,(\bar{u}_3\Gamma^n u_2) \tag{A.20}$$

Ingeneral, the spinors u_i refer to different particles.
It can be shown that

$$\mathcal{C}^{ij}_{mn} \;=\; \frac{1}{N_m N_n}\mathcal{T}r(\Gamma^i\Gamma^n\Gamma^j\Gamma^m) \tag{A.21}$$

Γ^i are assumed to be orthonormalized such that

$$\mathcal{T}r(\Gamma^i\Gamma^j) \;=\; N_i\,\delta_{ij} \tag{A.22}$$

The basic expansion relation in spinor components (a,b=1,2,3,4) is

$$(\bar{u}_{1a}\Gamma^i_{ab}u_{2b})\,(\bar{u}_{3c}\Gamma^j_{cd}u_{4d}) \;=\; \sum_{kl}\mathcal{C}^{ij}_{kl}(\bar{u}_{1a}\Gamma^k_{ad}u_{4d})\,(\bar{u}_{3c}\Gamma^l_{cb}u_{2b}) \tag{A.23}$$

Assume that u_a are all c-valued so that

$$\Gamma^i_{ab}\Gamma^j_{cd} \;=\; \mathcal{C}^{ij}_{kl}\Gamma^k_{ad}\Gamma^l_{cb} \tag{A.24}$$

(If u_a are anticommuting operators, there is an overall relative negative sign.) Multiplying both sides of this equation by $\Gamma^m_{bc}\Gamma^n_{da}$ and then summing over all the spinor indices we obtain $\mathcal{T}r(\Gamma^i\Gamma^n\Gamma^j\Gamma^m)$ where $\mathcal{T}r(\Gamma^i\Gamma^j) = N_i\,\delta_{ij}$ For Lorentz scalar products of bilinear covariants with all their lorentz indices contracted,

$$(\bar{u}_1\Gamma^i u_2)\,(\bar{u}_3\Gamma_i u_4) \;=\; \sum_j \mathcal{C}^i_j(\bar{u}_1\Gamma^j u_4)\,(\bar{u}_3\Gamma_j u_2) \tag{A.25}$$

Γ^i denote

$$\begin{aligned}
\Gamma^S &= 1 \\
\Gamma^V &= \gamma_\mu \\
\Gamma^T &= \sigma_{\mu\nu} \\
\Gamma^P &= \gamma_5 \\
\Gamma^A &= \gamma_\mu\gamma_5
\end{aligned}$$

The coefficients $\mathcal{C}_j^i$ assume the values given below :

	S	V	T	A	P
S	1/4	1/4	1/8	-1/4	1/4
V	1	-1/2	0	-1/2	-1
T	3	0	-1/2	0	3
A	-1	-1/2	0	-1/2	1
P	1/4	-1/4	1/8	1/4	1/4

Similar to equation A.25 is the relation,

$$(\bar{u}_1\Gamma^i u_2)\,(\bar{u}_3\Gamma_i\gamma_5 u_4) \;=\; \sum_j \mathcal{C}_j^i(\bar{u}_1\Gamma^j\gamma_5 u_4)\,(\bar{u}_3\Gamma_j u_2) \tag{A.26}$$

which comes with the same numerical coefficients $\mathcal{C}_j^i$. The above identities yield the following relations, very useful for the studies of weak processes :

$$[\bar{u}_1\gamma_\mu(1\pm\gamma_5)u_2]\,[\bar{u}_3\gamma^\mu(1\pm\gamma_5)u_4] \;=\; -\,[\bar{u}_1\gamma_\mu(1\pm\gamma_5)u_4]\,[\bar{u}_3\gamma^\mu(1\pm\gamma_5)u_2] \tag{A.27}$$

$$[\bar{u}_1\gamma_\mu(1\pm\gamma_5)u_2]\,[\bar{u}_3\gamma^\mu(1\mp\gamma_5)u_4] \;=\; 2\,[\bar{u}_1(1\mp\gamma_5)u_4]\,[\bar{u}_3(1\pm\gamma_5)u_2] \tag{A.28}$$

When anti-commuting fields ψ_i, rather than c-valued spinors u_i, appear in the bilinear products, the R.H.S. of the above equations (equation A.25, equation A.26, equation A.27 and equation A.28) will carry an additional overall "negative" sign.

Examples

Consider the term $[\bar{\nu}^c\, P_L\, d\, \bar{u}\, P_R\, e^c]$ and evaluate its Fierz Transform.

$$\begin{aligned}[\bar{\nu}^c\, P_L\, d\, \bar{u}\, P_R\, e^c] &= [\bar{\nu}^c\, \frac{1-\gamma_5}{2}\, d\, \bar{u}\, \frac{1+\gamma_5}{2}\, e^c] \\ &= \frac{1}{4}[\bar{\nu}^c\, d\, \bar{u}\, e^c \;-\; \bar{\nu}^c\, \gamma_5\, d\, \bar{u}\, e^c \;+\; \bar{\nu}^c\, d\, \bar{u}\, \gamma_5\, e^c \;-\; \bar{\nu}^c\, \gamma_5\, d\, \bar{u}\, \gamma_5\, e^c]\end{aligned} \tag{A.29}$$

Let us consider the 4 terms in square brackets on the R.H.S. of above equation one by one,

1. $[\bar{\nu}^c\, d\, \bar{u}\, e^c]$

$$\begin{aligned}[\bar{\nu}^c\, d\, \bar{u}\, e^c] &= \frac{1}{4}\,[\bar{u}\, d\, \bar{\nu}^c\, e^c \;+\; \bar{u}\, \gamma_\mu\, d\, \bar{\nu}^c \gamma^\mu e^c \;+\; \frac{1}{2}\,\bar{u}\, \sigma_{\mu\nu}\, d\, \bar{\nu}^c \sigma^{\mu\nu} e^c \;- \\ &\quad \bar{u}\, \gamma_\mu\, \gamma_5\, d\, \bar{\nu}^c\, \gamma^\mu\, \gamma_5\, e^c \;+\; \bar{u}\, \gamma_5\, d\, \bar{\nu}^c\, \gamma_5\, e^c] \\ &= \frac{1}{4}[S \;+\; V \;+\; \frac{1}{2}\,T \;-\; A \;+\; P]\end{aligned} \tag{A.30}$$

we have used equation A.25 with $\Gamma^i = \Gamma^S = 1$

2. $[-\bar{\nu}^c\, \gamma_5\, d\, \bar{u}\, \gamma_5\, e^c]$

$$\begin{aligned}-\,[\bar{\nu}^c\, \gamma_5\, d\, \bar{u}\, \gamma_5\, e^c] &= -\,\frac{1}{4}\,[\bar{u}\, d\, \bar{\nu}^c\, e^c \;-\; \bar{u}\, \gamma_\mu\, d\, \bar{\nu}^c \gamma^\mu e^c \;+\; \frac{1}{2}\,\bar{u}\, \sigma_{\mu\nu}\, d\, \bar{\nu}^c \sigma^{\mu\nu} e^c \;+ \\ &\quad \bar{u}\, \gamma_\mu\, \gamma_5\, d\, \bar{\nu}^c\, \gamma^\mu\, \gamma_5\, e^c \;+\; \bar{u}\, \gamma_5\, d\, \bar{\nu}^c\, \gamma_5\, e^c] \\ &= \frac{1}{4}[-S \;+\; V \;-\; \frac{1}{2}\,T \;-\; A \;-\; P]\end{aligned} \tag{A.31}$$

we have used equation A.25 with $\Gamma^i = \Gamma^P = \gamma_5$

Adding 1 and 2 : we have the following terms

$$\Big\{[\bar{\nu}^c\, d\, \bar{u}\, e^c] \;+\; [-\bar{\nu}^c\, \gamma_5\, d\, \bar{u}\, \gamma_5\, e^c]\Big\}$$

$$\begin{aligned}&= \frac{1}{4}[S \;+\; V \;+\; \frac{1}{2}\,T \;-\; A \;+\; P] \;+\; \frac{1}{4}[-S \;+\; V \;-\; \frac{1}{2}\,T \;-\; A \;-\; P] \\ &= \frac{1}{2}(V \;-\; A)\end{aligned} \tag{A.32}$$

3. $[-\bar{\nu}^c\,\gamma_5\;d\,\bar{u}\,e^c]$

Note that since $\gamma_5^2 = 1$, we can write the above term and we will have $\Gamma^i = \Gamma^P = \gamma_5$

$$[-\bar{\nu}^c\,\gamma_5\,d\,\bar{u}\,e^c] \;=\; [-\bar{\nu}^c\,\gamma_5\,d\,\bar{u}\,\gamma_5\,\gamma_5\,e^c] \tag{A.33}$$

here we need to use equation A.26 instead of equation A.25 because of another γ_5 sitting before e^c.

$$\begin{aligned}
&= -\frac{1}{4}[\bar{\nu}^c\,\gamma_5\,e^c\,\bar{u}\,d \;-\; \bar{\nu}^c\,\gamma_\mu\,\gamma_5\,e^c\,\bar{u}\,\gamma^\mu\,d \;+\; \frac{1}{2}\,\bar{\nu}^c\,\sigma_{\mu\nu}\,\gamma_5\,e^c\,\bar{u}\,\sigma^{\mu\nu}\,d \\
&\quad +\; \bar{\nu}^c\,\gamma_\mu\gamma_5\,\gamma_5\,e^c\,\bar{u}\,\gamma^\mu\,\gamma_5\,d \;+\; \bar{\nu}^c\,\gamma_5\,\gamma_5\,e^c\,\bar{u}\,\gamma_5\,d] \\
&= -\frac{1}{4}[\bar{\nu}^c\,\gamma_5\,e^c\,\bar{u}\,d \;-\; \bar{\nu}^c\,\gamma_\mu\,\gamma_5\,e^c\,\bar{u}\,\gamma^\mu\,d \;+\; \frac{1}{2}\,\bar{\nu}^c\,\sigma_{\mu\nu}\,\gamma_5\,e^c\,\bar{u}\,\sigma^{\mu\nu}\,d \\
&\quad +\; \bar{\nu}^c\,\gamma_\mu\,e^c\,\bar{u}\,\gamma^\mu\,\gamma_5\,d \;+\; \bar{\nu}^c\,e^c\,\bar{u}\,\gamma_5\,d]
\end{aligned} \tag{A.34}$$

4. $[\bar{\nu}^c\,d\,\bar{u}\,\gamma_5\,e^c]$

Note that here we have $\Gamma^i = \Gamma^S = 1$ for the above expression and we will use equation A.26 instead of equation A.25 because of a γ_5 sitting before e^c.

$$\begin{aligned}
[-\bar{\nu}^c\,d\,\bar{u}\,\gamma_5\,e^c] \;&=\; \frac{1}{4}[\bar{\nu}^c\,\gamma_5\,e^c\,\bar{u}\,d \;+\; \bar{\nu}^c\,\gamma_\mu\,\gamma_5\,e^c\,\bar{u}\,\gamma^\mu\,d \;+\; \frac{1}{2}\,\bar{\nu}^c\,\sigma_{\mu\nu}\,\gamma_5\,e^c\,\bar{u}\,\sigma^{\mu\nu}\,d \\
&\quad -\; \bar{\nu}^c\,\gamma_\mu\gamma_5\,\gamma_5\,e^c\,\bar{u}\,\gamma^\mu\,\gamma_5\,d \;+\; \bar{\nu}^c\,\gamma_5\,\gamma_5\,e^c\,\bar{u}\,\gamma_5\,d] \\
&= \frac{1}{4}[\bar{\nu}^c\,\gamma_5\,e^c\,\bar{u}\,d \;+\; \bar{\nu}^c\,\gamma_\mu\,\gamma_5\,e^c\,\bar{u}\,\gamma^\mu\,d \;+\; \frac{1}{2}\,\bar{\nu}^c\,\sigma_{\mu\nu}\,\gamma_5\,e^c\,\bar{u}\,\sigma^{\mu\nu}\,d \\
&\quad -\; \bar{\nu}^c\,\gamma_\mu\,e^c\,\bar{u}\,\gamma^\mu\,\gamma_5\,d \;+\; \bar{\nu}^c\,e^c\,\bar{u}\,\gamma_5\,d]
\end{aligned} \tag{A.35}$$

Adding 3 and 4 : we have the following terms

$$\Big\{[-\bar{\nu}^c\,\gamma_5\;d\,\bar{u}\,e^c] \;+\; [\bar{\nu}^c\,d\,\bar{u}\,\gamma_5\,e^c]\Big\}$$

$$\begin{aligned}
&= -\frac{1}{4}[\bar{\nu}^c\,\gamma_5\,e^c\,\bar{u}\,d \;-\; \bar{\nu}^c\,\gamma_\mu\,\gamma_5\,e^c\,\bar{u}\,\gamma^\mu\,d \;+\; \frac{1}{2}\,\bar{\nu}^c\,\sigma_{\mu\nu}\,\gamma_5\,e^c\,\bar{u}\,\sigma^{\mu\nu}\,d \;+\; \bar{\nu}^c\,\gamma_\mu\,e^c\,\bar{u}\,\gamma^\mu\,\gamma_5\,d \\
&\quad +\; \bar{\nu}^c\,e^c\,\bar{u}\,\gamma_5\,d] \;+\; \frac{1}{4}[\bar{\nu}^c\,\gamma_5\,e^c\,\bar{u}\,d \;+\; \bar{\nu}^c\,\gamma_\mu\,\gamma_5\,e^c\,\bar{u}\,\gamma^\mu\,d \;+\; \frac{1}{2}\,\bar{\nu}^c\,\sigma_{\mu\nu}\,\gamma_5\,e^c\,\bar{u}\,\sigma^{\mu\nu}\,d \\
&\quad -\; \bar{\nu}^c\,\gamma_\mu\,e^c\,\bar{u}\,\gamma^\mu\,\gamma_5\,d \;+\; \bar{\nu}^c\,e^c\,\bar{u}\,\gamma_5\,d] \\
&= \frac{1}{2}[\bar{\nu}^c\,\gamma_\mu\,\gamma_5\,e^c\,\bar{u}\,\gamma^\mu\,d \;-\; \bar{\nu}^c\,\gamma_\mu\,e^c\,\bar{u}\,\gamma^\mu\,\gamma_5\,d]
\end{aligned} \tag{A.36}$$

Adding equation A.32 and equation A.36 and dividing by a factor of 4, we get the full Fierz Transformed current, i.e.,

$$\begin{aligned}
[\bar{\nu}^c\, P_L\, d\, \bar{u}\, P_R\, e^c] &= \frac{1}{4}\,[1+2+3+4] \\
&= \frac{1}{4}\,\cdot\,\frac{1}{2}\,[\bar{u}\,\gamma_\mu\, d\,\bar{\nu}^c\gamma^\mu e^c \;-\; \bar{u}\,\gamma_\mu\,\gamma_5\, d\,\bar{\nu}^c\,\gamma^\mu\,\gamma_5\, e^c \;+ \\
&\quad \bar{\nu}^c\,\gamma_\mu\,\gamma_5\, e^c\,\bar{u}\,\gamma^\mu\, d \;-\; \bar{\nu}^c\,\gamma_\mu\, e^c\,\bar{u}\,\gamma^\mu\,\gamma_5\, d] \\
&= \frac{1}{8}\,[\bar{\nu}^c\,\gamma_\mu\,(1\;+\;\gamma_5)\, e^c\,\bar{u}\,\gamma^\mu\, d \;-\; \bar{\nu}^c\,\gamma_\mu\, e^c\,\bar{u}\,\gamma^\mu\,(1\;+\;\gamma_5)\, d] \\
&= \frac{1}{8}\,[\bar{\nu}^c\,\gamma_\mu\,(2\,P_R)\, e^c\,\bar{u}\,\gamma^\mu\,(1\;-\;\gamma_5) d] \\
&= \frac{1}{2}\,[\bar{\nu}^c\,\gamma_\mu\, P_R\, e^c\,\bar{u}\,\gamma^\mu\, P_L d] \\
&= \frac{1}{2}\,[\bar{e}\,\gamma_\mu\, P_L\,\nu\,\bar{u}\,\gamma^\mu\, P_L d]
\end{aligned} \tag{A.37}$$

Finally there will be an overall minus sign, since we are using fields instead of spinors. Therefore,

$$[\bar{\nu}^c\, P_L\, d\, \bar{u}\, P_R\, e^c] \;=\; -\,\frac{1}{2}\,[\bar{e}\,\gamma_\mu\, P_L\,\nu\,\bar{u}\,\gamma^\mu\, P_L d] \tag{A.38}$$